Communication between the Endoplasmic Reticulum and Peroxisomes in Mammalian Cells

by

Rong Hua

A thesis submitted in conformity with the requirements
for the degree of Doctor of Philosophy

Department of Biochemistry
University of Toronto

Communication between the Endoplasmic Reticulum and Peroxisomes in Mammalian Cells

Rong Hua

Doctor of Philosophy

Department of Biochemistry
University of Toronto

2017

Abstract

Peroxisomes are important metabolic organelles found in virtually all eukaryotic cells. Since their discovery, peroxisomes have long been seen in close proximity to the endoplasmic reticulum (ER). The interplay between the two organelles is suggested to be important for peroxisome biogenesis as the ER may serve as a source for both lipids and peroxisomal membrane proteins (PMPs) for peroxisome growth and maintenance. On the other hand, various lipid molecules are exchanged between them for the biosynthesis of specialized lipids such as bile acids, plasmalogens and cholesterol. However, how proteins and lipids are transported between the two organelles is not yet fully understood. Previously, the peroxisomal biogenesis factor PEX16 was shown to serve as a receptor for PMPs in the ER and also as a mediator of the subsequent transport of these ER-targeted PMPs to peroxisomes. Here, I extended these results by carrying out a comprehensive mutational analysis of PEX16 aimed at gaining insights into the molecular targeting signals responsible for its ER-to-peroxisome trafficking and the domain(s) involved in its PMP recruitment function at the ER. I also showed that the recruitment function of PEX16 is conserved in plants. To gain further mechanistic insight into PEX16 function, the proteins proximal to

PEX16 were identified using the proximity-dependent BioID analysis. From this data, I identified proteins that tether the ER and peroxisomes in mammalian cells. The tether between the two organelles is mediated by the ER resident VAP proteins (VAPA and VAPB) and the peroxisomal protein ACBD5. Disruption of this VAP-ACBD5 tether was shown to interfere with peroxisomal membrane expansion as well as cellular plasmalogen and cholesterol levels, suggesting the importance of this tether in lipid transfer between the two organelles. Overall, my work provides new insights into the mechanisms for protein and lipid exchange between the ER and peroxisomes. Collectively, the results presented here highlight the importance of the ER for peroxisome growth and functions.

Acknowledgements

This thesis was completed with the generous support from a lot of people. First, I would like to thank my supervisor, Dr. Peter Kim, who I have been working with since I was still an undergraduate student. His passion for science, motivation, and knowledge inspired me to join the lab. Over the past 8 years, Peter has been a great mentor who not only guided me scientifically to complete this project, but also helped me to improve both my writing and presentation skills. I also would like to express my sincere thanks to my committee members, Dr. David Williams and Dr. William Trimble, for their insightful comments and encouragement. I could not have imagined having a better supervisory committee for my PhD study.

I would also like to express my profound gratitude to all the past and present members in the Kim lab. A very special gratitude to Liz, who taught me cloning and many other techniques in the lab, and to Sasha and Derrick, who provide a helping hand in completing the two manuscripts.

A very special gratitude goes out to all the collaborators for their unfailing support and assistance, especially Étienne and Joel.

I am grateful to my parents who have provided me with moral and emotional support in my life. I am also grateful to my other family members and friends who have supported me along the way. With a special mention to my best friends, Li Qi and Ami.

Thanks for all your encouragement!

Table of Contents

List of Figures

List of Tables

List of Abbreviations and Acronyms

a.a.	Amino acid
ALS	Amyotrophic lateral sclerosis
A. thaliana	Arabidopsis thaliana
Cer	Cerulean
Ctrl	Control
DLP1	Dynamin like protein 1
EM	Electron microscopy
ER	Endoplasmic reticulum
FIS1	Fission 1
H. polymorpha	*H. polymorpha*
MCS	Membrane contact site
MFF	Mitochondrial fission factor
OMP25	Outer membrane protein 25
ORF	Open reading frame
PBD	Peroxisomal biogenesis disorder
PMP	Peroxisomal membrane protein
PPAR	Peroxisome proliferator activated receptor
PPV	Preperoxisomal vesicle
PTS	Peroxisomal targeting sequence
P. pastoris	*Pichia pastoris*
S. cerevisiae	*Saccharomyces cerevisiae*
SMA	Spinal muscular atrophy
TAG	Triacylglycerol
TM	Transmembrane
UB	Ubiquitin
UPR	Unfolded protein response
VLCFA	Very long chain fatty acid
Y. lipolytica	*Yarrowia lipolytica*

Chapter 1

Introduction

Part of this chapter is adapted from a review originally published as:

- Hua R., and Kim P.K. 2016. Multiple paths to peroxisomes: Mechanism of peroxisome maintenance in mammals. *Biochim Biophys Acta*. 1863(5): 881-891.

1.1 Overview

Peroxisomes are single membrane-bound organelles found in virtually all eukaryotic organisms. Their matrix encloses at least 50 different enzymes associated with various metabolic functions depending on species, cell types, and environmental stimuli. In mammalian cells, peroxisomes are mainly responsible for β-oxidation of very long chain fatty acids (VLCFA), detoxification of hydrogen peroxide, as well as the biosynthesis of bile acids and ether lipids, such as plasmalogens (1-3). The importance of these catabolic and anabolic reactions is best illustrated by a group of genetically heterogeneous metabolic diseases known collectively as the peroxisomal disorders, resulting from genetic defects in peroxisomal enzymes, or peroxins, which are the proteins required for their formation (4).

Peroxisomes can rapidly increase in size and number to adapt to various cellular stimuli. In mammalian cells, peroxisome proliferation is induced by the activation of a group of nuclear receptors called peroxisome-proliferator-activated receptors (PPAR) that act as lipid sensors and modulate the expression of genes associated with lipid metabolism, including genes involved in peroxisome proliferation (5-8). Genetic and proteomic screens in yeast (9) and mutated Chinese hamster ovary (CHO) cells (10) with defects in peroxisome number have led to the identification of 32 yeast genes and 13 mammalian genes, termed PEXs encoding peroxins that are required for the formation of peroxisomes (11-13). Mutation in any of these PEX genes leads to the development of a group of inheritable diseases known as the peroxisomal biogenesis disorders (PBDs). Defects in most of these peroxins result in membrane structures commonly called ‘peroxisomal membrane ghosts’ that are devoid of matrix proteins (14), reflecting that most of these peroxins are involved in the import of peroxisomal matrix proteins into peroxisomes. However, deletions or non-functional mutations in mammalian PEX3, PEX16, or PEX19 (15-22), and Pex3p or Pex19p in yeast result in the complete disappearance of peroxisomal membrane structures (23, 24), implying that these peroxins are required in the early stages of peroxisome biogenesis. Other proteins that were not initially identified as peroxins and later shown to act on peroxisome maintenance are dynamin-like protein 1 (DLP1/Drp1) (25-28), fission 1 (FIS1) (29, 30), and mitochondrial fission factor (MFF) (31-34). These proteins cooperate with the PEX11 family to mediate the fission of peroxisomes (13).

Like any other organelles, peroxisomes need to interact and communicate with their surroundings or other intracellular compartments to coordinate and balance their metabolic functions. Functional interplay between organelles can be achieved by numerous mechanisms including vesicular transport and signal transduction pathways (i.e., exchange of signaling molecules or metabolites). Moreover, it is becoming evident in the last few years that a common way of intracellular communication is via the membrane contact site (MCS) where the opposing membranes of two organelles are tethered in close proximity (within 30 nm), thus allowing for the exchange of molecules and signals between them (35, 36). Electron micrographs of peroxisomes from various species have demonstrated that peroxisomal membranes are found juxtaposed to other organelles, especially the endoplasmic reticulum (ER) (37, 38). Peroxisomes are not only found proximal to the ER, but also they are surrounded by lamellar-like structures that appear to be continuous with rough ER (39), suggesting that contact sites may form between the two organelles. Over the years, it became apparent that the ER plays a role in peroxisome biogenesis even though its contribution varies in species and conditions, as the ER serves as sources for both lipids and proteins for peroxisome growth (40). Another aspect of cooperation between peroxisomes and the ER is to facilitate lipid-related metabolic pathways including the biosynthesis of ether phospholipids, cholesterol, and bile acids (37). The synthesis of these specialized lipids is initiated in peroxisomes, and completed in the ER following the transport of the lipids precursors from peroxisomes to the ER (41, 42).

Despite the long-held evidence for ER-peroxisome communication, the understanding of its molecular basis is very limited. How proteins and lipids are trafficked between the two organelles is not fully understood. The existence of physical contact between peroxisomes and the ER has been demonstrated in a number of yeast (43-45), however, whether such *bona fide* contact sites are present in mammalian cells is not known. The molecular components and physiological importance of these contact sites also remain to be identified.

1.2 Origin of mammalian peroxisomes

1.2.1 Historical model

Peroxisomes were first observed in mouse renal cells by J. Rhodin using electron microscopy

in 1954 (46) and by W. Bernhard & C. Rouiller in rat liver in 1956 (47). At that time, peroxisomes were referred as “microbodies” which is a morphological term used for describing a single-membrane bound subcellular structure with a diameter between 0.2 to 1.0 μm. The term “peroxisome” was first introduced in 1966 by C. de Duve & P. Baudhuin who isolated peroxisomes from rat liver and demonstrated that the peroxisomal matrix contains an oxidase that produces H_2O_2, as well as catalase, which is a H_2O_2-decomposing enzyme (48). In this early characterization of peroxisomes, several electron micrographs published during the early 1960s were interpreted as showing peroxisomes in close juxtaposition with the ER (49, 50). In addition, catalase had been reported to be present in the microsomal fraction of rat liver by T. Higashi & T. Jr. Peters in 1963 (51). Taken together, C. de Duve & P. Baudhuin proposed in their early review that peroxisomes formed by budding from the ER (48). This hypothesis was further supported by several subsequent electron micrographs showing that peroxisomes were surrounded by and continuous with the smooth ER in both pig intestinal cells and mouse hepatocytes (52, 53).

1.2.2 Discovery of growth and division model

In the mid 1980s, Paul B. Lazarow and Yukio Fujiki challenged the concept of ER budding with the introduction of the “growth and division” model (54). According to this model, peroxisomes are autonomous organelles, like mitochondria and chloroplasts, which proliferate by the fission of pre-existing peroxisomes. This postulation was based on a seminal finding that peroxisomal matrix and membrane proteins were synthesized on free polyribosomes in the cytosol and then imported post-translationally into peroxisomes (54-58). Supporting this view, it was discovered that the peroxisomal matrix proteins contain peroxisomal targeting signals (PTS) that are necessary and sufficient for the direct targeting of these proteins into the peroxisomal matrix (59, 60). By analogy to protein import into mitochondria and chloroplasts, peroxisomes were therefore considered as autonomous organelles that are derived from pre-existing ones from division, i.e., not *de novo*.

Today, we know that most peroxisomal matrix proteins contain one of the two peroxisomal targeting signals, i.e., PTS1 or PTS2, that is recognized by the soluble receptor PEX5 or PEX7 respectively (61, 62). The cargo-loaded receptors will target directly to peroxisomes

via their interaction with the docking complex at the peroxisomal membranes. After being translocated across the membranes, the cargo is then released into the matrix of the peroxisome and the receptor is recycled back to the cytosol (11, 62-64). Peroxisomal membrane proteins (PMPs), on the other hand, contain the integral membrane targeting sequences (mPTS), which typically consist of a transmembrane (TM) domain flanked by charged residues on either side (63, 65-67). These mPTSs are recognized by the cytosolic chaperone PEX19 that guides the PMPs to peroxisomal membranes via its interaction with the docking factor PEX3 (68-70).

The growth and division of peroxisomes is mediated by components of the elongation and fission machinery, including the PEX11 family, dynamin like protein 1 (DLP1/Drp1), MFF and fission 1 (FIS1) (25-28). During peroxisome proliferation, the PEX11 family proteins mediate the protrusion of peroxisomal membranes and recruit both FIS1 and MFF to the site of membrane elongation. FIS1/MFF then recruits cytosolic DLP1 to its site of action and cooperate with it to mediate the final scission of the peroxisomal membranes (25, 29, 30, 33, 71).

1.2.3 Remerge of the ER in peroxisome biogenesis

In the last 20 years, the concept that the ER acts as a contributor for peroxisome biogenesis has experienced renewed enthusiasm. A common notion for the “growth and division” model is that new peroxisomes can only be formed from pre-existing peroxisomes. The view that peroxisomes multiply solely by growth and division was challenged by the fact that peroxisomes can form *de novo* in peroxisome-deficient cells that lack pre-existing peroxisomes upon re-introduction of the wild-type peroxin. The three peroxins that have been identified to be essential for peroxisomal membrane biogenesis in mammalian cells are PEX3, PEX16, and PEX19 (15-22). Peroxisomal membrane ghosts are completely absent in the fibroblasts from Zellweger syndrome patients with deletion or non-functional mutation in any of the three genes (15-22). Upon re-introduction of the gene encoding the corresponding wild-type peroxin, peroxisomal membrane structures could be detected within a short time frame, followed by the restoration of peroxisomal matrix protein import (15-22). This observation raises the possibility that peroxisomes could be formed from yet-to-be-identified

pre-peroxisomal structures or be derived from other organelles. In fact, several studies in yeast have discovered the existence of such small pre-peroxisomal vesicles that carry PMPs or even matrix proteins. The discovery of pre-peroxisomal vesicles was first reported in *Y. lipolytica* in which six distinct vesicle pools, designated P1 to P6, were identified and purified (72). The fusion of P1 and P2 *in vitro* was shown to require two peroxisomal AAA ATPases, Pex1p and Pex6p, resulting in the formation of a larger and more dense vesicle type (P3). The P3 vesicles were thought to gradually import matrix proteins (P4 and P5), and eventually mature into a newly formed peroxisome (P6). More recently, these preperoxisomal vesicles were further characterized into two biochemically distinct pools (73). In yeast *S. cerevisiae*, two distinct populations of preperoxisomal vesicles that each carry half a peroxisomal translocon complex (i.e., the docking or RING complex) were shown to bud from the ER. These preperoxisomal vesicles did not fuse with pre-existing peroxisomes, but instead, undergo heterotypic fusion, leading to the formation of new peroxisomes. The existence of these pre-peroxisomal structures has also been demonstrated in *H. polymorpha* where the lack of Pex3p and a key autophagy factor Atg1 resulted in the accumulation of reticular and vesicular structures that contain a selective group of peroxins (74). It was argued that these pre-peroxisomal structures were previously missed as they are rapidly degraded via autophagy (74).

What remains unclear is whether similar structures exist in mammalian cells and whether the ER is the source of these pre-peroxisomal structures. However, a number of studies have pointed to the ER as a potential contributor for the *de novo* formation of mammalian peroxisomes. Electron microscopy and 3D image reconstruction from EM tomography of peroxisomal structures in mouse dendritic cells revealed that peroxisomes are surrounded by lamellar-like structures that are enriched with integral membrane proteins PEX3 and PMP70 (39). These lamellar extensions appeared to be continuous with rough ER (39). Similar double-membrane structures that were associated with the ER were also observed in CHO cells deficient in PEX6, a component of the peroxisomal AAA ATPase that acts to remove ubiquitinated peroxisomal proteins (75). However, unlike the lamellar-like structures, these double-membrane structures were found to form looped structures surrounding spherical bodies (75). Similar structures were also observed in the hepatocytes of PEX5 knockout mice (76).

A number of mammalian peroxisomal membrane proteins have also been shown to traffic to peroxisomes through the ER, including PEX16, which is involved in the early stages of peroxisome biogenesis (77-79). When being exogenously expressed, PEX16 is localized to the ER in both *pex19*- and *pex3*-deficient human fibroblast cells, which do not contain any peroxisomal structures, as well as in COS7 cells (77). *In vitro* membrane targeting assays showed that PEX16 targeted to the ER co-translationally, suggesting that PEX16 could target directly to the ER presumably by the SRP pathway (77). Using time-lapse imaging combined with PEX16 tagged with a photoconvertible fluorescent protein, PEX16 was shown to be able to traffic from the ER to pre-existing peroxisomes (77-79). Similarly, PEX3 tagged with a *bona fide* SRP-recognized ER targeting sequence not only targeted to pre-existing peroxisomes, but also was able to complement *pex3*-deficient cells (78, 80). Given the number of peroxisomal membrane proteins that were demonstrated to target to the ER in both yeast and mammals, the ER is likely the membrane source for these pre-peroxisomal structures.

Taken together, it is now clear that peroxisomes can form *de novo* from the ER, although the mechanism of pre-peroxisomal vesicle/membrane formation from the ER is unclear. However, the formation is unlikely to be similar to vesicle formation from the ER exit sites which is involved in transporting proteins between the ER and Golgi apparatus, since the transport of PEX16 and other PMPs from the ER to peroxisomes was shown to be independent of COPI or COPII (81, 82). This observation has also been interpreted to suggest that peroxisomes are not derived from the ER, but instead formed from pre-peroxisomal structures derived from other sources (81, 83). Interestingly, Sec16B, a secretory scaffold protein that interacts with COPII components for the formation of ER exit sites, has recently been shown to be required for the transportation of PEX16 from the ER to peroxisomes, and the stabilization of PEX3 expression (84). Given that the inhibition of COPII does not affect peroxisome formation (81, 82), Sec16B likely cooperates with other coat or vesicle-forming factors to traffic the ER localized PMPs to peroxisomes, or to mediate the maturation of pre-peroxisomal structures into functional peroxisomes.

1.3 Peroxisomal membrane protein targeting

1.3.1 Targeting of peroxisomal membrane proteins

Functionally, PMPs can be divided into three groups: 1) the membrane modulating PMPs, which include the PEX11 family, FIS1 and MFF; 2) PMPs required for the import of matrix proteins (PEX13, PEX14, peroxisomal E3 ligases, and the peroxisomal AAA ATPase complex); and 3) the peroxisomal metabolite transporters (e.g., the ABCD family of transport proteins, and PMP34). The first two groups of PMPs are required for the formation and assembly of peroxisomes, while the third group is necessary for peroxisomal functions. As mentioned above, the recruitment of most if not all PMPs to membranes requires PEX3, PEX16, and PEX19, although it is not clear whether PEX16 works cooperatively with PEX3 and PEX19 or independently from them (79). In the absence of these genes, cells are devoid of any peroxisomal membrane structures, and other PMPs are either rapidly degraded or localized to the cytosol or other organelles, such as the mitochondria (15-19, 77). The current model for PMP targeting suggests that PMPs can be targeted to peroxisomes via two distinct but not mutually exclusive pathways: one via the ER (i.e., the indirect Group I pathway) and one from the cytosol (i.e., the direct Group II pathway) (85, 86).

Most PMPs are synthesized on free ribosomes in the cytosol and target post-translationally to peroxisomes (57, 87-90). These PMPs usually contain the so-called class I mPTS (mPTS1) which serves as a binding site for PEX19 (70, 91). PEX19 acts as a soluble receptor that binds to the mPTS1 of the newly synthesized PMPs and stabilizes them in a soluble state in the cytosol (18, 91-93). The cargo-loaded PEX19 complex is then guided to peroxisomal membranes via the direct interaction between PEX19 and the docking factor, PEX3 (70, 94, 95) (Fig. 1.1A). PEX3 itself is targeted post-translationally to peroxisomes by PEX19 though its interaction with PEX16 on the membranes (96) (Fig. 1.1B). On the other hand, PEX16 is proposed to contain a class I mPTS which targets it to peroxisomes by the PEX3-PEX19 complex (70, 91). This mutual import hypothesis raises the classic question of ‘the chicken or the egg’. However, as further discussed below, the role of the ER as a source of both membrane and a subset of PMPs for peroxisomes can address this conundrum.

The ER-to-peroxisomes targeting pathway has been described in multiple organisms, with

the most extensive work done in yeast. Pex2p and Pex16p in *Y. lipolytica* were shown to be core-glycosylated in the ER lumen and transported to peroxisomes in the glycosylated form (97). In *S. cerevisiae*, Henk Tabak's group has provided evidence that in both wild-type cells and peroxisome-less cells that are complemented with the corresponding full-length version of the mutant gene, a set of 16 PMPs are inserted into the ER first en route to peroxisome. This insertion of PMPs into the ER requires the ER translocator complexes, Sec61p or Get3p (98) (Fig. 1.1C). In the mammalian system, the ER targeting of PMPs is proposed to depend on PEX16 (77-79) (Fig. 1.1D). PEX16 is a PMP with dual localization, in both the ER and peroxisomes. Interestingly, in the yeast *Y. lipolytica*, the *PEX16* gene (YIPex16p) differs from its mammalian homolog in that it is a peripheral membrane protein located at the matrix side of peroxisomal membranes, and is required for the division of pre-existing peroxisomes (85, 99, 100). At the peroxisomal membranes, PEX16 is suggested to function as the membrane receptor for the direct targeting and insertion of PEX3 into peroxisomal membranes (96). When localized at the ER, PEX16 is able to recruit two other PMPs, PEX3 and PMP34, to the ER membranes from where they are subsequently transported to pre-existing peroxisomes (77-79). Moreover, by analyzing the kinetics of PMP trafficking to peroxisomes, we have previously shown that these PMPs target to peroxisomes via the ER in a PEX16-dependent manner, suggesting a potential function for PEX16 as a general PMP receptor at the ER (78). However, the precise role(s) that PEX16 plays in this ER-to-peroxisome protein targeting pathway remains unclear.

1.3.2 Targeting of mammalian PEX16

For the targeting of mammalian PEX16, there is some debate as to how PEX16 itself targets to peroxisomes (Fig. 1.2). For instance, by using yeast two-hybrid assays, Fransen et al. showed that the amino acids 59 to 219 of PEX16 bind to PEX19, which were thought to act as the mPTS for the targeting of PEX16 to peroxisomes (101). This result is consistent with the finding by the Fujiki group that the region (a.a. 1-140) that comprises the positively-charged amino acid cluster at position 66-81 and the adjacent transmembrane domain contains the necessary information for the peroxisomal targeting of PEX16 (102). A distinct mPTS in PEX16 was also reported to exist within the C-terminal half of the protein (a.a. 221-336) (70, 91). This region was shown to bind to PEX19 and its targeting to peroxisomes

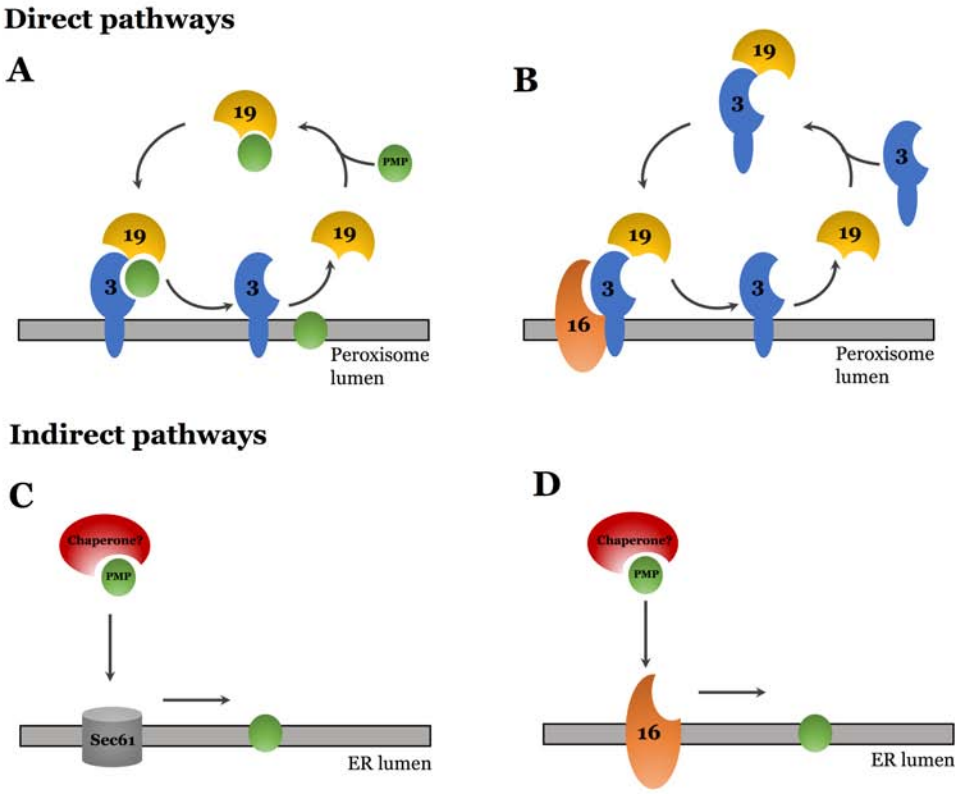

Figure 1.1 Models for PMP targeting. PMPs can be targeted to peroxisomes either directly from the cytosol (A-B) (i.e., the direct Group II pathway) or via the ER (C-D) (i.e., the indirect Group I pathway). (A) The main mechanism of direct PMP targeting to peroxisomes depends on PEX3 and PEX19. PEX19 acts as a soluble receptor that binds to the mPTS1 of the newly synthesized PMPs, stabilizes them in a soluble state in the cytosol. The cargo-loaded PEX19 complex will then be guided to peroxisomal membranes via the direct interaction between PEX19 and the docking factor, PEX3. (B) PEX3 itself is targeted post-translationally to peroxisomes by PEX19 though its interaction with PEX16 on the membranes in mammalian cells. (C) In the yeast *S. cerevisiae*, PMPs including Pex3p have been shown to be inserted into the ER first en route to peroxisomes. This insertion of PMPs into the ER requires the ER translocator complexes, Sec61p or Get3p. (D) In mammalian cells, the ER targeting of PMPs is proposed to depend on PEX16.

depended on PEX3 and PEX19 (70, 91), suggesting that PEX16 may target directly to peroxisomes in a PEX3- and PEX19-dependent manner with a C-terminal mPTS1. The above results contrast with the later finding that PEX16 is cotranslationally inserted to the ER in an *in vitro* targeting assay (77). Furthermore, results from a kinetic assay that measured the rate of import of PMPs to peroxisomes indicate that the peroxisomal import of PEX16 is slower than that of PEX3 and PMP34, but is more similar to a version of PEX3 that is "forced" to the ER by an appended signal sequence (78). Since it was proposed that the rate of import for the direct pathway is faster than that of the indirect pathway (via the ER), these results suggest that PEX16 follows the Group I pathway in which it is first inserted to the ER before routing to peroxisomes. Therefore, identification of targeting signals and/or other functional domains in PEX16 will shed light on the mechanism(s) in which PEX16 targets to peroxisomes as well as the roles that PEX16 serves in the PMP targeting pathway.

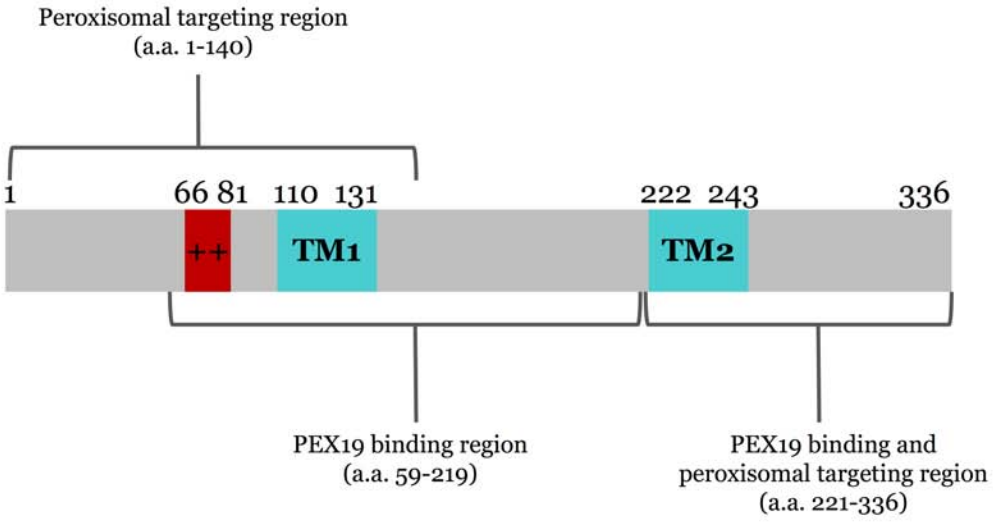

Figure 1.2 Domain architecture of mammalian PEX16. Full-length PEX16 is predicted to contain two transmembrane (TM) domains, TM1 and TM2, resulting in the protein being oriented in membranes with both of its N and C termini facing the cytosol. Two regions within the N-terminal half (a.a. 59-219 and 1-140) and a distinct region within the C-terminal half (a.a. 221-336) of the protein were purposed to act as the mPTS for the targeting of PEX16 to peroxisomes.

1.4 Peroxisomal lipid trafficking

1.4.1 General features of lipid transfer between organelles

Besides proteins, peroxisomes also need to exchange lipid molecules with the surroundings to regulate and balance their proliferation and cellular functions. For example, peroxisomes in all species lack most enzymes required for phospholipid biosynthesis, implying that the membrane lipids required for the enlargement of peroxisomal membrane during growth and division as well as during the maturation process of the pre-peroxisomal structures must be transferred from donor membranes of other organelles (103). Peroxisomes also need to exchange metabolites with other organelles, especially the mitochondria, for their metabolic functions such as β-oxidation of VLCFA and detoxification of hydrogen peroxide (1-3). However, how lipids are exchanged between peroxisomes and other organelles is not fully understood.

The asymmetrical distribution of lipid species inside the cell suggests that lipids need to be sorted between organelles. One of the common ways for intracellular lipid transfer is via the vesicular transport system in which lipids are shuttled together with proteins between organelles in the endomembrane system (36). Despite the rapid and perpetual membrane exchange between organelles via vesicular transport, organelles still maintain their unique lipid compositions for specific cellular functions, suggesting the existence of a highly regulated lipid sorting mechanism. Moreover, lipid transport has also been seen between organelles that are not connected with the vesicular transport system, such as mitochondria (104). Therefore, nonvesicular lipid trafficking through membrane contact sites (MCSs), which are the regions where membranes of two organelles are in close proximity (within 10-30 nm) (36), has been shown to be responsible for the transfer of specific lipids between the two opposing organelles.

Lipid exchange occurring at MCSs can be mediated by several mechanisms, one of which is that lipid monomers are transported between membranes by soluble lipid transport proteins (LTPs) (35, 104, 105). Many LTPs are known to function at the MCSs, as the short distance between the two opposing membranes helps to accelerate the rate of lipid transfer. According to their sequence and structural similarity, LTPs have been divided into several subfamilies,

but most of them contain a hydrophobic pocket that binds lipid monomers and often a lid domain that helps to shield the bound lipid from the aqueous environment (35, 104, 106). Many LTPs also contain domains that target them or facilitate their binding with the two opposing membranes at the MCS. For example, at ER-mitochondria MCSs, both the oxysterol binding protein (OSBP) and the ceramide transport protein CERT contain a FFAT domain that binds to the ER-resident VAP proteins, and a pleckstrin homology (PH) domain that interacts with the Golgi PI(4)P (see Section 1.5.1 for more detail) (107-109). Therefore, the simultaneous binding to both the ER and mitochondrial membranes allow these LTPs to facilitate lipid shuttling between the two membranes.

Lipid exchange at MCSs can also occur independent of LTPs. One such type of lipid transfer may be mediated by a hydrophobic channel or tunnel bridging the two membranes at a MCS (35). The synaptotagmin-like mitochondrial lipid-binding protein (SMP) domain has been proposed to possess the ability to form channels at MCSs (110). Another possible mechanism for lipid transfer at MCSs that does not require LTPs is via membrane hemifusion (35). Such hemifusion has been observed between peroxisomes and lipid droplets (LDs) in yeast (see Section 1.4.4 for more detail) (111) and between the ER and chloroplasts in plants (112), allowing for rapid exchange of large amounts of lipid and protein between the two cellular compartments. Whether membrane hemifusion also occurs at MCSs in the mammalian system is not known.

In summary, lipid exchange between various cellular compartments can be mediated by both the vesicular transport mechanism and nonvesicular mechanisms. The bulk transfer of lipids occurs when vesicles derived from the donor membrane fuse with the receiving membrane. On the other hand, specific lipid molecules can be transferred at MCSs between two compartments, either in a LTP-dependent manner or via hemifusion or channel formation between the two opposing membranes. The implications of various lipid sorting mechanisms for lipid transfer between peroxisomes and other organelles will be discussed in detail below.

1.4.2 Interplay between peroxisomes and the ER

As discussed earlier, it is now widely accepted that the ER contributes to the *de novo* biogenesis, growth and division of peroxisomes, as a subset of PMPs are delivered to

peroxisomes via the ER. However, the mechanism of such protein transport is still unclear. Moreover, since the ER is the major site of membrane lipid synthesis inside cells, another potential function of the ER for peroxisome biogenesis is to provide lipids to allow for the development of the peroxisomal endomembrane system. In the yeast *Y. lipolytica*, a specialized subcompartment of the ER has been suggested to act as a donor of phosphatidylcholine (PC) for the receptor membranes of the P3 and P4 peroxisomes that are in close opposition with the ER membranes (100). In plant cotton oilseeds, nonpolar lipids and PC required for glyoxysome (specialized peroxisomes in plants) enlargement during post-germinative seedling growth are supplied by ER-derived lipid bodies (113). Much of our knowledge about the phospholipid transfer between the ER and peroxisomes is gained from the studies done in yeast. Lipid transfer between the two organelles in the yeast *S. cerevisiae* was monitored by the conversion of phosphatidylserine (PtdSer) to phosphatidylethanolamine (PtdEtn) to phosphatidylcholine (PtdCho) (45). While all the enzymes required for this conversion were found in the ER, the enzyme required for the conversion of PtdSer to PtdEtn, phosphatidylserine decarboxylase (Psd), was specifically targeted to the peroxisomal matrix. By using this Psd assay, these authors demonstrated that phospholipids are able to move between the ER and peroxisomes, and this transfer of lipid is likely to be mediated by a nonvesicular pathway (45). Similar mechanisms may also be used to transport lipid metabolites, such as very long chain fatty acids (VLCFA), to peroxisomes for their metabolism, or lipid intermediates for the biosynthesis of specialized lipids such as plasmalogens, bile acids and cholesterol (1-3).

Although the mechanism of this nonvesicular transfer of lipids is not fully understood, it has been suggested that close contact (i.e., membrane contact sites) between the two organelles may be required for the transfer (114). This hypothesis is in line with the observation that extensive contacts between peroxisomes with the ER and lipid droplets were induced when yeast cells were shifted to oleic acid medium (111, 115). However, the specific function or mechanism of lipid transfer in mammalian cells is not yet known. Although close association between microperoxisomes and lipid droplets has been reported in mammalian white adipose tissues (116), whether the close contacts between these two organelles play a similar role in mammalian lipid transfer or if the same vesicular pathway that is involved in PMP trafficking is required for this process remains to be elucidated.

So far two protein complexes have been identified in yeast to mediate the tethering between peroxisomes and the ER. A large macromolecular complex involving the integral peroxisomal membrane protein Pex30p together with the ER reticulon proteins, Rnt1, Rnt2, and Yop1 has been suggested to facilitate the contact between the two organelles (44). The fact that Pex30p in the yeast *P. pastoris* localized to both the ER and peroxisomes support a role of this protein in the ER-peroxisome contact sites (43). In cells where the integrity of the cortical ER tubular network was disrupted by the deletion of these ER reticulons, peroxisome proliferation was largely affected, supporting an essential role of the ER in peroxisome maintenance. Interestingly, cells lacking either Pex30p or the reticulons showed an enhanced efficiency of *de nov*o peroxisome biogenesis, implying that the Pex30p complex negatively regulates this process. Therefore, these authors speculate that Pex30p is transported through the ER network and accumulates at specific subdomains on the cortical ER where it interacts with the ER reticulons to facilitate the formation of ER-to-peroxisome contact sites (EPCONS). These EPCONS bring the two organelles in close opposition and allow for the transfer of materials between them, thereby providing a platform for the formation of peroxisomes (44). In the budding yeast *S. cerevisiae*, the peroxisome inheritance is suggested to be regulated by a tethering complex consisting of Pex3p, the peroxisomal biogenic protein that localizes to both peroxisomes and the ER, and the peroxisome inheritance factor Inp1p (117). Inp1p acts as a molecular hinge between the ER-bound Pex3p and peroxisomal Pex3p, thereby tethering peroxisomes to the ER. Peroxisomes that are anchored to the ER by this Pex3p-Inp1p tether are retained in the mother cells. In cells lacking Inp1p, peroxisomes are found to accumulate in the daughter cells, reinforcing the importance of the ER-peroxisome tether in controlling peroxisome population. Furthermore, the authors also postulated that peroxisomes enriched for Inp2p are transported to the bud along microtubules via Myo2 (class V myosin motor protein 2) (117). However, no known homologue of Pex30p or Inp1p has been identified in mammalian cells, so whether similar tethers exist in mammals is not known.

In summary, although several tethering complexes have been identified in yeast, and a variety of cellular functions including peroxisome maturation, proliferation, inheritance, and exchange of molecules have been proposed for the close apposition (i.e., membrane contact

sites) between the ER and peroxisomes, the protein components of the tethers in mammalian cells and their physiological functions are still unclear.

1.4.3 Interplay between peroxisomes and mitochondria

Peroxisomes and mitochondria are two organelles that share many common characteristics and functions, and they cooperate closely with each other. For example, the pro-lipid metabolism nuclear receptors, PPARs, control the biogenesis of both organelles (5, 118-123). The β-oxidation of fatty acids occurs almost exclusively in these two organelles in mammalian cells. Peroxisomal β-oxidation acts as a chain-shortening system for very-long-chain (>20) fatty acids , and the shortened chains are transported subsequently via an unknown mechanism to mitochondria for complete breakdown (124). Given that mitochondria and the ER exchange lipids via their membrane contact sites (114), peroxisomes and mitochondria may also exchange lipids via a similar mechanism. Recently, peroxisomes in *S. cerevisiae* have been demonstrated to localize to specific mitochondrial subdomains such as ER-mitochondria junctions (ERMES) and the site of acetyl-CoA synthesis (125). Indeed, a tethering complex has been identified in yeast that consists of the integral peroxisomal membrane protein Pex11p that is involved in peroxisome elongation and fission, and the mitochondrial ERMES complex (126). The direct interaction between Pex11p and the ERMES protein Mdm34 was suggested to mediate the contact between peroxisomes and mitochondria (126). Interestingly, the Pex11p-Mdm34 interaction affects peroxisome morphology and Pex11p localization only in cells growing in the glucose-containing medium, but not in those growing in medium containing fatty acids but lacking glucose. Therefore, these authors speculate that Pex11p may act as a sensor of the metabolic state of the peroxisome matrix. In response to metabolic stimuli, Pex11p physically interacts with Mdm34 to tether peroxisomes to the mitochondria, allowing for the efficient transfer of metabolites between them, and thereby helps to maintain the cellular lipid homeostasis (126). In mammalian cells, the ATP binding cassette (ABC) transporter ABCD1 is suggested to be involved in the interaction between peroxisomes and mitochondria for the metabolism of very-long-chain (>22) fatty acids. The loss of this gene is associated with X-linked adrenoleukodystrophy (X-ALD). The elevated levels of VLCFAs seen in both X-ALD human and ALD mouse tissues are suggested to be attributed to reduced contact between

peroxisomes and mitochondria. In line with this, mitochondrial structural abnormalities were also observed in adrenal cortical cells of ALD mice (127). Further work needs to be done to identify the molecular components involved in this contact and to understand the underlying mechanism for the transfer of lipid molecules between the two organelles.

On the other hand, it is also possible that mitochondria and peroxisomes may exchange their lipid composition by vesicular transport. Recently, a novel vesicular trafficking pathway between these two organelles has been reported in the mammalian system (128). In this study, the McBride group demonstrated the existence of mitochondria-derived vesicles (MDVs) that contain a new outer-membrane mitochondria-anchored protein ligase (MAPL) in HeLa cells. These MDVs are 70-100 nm in diameter and fuse with a subpopulation (~10 % of total) of peroxisomes (128). Later on, the same group provided evidence that the transport of these MAPL-containing vesicles to peroxisomes requires the retromer complex Vps35/Vps26A (129). It is not surprising that mitochondria and peroxisomes may exchange lipids, as various membrane proteins are found to target and function in both organelles, especially the membrane modulating proteins such as MFF, FIS1 and DLP1 (130, 131). This being said, this pathway has only been described as unidirectional, as there is no evidence for the transport of vesicles from peroxisomes to mitochondria.

However, the functional and physiological significance of this MDV-mediated vesicular transport route to peroxisomes is not clear, since the content of the MAPL positive vesicles has not yet been identified (119). Given the functional similarities and the evidence for vesicular communication between the two organelles, is it plausible that mitochondria may contribute to the biogenesis of peroxisomes? Many mammalian PMPs have been observed on mitochondria in cells devoid of peroxisomes, or when over-expressed in cultured cells (15-19, 70, 77, 78). It is not clear whether the mitochondrial targeting of PMPs is a common mis-targeting artifact in the over-expression system or if the mitochondrial route of peroxisomal proteins naturally exists. Membrane proteins of both organelles are imported by a post-translational mechanism; therefore it is possible that overexpression of PMPs or the lack of peroxisomes may lead to the mis-targeting of PMPs to mitochondria. The similarity in their targeting mechanisms is best exemplified by a number of shared tail-anchored membrane proteins, such as MFF and FIS1 (29-34).

There is some evidence that peroxisomes may be able to form from mitochondria. The mammalian PEX3 readily targets to mitochondria in cells devoid of peroxisomes (70, 77, 78). The feasibility of the model that mitochondria may serve as a platform for the *de novo* biogenesis of peroxisomes was first demonstrated in the yeast *S. cerevisiae* (132). In this study, Pex3p was "forced" to target to mitochondria by an appended mitochondrial targeting signal from Tom20p. Upon introduction of mitochondrial Pex3p in *pex3p*-deficient cells, functional peroxisomes were successfully formed *de novo*, suggesting that mitochondria contain the essential machinery for the *de novo* biogenesis of peroxisomes. Recently, it has been reported that adenoviral expression of PEX3-YFP in human patient fibroblasts lacking PEX3 restores peroxisomal biogenesis in which PEX3 is found enriched within mitochondria-derived pre-peroxisomal structures (133). Moreover, by performing whole-cell fusion experiments using a *pex16* mutant human fibroblast cell line that expresses PEX3-YFP and a *pex3* mutant cell line that expresses PEX16-mRFP, the authors demonstrated that the ER-derived PEX16-positive structures fuse with PEX3 enrichments along mitochondria, followed by the release of a single structure from mitochondria (133). These results suggest a hybrid nature of newly formed peroxisomes and an important role of mitochondria in the *de novo* biogenesis of peroxisomes in mammalian cells (133). However, whether such heterotypic fusion between the ER-derived and mitochondria-derived vesicles also occurs in normal human cells is not known.

1.4.4 Interplay between peroxisomes and lipid droplets

Lipid droplets (LDs) are the lipid storage organelles found in all organisms due to their ability to accumulate neutral lipids such as triacylglycerols (TAGs) and cholesterol ester (134, 135). It is vital for cells to tightly regulate energy levels by balancing lipid storage and mobilization. Excessive storage of lipids will lead to metabolic diseases such as diabetes and obesity; while inability to store lipids as seen in diseases such as lipodystrophy is also detrimental to the health of humans. Rather than being a solely storage organelle, there is growing evidence supporting the multifunctional nature for LDs. The highly complex LD proteome suggests that LDs could interact with other organelles including the ER, peroxisomes, lysosomes, and mitochondria (134, 136). Therefore, LDs are not only involved

in lipid metabolism, but they are also implicated in protein degradation and pathogen replication (134, 137).

The close proximity between peroxisomes and LDs has long been seen in electron micrographs (138). Later, this interaction between the two organelles was confirmed in multiple organisms including the plant *A. thaliana* (139), mammalian COS7 cells (140) and the yeast *Y. lipolytica* (115). Since LDs are the site of storage for fatty acids, which are the substrates of peroxisomal β-oxidation, the connection between these two metabolic organelles was suggested to be associated with the link between lipolysis in LDs and β-oxidation of fatty acids in peroxisomes (111). Moreover, the fact that changes in LD morphology was observed in multiple organisms where peroxisome biogenesis and/or functions are impaired reinforces a connection between them. For example, LDs were shown to accumulate in mouse hepatocytes that lacking peroxisomes (141). Enlarged LDs were observed in the nematode *C. elegans* in which peroxisomal β-oxidation activity was impaired (142).

However, the underlying molecular mechanism(s) of peroxisome-LD communication is still unclear. By using a biomolecular fluorescence complementation assay, an interaction map of protein-protein contacts of LDs with mitochondria and peroxisomes has been generated in *S. cerevisiae*. The LD proteins Erg6 and Pet10 were found to be involved in 75 % of all interactions detected, including some with peroxisomal proteins (143). However, further experiments need to performed to validate these interactions between the LD and peroxisomal proteins. Whether these proteins could serve as a tether between the two organelles and their physiological functions are interesting questions to be uncovered. In *S. cerevisiae* that were growing in oleate culture, peroxisomes were not only found to tightly bound to LDs, but they also penetrated them. The extensions of peroxisomes, termed pexopodia, extended into the core of LDs, as a result of hemifusion between the single leaflet of the LD membrane and the outer leaflet of the peroxisomal membrane. Furthermore, proteomic analysis of purified LDs showed that pexopodia and LD inclusions are enriched for enzymes of fatty acid β-oxidation, Therefore, these authors speculated that the interaction between LDs and peroxisomes mediated by pexopodia allows the direct contact between the inner peroxisomal leaflet with the LD core, thereby facilitating the transfer of fatty acids

from LDs to peroxisomes for β-oxidation (111). However, whether the formation of these peroxisome protrusions represents a common means of peroxisome-LD lipid exchange in other organisms is not known.

Remarkably, proteins can also be transferred between peroxisomes and LDs. The *A. thaliana* Sugar-Dependent 1 (SPD1), a major TAG lipase involved in lipid reserve mobilization during seeding establishment in plants, has been reported to initially localize to peroxisomes and then migrate to LDs during the course of seedling growth. The authors also demonstrated that the translocation of SPD1 from peroxisomes to LDs is mediated by peroxisomal tubular extensions and requires a functional core retromer complex (144). Recently, the two peroxisomal biogenesis factors, PEX3 and PEX19, were suggested to be involved in the insertion of the UBXD8, a hairpin-protein localized to both the ER and LDs, into the cytoplasmic leaflet of the ER bilayer. Based on their findings that the peroxisomal membrane proteins and LD-destined hairpin proteins share the same targeting machinery, these authors propose a coordinated relationship between peroxisomes and LDs in the ER (145). This mutual control for both peroxisome and LD biogenesis allows the cell to tightly regulate and balance energy levels in response to metabolic stimuli.

1.4.5 Interplay between peroxisomes and lysosomes

For a long time, the studies on the interaction between peroxisomes and lysosomes were mainly focused on pexophagy in which peroxisomes are selectively degraded in lysosomes via a process called autophagy. However, recently a novel peroxisome-lysosome contact site (termed LPMC) was identified in mammals, and its role in cholesterol transport has been suggested (146). Cholesterol is an important lipid that plays diverse functions in eukaryotic cells. After being synthesized in the ER, it is transported to various intracellular compartments with the majority (~60-80 %) ending up in the plasma membrane (PM) (147). Besides *de novo* biosynthesis in the ER, mammalian cells also acquire exogenous cholesterol through receptor-mediated endocytosis of plasma low density lipoprotein (LDL) (148, 149). After receptor binding and internalization, the LDL-derived cholesteryl esters undergo hydrolysis by acid lipases and the resulting free cholesterol emerges in the late endosome/lysosome from where it is further transported to various cellular compartments

including the ER, PM, and mitochondria (149). However, the mechanism underlying the transport of cholesterol from lysosomes to various downstream organelles is not well documented. By using a genome-wide pooled shRNA screen for delayed LDL-cholesterol transport, B.B. Chu and colleagues identified 341 hits that included 10 peroxisomal genes. A tether that consists of the lysosomal membrane protein synaptotagmin VII (Syt7) and $PI(4,5)P_2$ on the peroxisomal membrane was shown to bring the two organelles in close apposition. By using an *in vitro* reconstitution assay and confocal microscopy in HeLa cells, the authors also demonstrated that cholesterol can be transported from lysosomes to peroxisomes though LPMC. In line with this, accumulation of cholesterol was observed in cultured fibroblasts of patients with peroxisomal disorders including X-ALD, Infantile Refsum disease (IRD) and Zellweger syndrome (ZS). Therefore, the authors speculate that cholesterol transport from lysosomes to peroxisomes through LPMS could serve as a potential mechanism for cholesterol efflux from lysosomes (146). After reaching peroxisomes, it is not known whether the LDL-cholesterol is further processed in peroxisomes or it is subsequently transported to other organelles. Further studies are needed to uncover the precise role(s) of LPMS and/or peroxisomes in cholesterol transport.

1.5 Proteins in ER contact sites

Most of our current knowledge about membrane contact sites was gained from the studies on the contact between the ER and other organelles. Within the cell, the ER is a large, interconnected organelle that spreads throughout the cytoplasm and performs multiple functions including biosynthesis of proteins and lipids and regulation of intracellular calcium levels. In order to perform and regulate various cellular functions, the ER needs to cooperate with other organelles including peroxisomes. One of the most common ways for the ER to interact with other organelles is to establish membrane contact sites (MCSs) with them. Indeed, the ER has been found in close opposition with almost all membrane-bound organelles, such as the PM, endosomes, peroxisomes, LDs, Golgi and mitochondria (150). The hallmark of MCSs is that the two organelles are brought into close proximity by a tether that is either a protein or a complex of proteins (35). One group of such proteins that has been implicated in ER contact sites are VAMP-associated proteins A and B (VAPA and VAPB).

1.5.1 VAPs in ER contact sites

The VAPs are highly conserved ER-resident proteins expressed in all eukaryotes. In addition to their ER localization, they are also found in multiple membrane compartments, including the Golgi, Golgi-ER intermediate compartment (107, 151, 152), late endosomes (153, 154), mitochondria (155), and the PM (156). Indeed, VAPs have been shown to play important roles at the contact sites between the ER and these organelles.

Mammalian VAPA and VAPB share 63 % sequence similarity and both contain three conserved domains: an N-terminal 7-β strand globular domain in the major sperm protein (MSP) family, a coiled-coil linker region, and a C-terminal TM helix tail that inserts into the ER membrane (157). Much of our knowledge about VAP functions was obtained from the identification of VAP-interacting proteins. Among all VAP-interacting proteins identified so far, the group of proteins that is most well documented and studied is the FFAT (two phenylalanines in an acidic tract)-motif-containing proteins (158, 159). Indeed, many VAP-interacting FFAT proteins have known functions in lipid binding, lipid sensing, and lipid transport, suggesting an important role of these VAP-mediated MCSs in nonvesicular transfer of lipids between organelles (160). At the ER-Golgi contact site, VAPA has been shown to interact with oxysterol binding protein (OSBP) that contains a FFAT domain, a pleckstrin homology (PH) domain that interacts with the Golgi PI(4)P, and a lipid binding domain (ORD). The interaction between VAPA and OSBP allows the tethering between the ER and Golgi, thereby facilitating the transfer of sterols between the two organelles (107). Another tether at ER-Golgi contact sites is mediated by the interaction between VAPA and the ceramide transport protein CERT. CERT contains multiple functional domains that allow it to be associated with the Golgi membrane (via its PH domain that binds to Golgi PI(4)P), bind to ER-resident VAPA (via its FFAT motif), and catalyze the intermembrane transfer of ceramides (via its steroidogenic acute regulatory protein-related (START) domain). These VAP-CERT mediated contact sites function to facilitate the transfer of ceramide from the ER to the *trans*-Golgi region for the synthesis of sphingomyelin (108, 109). By monitoring sterol transport from the PM to the two acceptor compartments, the ER and LDs, M. Jansen and colleagues suggested that the ER is an intermediate station in sterol PM-LD delivery; and the sterol transfer from the PM to the ER is indeed facilitated by the interaction between VAPs

and the FFAT motif-containing ORPs (i.e., ORP1S and ORP2) (161). Moreover, VAPA has also been shown to interact with the cholesterol-sensing protein ORP1L. This interaction induces the formation of ER-late endosome contact sites, thereby allowing VAPA to interact in trans with the Rab7-RILP receptor to regulate late endosome positioning in response to cholesterol level changes (154). VAPB is also able to interact with the outer mitochondrial membrane protein, protein tyrosine phosphatase-interacting protein 51(PTPIP51), to bridge the contact between the ER and mitochondria. The tethering between the two organelles allows for the uptake of Ca^{2+} by mitochondria following release from ER stores (155).

Besides functioning at the ER contact sites, VAPB has also been implicated in a variety of other cellular processes. For example, expression of wild-type VAPB was demonstrated to induce ER stress and promote the unfolded protein response (UPR) via activating the IRE1/XBP1 pathways (162, 163). Also there is evidence suggesting that the MSP domain of VAPB can be cleaved, secreted and act as a diffusible hormone for Eph receptors (164).

In summary, VAPs are found in various subdomains throughout the ER network, where they interact with FFAT-motif-containing proteins in the membranes of the opposing organelles, thereby tethering them. However, whether VAPs also localize to ER-peroxisome contact sites and what their potential function(s) might be at these contact sites have not yet been examined, although the two organelles are always seen in close proximity with each other.

1.5.2 VAPB in ALS

As discussed above, VAPs play multiple vital functions inside the cell. A proline-to-serine substitution at position 56 (P56S) in the MSP domain of VAPB is associated with rare motor neuron diseases, late-onset Spinal Muscular Atrophy (SMA) and Amyotrophic Lateral Sclerosis-type 8 (ALS8) (165). ALS is the most common adult-onset neuron disease caused by degeneration of upper and lower motor neurons, accompanied by progressive weakness, muscle atrophy, and various cognitive and behavioral dysfunctions (166). However, it is still a matter of debate as to how this ALS-linked mutation in VAPB leads to neurodegeneration and muscle wasting in patients.

Like many other neurodegenerative diseases, VAPB(P56S) forms insoluble aggregates that sequester wild-type VAPA and VAPB (163, 167). Over-expression of either the wild-type or mutant VAPB(P56S) in primary motoneurons by an Adeno-associated viral vector was shown to impair intracellular Ca^{2+} homeostasis and induce ER stress that leads to the activation of IRE1, thereby triggering the selective death of cultured motoneurons. Calpains and caspase 12 and 3 were also shown to be involved in this Ca^{2+}-sensitive, ER-derived cell death. Therefore, the authors speculated that the aberrant Ca^{2+} levels and ER-derived (i.e., the unfolded protein response, UPR) death pathways are implicated in the degenerative process of motoneurons expressing the ALS-associated VAPB mutant, implying a gain-of-function mechanism for the VAPB(P56S)-induced ALS (168). However, an opposite effect of VAPB(P56S) on UPR activity was presented in several other studies. Over-expression of wild-type or mutant VAPB in HEK293 cells was shown to inhibit ATF6-regulated transcription that serves as a sensor/transducer of the UPR (169). Over-expression of wild-type VAPB in the motor neural NSC34 cells was shown to induce UPR, but not the P56S mutant; thereby the authors speculate that the P56S mutant reduces the wild-type VAPB function (i.e., the UPR activation) by sequestering it in insoluble aggregates (162). Interestingly, overexpression of wild-type or mutant VAPB in transgenic mice does not cause motor neuron dysfunction or degeneration. In the VAPB mutant transgenic line, no typical ALS pathology, ER structural change, or coaggregation with VAPA was detected. Furthermore, overexpression of wild-type or mutant VAPB does not modulate the course of the ALS in the SOD1G93A (i.e., a mutation in Cu/Zn superoxide dismutase-1 that is linked to ALS) mice (170), implying that VPAB has no significant effect on the development of ALS that is not associated with VAPB mutant. Therefore, a loss-of-function mechanism is proposed for the VAPB mutant-associated ALS (166).

Another possible linkage between VAPB(P56S) and neurodegeneration may be attributed to its involvement in ER contact sites. It has been shown that VAPB(P56S) displays an increased binding affinity to mitochondrial PTPIP51 as compared to wild-type VAPB, thereby inducing mitochondria clustering with the VAPB(P56S) aggregates. The enhanced interaction between the ER and mitochondria leads to an increase in Ca^{2+} uptake by mitochondria following release from the ER, resulting in the disruption of Ca^{2+} homeostasis inside cells (155). Therefore, the authors propose that damage to the ER, mitochondria, and

cellular Ca^{2+} homeostasis may all contribute to the development of ALS induced by the VAPB mutant. Since VAPB is found in multiple contact sites between the ER and other organelles, further studies are needed to examine whether the ALS-linked VAPB(P56S) mutant also causes damage to other organelles, and whether the dysfunction of these organelles has any relevance to ALS.

1.6 Rationale and Approach

Since their discovery in the early 1950s, peroxisomes have long been seen in close apposition with the ER. Yet, the functional relationship between these two organelles and the underlying molecular mechanism(s) remain unresolved. For my PhD thesis project, I aimed to uncover the mechanism(s) of the ER-to-peroxisome pathways in the mammalian system, and examine potential physiological functions mediated by the communication between the two organelles.

The functions for the interplay between the ER and peroxisomes can be grouped into two aspects: 1) peroxisome biogenesis as the ER was postulated to provide peroxisomes with both lipids and essential peroxisomal membrane proteins for its growth and maintenance; 2) metabolic pathways as enzymes for the biosynthesis of a number of specialized lipids are found in both the ER and peroxisomes, implying that lipid precursors may be exchanged between them. However, the mechanism(s) as to how lipids and proteins are transported between the two organelles is not fully understood. Although there is evidence suggesting that the peroxisomal biogenesis factor PEX16 may serve as a receptor for PMPs in the ER and also mediate the subsequent transport of these ER-targeted PMPs to peroxisomes, the precise role(s) that PEX16 serves in this process is still unclear. Therefore, in order to uncover the mechanism underlying the ER-to-peroxisome protein targeting pathway and especially the role that PEX16 plays in this process, I performed a comprehensive mutational analysis of human PEX16 in order to identify and characterize the targeting signals responsible for its initial sorting to the ER and then from the ER to peroxisomes, as well as the domain responsible for its PMP recruitment function. Furthermore, whether the ability of PEX16 to recruit PMPs to the ER is conserved among evolutionarily diverse organisms was also tested. The implications of these results in terms of the roles of PEX16 in the

maintenance of peroxisomes from the ER are discussed (Chapter 3).

On the other hand, a widespread mechanism for selective transfer of lipids between organelles is via the membrane contact sites. As peroxisomes are always found in close proximity to the ER, it is possible that lipid exchange between the two organelles occurs at MCSs. However, despite the fact that two ER-peroxisome tethering complexes have been identified in yeast, it is not known whether such a *bona fide* contact site exists in mammals. Here, I conducted the BioID analysis on PEX16 to search for proteins that may be involved in mediating the ER-peroxisome contact. A group of candidate proteins that are implicated in ER contact sites with many other organelles were identified in the screen. The ability of these candidate proteins to act as a tether between the ER and peroxisomes was tested and the potential physiological functions of this contact were examined. I identified a novel tether between the ER and peroxisomes in mammalian cells that consists of the ER-resident VAPs and peroxisomal ACBD5. I also provided evidence supporting the importance of this VAP-ACBD5 tether for peroxisome biogenesis and cellular lipid homeostasis (Chapter 4).

Overall, the implication of these results in peroxisome biogenesis and membrane contact sites between organelles is discussed. By taking together recent novel findings, a model for peroxisome maintenance in the mammalian system is proposed (Chapter 5).

Chapter 2

Materials and Methods

Part of this chapter is adapted from articles originally published as:

- Hua R., Gidda S.K., Aranovich R.T., Mullen R.T., Kim P.K. 2015. Multiple Domains in PEX16 Mediate its Trafficking and Recruitment of Peroxisomal Proteins to the ER. *Traffic*. 16: 832-852.
- Hua R., Cheng D., Coyaud É., Freeman S., Pietro E.D., Wang Y., Vissa A., Yip C.M., Fairn G.D., Braverman N., Brumell J.H., Trimble W.S., Raught B., Kim P.K. 2017. VAPs and ACBD5 tether peroxisomes to the ER for peroxisome maintenance and lipid homeostasis. *Journal of Cell Biology*. 216(2):367-377.

2.1 Plasmids and siRNA

PEX16-GFP, PEX16NT-GFP, PEX16(Δ66-81)-GFP, saPEX16-GFP, UB-RFP-SKL, ssGFP-KDEL and ssRFP-KDEL have been described previously (77). All other PEX16 mutant constructs used were generated using standard recombinant DNA procedures and were verified by automated sequencing at the Centre for Applied Genomics. Oligonucleotides were produced by Sigma-Genosys. Mutagenesis was carried out using appropriate forward and reverse mutagenic primers and polymerase chain reaction (PCR)-based mutagenesis protocols.

Cer-PEX26$_{TM}$, which is a chimera of mCerulean (Cer) fused to the C-terminal portion of human PEX26 (a.a. 135–269), was constructed in two steps. First, the human PEX26 open reading frame (ORF) from pSPORT-PEX26 (Invitrogen) was subcloned into the *Eco*RI and *Sal*I sites of mCerulean-C1 (Invitrogen). Second, the PEX26 ORF was truncated using PCR-based site-directed mutagenesis. PEX11β-Cer was generated by subcloning the human PEX11β ORF from pOTB7-PEX11β (Invitrogen) into the *Eco*RI and *Sal*I sites of mCerulean-N1 (Invitrogen). PEX10-Cer was constructed in two steps. First, the human PEX10 ORF from pDONR223-PEX10 (SPARC BioCentre, Hospital for Sick Children) was subcloned into the *Xho*I and *Eco*RI sites of pEGFP-N1 (Invitrogen) to yield PEX10-GFP. Second, the PEX10 ORF was excised from PEX10-GFP by digestion with *Nhe*I and *Kpn*I and then ligated into the equivalent sites in mCerulean-N1 to yield PEX10-Cer. Fis1-Myc was described previously (171). Cer-OMP25$_{TM}$, which is a chimera of Cerulean and the C-terminal membrane targeting domain of the mitochondrial outer membrane protein 25 (OMP25), including its single TM domain, was generated by excising (via digestion with *Nhe*I and *Bsr*GI) the Cer ORF from mCerulean-C1. Thereafter, the resulting fragment was ligated into *Nhe*I and *Bsr*GI-digested EGFP-OMP25$_{TM}$ [provided by Dr R. Gupta (McMaster University)].

pET32a-Vamp1A was a kind gift from Dr. William S. Trimble (Hospital for Sick Children, Canada). The Vamp1A ORF was amplified by PCR and cloned into the *Bgl*II and *Sal*I sites of pEGFP-N1 to yield Vamp1A-GFP. saPEX16(1–109)-Vamp1A(TM)-GFP was constructed as follows. First, sequences corresponding to amino acid residues downstream of position

109 in PEX16 were removed from PEX16NT-GFP by PCR. Second, complementary annealed oligonucleotides encoding the C-terminal membrane targeting domain of Vamp1A, including its single TM domain (a.a 83–118), were inserted into the *Hind*III site of $PEX16_{1–109}$-GFP, yielding PEX16(1–109)-Vamp1A(TM)-GFP. PEX16(1–109)-Vamp1A(TM)-GFP was then excised by digestion with *Bgl*II and *Sal*I and ligated into the equivalent sites in saPEX16-GFP, yielding saPEX16(1–109)-Vamp1A(TM)-GFP.

Plant expression vectors encoding *Arabidopsis* PEX16 or modified versions thereof were generated as follows. AtPEX16-GFP was constructed by cloning the full-length PEX16 ORF (obtained by RACE-PCR using cDNA synthesized from *A. thaliana* suspension-cultured cell mRNA and the gene-specific primers) into *Nhe*I-digested pUC18-*Nhe*I-GFP (172). saAtPEX16-GFP was constructed in several steps. First, sequences encoding the tung tree (*Vernicia fordii*) ER membrane protein NADH:cytochrome b_5 reductase isoform 1A (CBR1A) (173) were amplified by PCR and subcloned into pUC18-MCS-GFP (172), yielding CBR1A-GFP. Second, a novel *Bgl*II site was introduced (via PCR-based mutagenesis) into CRB1A-GFP, immediately downstream of the CBR1A 21 amino-acid-long signal anchor sequence, and following digestion with *Bgl*II the vector was religated, yielding saGFP. Lastly, sequences encoding the AtPEX16 ORF were amplified along with *Bgl*II and *Nhe*I sites and then ligated into the equivalent sites in saGFP, yielding saAtPEX16-GFP. saPEX16(mut)GFP, whereby the amino acid sequence -RKYGRVS- in PEX16 responsible for its peroxisomal targeting was replaced with glycines (174), was generated using PCR-based mutagenesis and saPEX16-GFP as template. Myc-AtPEX3, encoding N-terminal Myc-epitopte-tagged *Arabidopsis* PEX3 was constructed by cloning the full-length PEX3 ORF (obtained by RACE-PCR using cDNA synthesized from *A. thaliana* suspension-cultured cell mRNA and the gene-specific primers) into *Xba*I and *Xma*I-digested pRTL2-Myc-MCS (172). PMP36-Myc, encoding C-terminal Myc-epitope-tagged *Arabidopsis* PMP36, was generated by subcloning the PMP36 ORF from pUNI51-PMP36 (Arabidopsis Biological Resource Center) into pRLT2/MCS-Myc (173). The human codon-optimized version of *Arabidopsis* PEX16 (At^{Hs}PEX16) was generated by GenScript and was based on the codons with the highest usage frequency for each amino acid in humans [GenScript Codon Usage Frequency Table (http://www.genscript. com/cgi-

bin/tools/codon_freq_table)]. The At^{Hs}PEX16 ORF was then cloned into the *Bgl*II and *Sal*I sites of pEGFP-N1 or saPEX16-GFP to yield At^{Hs}PEX16-GFP or saAt^{Hs}PEX16-GFP, respectively.

Myc-VAPA, and VAPB-GFP were kind gifts from Dr. William S. Trimble (Hospital for Sick Children, Canada). Myc-VAPB and Myc-VAPB(P56S) were kind gifts from Dr. Christopher C.J. Miller (King's College London, UK) (155). The FFAT-motif mutant ACBD5, Myc-VAPB(FFATmut), was generated in which all residues in its FFAT domain (a.a. 262-271) (157) were replaced by Ala. Mutagenesis was carried out using appropriate forward and reverse mutagenic primers and polymerase chain reaction (PCR)-based mutagenesis protocols. The ACBD5 ORF was purchased from SPARC BioCentre (SIDNET ID: 1004942), and cloned into the Myc-N1 vector by standard PCR-based methods.

siRNAs were all from Invitrogen. siRNA sequences were: siCtrl - AAUAAGGCUAUGAAGAGAUAC, siVAPA - GCGAAAUCCAUCGGAUAGAAA, siVAPB - GCUCUUGGCUCUGGUGGUUUU, siACBD5-1 (or simply refer as siACBD5) - GCACAGUGGUUGGUGUAUUUA, siACBD5-2 – CCGUUAAUGGUAAAGCUGAAA, siDLP1(Santa Cruz: sc-43732).

2.2 Mammalian cell culture and transfection

COS7, HEK293T, and HeLa cells were obtained from the American Type Culture Collection (ATCC). PBD400-T1 and PBD399-T1 cells were gifts from Dr. S. South (Johns Hopkins University). All cells were cultured in DMEM (Thermo Scientific HyClone) supplemented with 10 % fetal bovine serum (FBS; Gibco) and 2 mM L-glutamine (Thermo Scientific HyClone) at 37°C in humidified air containing 5 % CO_2. Plasmids and siRNAs were transfected using Lipofectamine-2000 (Invitrogen) according to the manufacturer's instructions. Prior to live-cell imaging, the medium was changed to CO_2-independent (Invitrogen) containing 10 % FBS and 2 mM L-glutamine.

2.3 Plant cell culture, transformation and processing for microscopy

Tobacco (*Nicotiana tabacum* cv Bright Yellow-2 [BY-2]) suspension cell cultures were maintained and prepared for transformation via biolistic particle bombardment as described previously (175). Bombarded cells were incubated for 4 or 8 h to allow for expression and sorting of the introduced gene product(s), then fixed in paraformaldehyde (Electron Microscopy Sciences), permeabilized using 0.1 % Triton X-100 (Fisher Scientific) in PBS, and incubated with the appropriate primary and secondary antibodies as previously described (175).

2.4 Co-immunoprecipitation and immunoblot analysis

For co-immunoprecipitation, transfected HEK293T cells were lysed in 1 mL lysis buffer (150 mM NaCl, 50 mM HEPES, 1% Triton X-100, 10% glycerol, 1.5 mM $MgCl_2$, 1.0 mM ethylene glycol-bis[β-aminoethyl ether]-N,N,N′,N′-tetraacetic acid) supplemented with protease inhibitors. For each immunoprecipitation, a 0.9 mL aliquot of the lysate was incubated with 0.9 µg of Myc antibody (EMD Millipore) and 378 µL of a 1:1 slurry of Protein G Sepharose (Bioshop) overnight. Sepharose beads were washed 3× with 1 mL high salt lysis buffer containing 0.5 M NaCl. The precipitates were analyzed by standard immunoblot procedures.

2.5 Biotin-streptavidin affinity purification

BioID (176) was carried out as previously described (177). Briefly, the full length human PEX16 coding sequence was amplified by PCR from MGC clone BC004356, and cloned with *AscI* and *NotI* restriction sites into pcDNA5 FRT/TO FLAGBirA* expression vector, and 293 T-REx Flp-In cells stably expressing FLAGBirA*-PEX16 were generated. After selection (DMEM + 10% FBS + 200 µg/ml Hygromycin B), 5 x 15 cm diameter plates of sub-confluent (60 %) cells were incubated for 24 hr in complete media supplemented with 1 µg/ml tetracycline (Sigma) and 50 µM biotin (BioShop). Cells were collected and pelleted (2,000 rpm, 3 min), the pellet was washed twice with PBS, and dried pellets were snap frozen. Cell pellets were resuspended in 10 mL of lysis buffer (50mM Tris-HCl pH7.5,

150mM NaCl, 1mM EDTA, 1mM EGTA, 1 % Triton X-100, 0.1 % SDS, 1:500 protease inhibitor cocktail (Sigma-Aldrich), 1:1000 benzonase nuclease (Novagen)) and incubated on an end-over-end rotator at 4°C for 1 hour, briefly sonicated to disrupt any visible aggregates, then centrifuged at 16,000 x g for 30 min at 4°C. Supernatant was transferred to a fresh 15 mL conical tube. 30 µL of packed, pre-equilibrated streptavidin sepharose beads (GE) were added and the mixture was incubated for 3 h at 4°C with end-over-end rotation. Beads were pelleted by centrifugation at 2000 rpm for 2 min and transferred with 1mL of lysis buffer to a fresh Eppendorf tube. Beads were washed once with 1 mL lysis buffer and twice with 1 mL of 50 mM ammonium bicarbonate (ammbic; pH=8.3), transferred in ammbic to a fresh Eppendorf tube and washed two more times with 1 mL ammbic. Washed beads were incubated with 1 µg MS grade TPCK trypsin (Promega, Madison, WI) dissolved in 200 µL of 50 mM ammbic (pH 8.3) overnight at 37°C. The following morning, 0.5µg MS-grade TPCK trypsin was added, and beads were incubated 2 additional hours at 37°C. Beads were pelleted by centrifugation at 2000g for 2 min, and the supernatant was transferred to a fresh Eppendorf tube. Beads were washed twice with 150 µL of 50 mM ammonium bicarbonate, and these washes were pooled with the first eluate. The sample was lyophilized, and resuspended in buffer A (0.1 % formic acid). One fifth of the sample was analyzed per MS run.

2.6 Mass spectrometry

Liquid chromatography analytical columns (75 µm inner diameter) and pre-columns (100 µm inner diameter) were made in-house from fused silica capillary tubing from InnovaQuartz (Phoenix, AZ) and packed with 100 Å C18-coated silica particles (Magic, Michrom Bioresources, Auburn, CA). Peptides were subjected to nanoflow liquid chromatography - electrospray ionization - tandem mass spectrometry (nLC-ESI-MS/MS), using a 120 min reversed phase (10-40 % acetonitrile, 0.1 % formic acid) buffer gradient running at 250 nL/min on a Proxeon EASY-nLC pump in-line with a hybrid linear quadrupole ion trap (Velos LTQ) Orbitrap mass spectrometer (Thermo Fisher Scientific, Waltham, MA). A parent ion scan was performed in the Orbitrap, using a resolving power of 60,000. Simultaneously, up to the twenty most intense peaks were selected for MS/MS (minimum ion

count of 1000 for activation) using standard CID fragmentation. Fragment ions were detected in the LTQ. Dynamic exclusion was activated such that MS/MS of the same m/z (within a 10 ppm window, exclusion list size 500) detected three times within 45 sec were excluded from analysis for 30 s. Data were analyzed using the trans-proteomic pipeline (TPP) (178, 179) via the ProHits software suite (180). For protein identification, Thermo .RAW files were converted to the .mzXML format using Proteowizard (181), then searched using X!Tandem (182) and Comet (183) against Human RefSeq Version 45 (containing 36113 entries). Search parameters specified a parent ion mass tolerance of 10 ppm, and an MS/MS 435 fragment ion tolerance of 0.4 Da, with up to two missed cleavages allowed for trypsin. Variable modifications of +16@M and W, +32@M and W, +42@N-terminus, +1@N and Q were allowed. Proteins identified with a ProteinProphet cut-off of 0.90 (corresponding to ≤1% FDR) and with ≥ 2 unique peptides were analyzed with SAINT Express v.3.3. Each biological replicate was analyzed using two technical replicates. Data were compared to 12 control runs (FlagBirA* alone and no bait control lysates), collapsed to the 2 highest spectral counts for each prey protein, and the SAINT score cut-off value was set to 0.80 (BFDR <1%) to define high confidence interactors.

2.7 LC-MS/MS analysis of plasmalogens and VLCFAs

Cell pellets were homogenized in PBS (ThermoFisher Scientific). An extraction solution of methanol containing 10 ng each of the internal standards, 16:0-D4 lyso-PAF (15.6 pmol) (Cayman Chemical Co.) and D4-26:0-lyso-PC (Avanti Polar Lipids) was added to 50 µg protein cell extract in a glass tube. The samples were incubated on a shaker at room temperature for 1 hr. The samples were transferred to Corning Costar spin-X centrifuge tube filters and centrifuged for 5 min. The filtrates were then transferred to autosampler Verex vials (Phenomenex) for analysis by LC-MS/MS. A Waters TQD interfaced with an Acquity UPLC system was employed for positive ion electrospray (ESI)-MS/MS ionization. Plasmalogen species were detected by monitoring multiple reaction monitoring (MRM) transitions representing fragmentation of [M+H]+ species to m/z 311, 339, 361, 385, 389, 390 for compounds with 16:1, 18:1, 20:4. 22:6, 22:4 and 18:0, respectively at the sn-2 position. Elution of lyso_PCs was detected by monitoring multiple reaction monitoring (MRM) transitions representing fragmentation of [M+H]+ to m/z 104. Chromatographic

resolution was achieved via the use of a 2.1 x 50 mm, 1.7 µm Waters Acquity UPLC BEH column. The solvent systems used were: mobile phase A = 54.5 % water/45 % acetonitrile/0.5 % formic acid mobile phase B = 99.5 % acetonitrile/0.5 % formic acid with both solutions containing 2 mM ammonium acetate. Injections of extracts dissolved in methanol were made with initial solvent conditions of 85 % mobile phase A/15 % mobile phase B. The gradient employed was from 15 % to 100 % mobile phase B over a period of 2.5 min, held at 100 % mobile phase B for 1.5 min before reconditioning the column back to 85 % mobile phase A/15 % mobile phase B for 1 min at a solvent rate of 0.7 ml/min. A column temperature of 35 °C and an injection volume of 5 µl for plasmalogens and 10 µl for lysoPCs were used.

2.8 SIM image processing and analysis

Structured illumination microscopy (SIM) is a super-resolution fluorescence microscopy technique that increases resolution by exploiting interference patterns (moiré fringes) generated when the sample is illuminated using spatially patterned light (184). Raw SIM image stacks were processed in Zen under the Structured Illumination toolbar. A series of parameters were set to generate an optical transfer function (OTF) used for 3D reconstruction. The noise filter for Wiener de-convolution was set to a value of 1.0×10^{-4} to maximize the recovery of high spatial frequency information while minimizing illumination pattern artifacts. The maximum isotropy option was left unselected to recover all available frequency information at exactly the 120° rotation angles. Super-resolution frequency weighting was set 1.0. Negative values arising as an artifact of the Wiener filter were clipped to zero using the Baseline Cut option. Sectioning filters used to remove the 0-frequencies from the 0^{th} order and non-shifted 1^{st} order (+1, -1) were set to default values of 100 and 83, respectively. Processed SIM images were then aligned via an affine transformation matrix of pre-defined values obtained using 100 nm multicolor Tetraspeck fluorescent microspheres (ThermoFisher). SIM data was analyzed for peroxisome-ER association by generating 3D-surface projections in Zen.

2.9 Microscopy and analysis

Fluorescence images of mammalian cultured cells were acquired using a Zeiss LSM 710 laser-scanning confocal microscope with a 63×1.4 NA oil immersion objective. Images of plant (BY-2) cells were acquired using a Leica DM RBE microscope with a Leica 63x Plan Apochromat oil-immersion objective. For peroxisome diffusion analysis, the images were acquired using a Leica DMI6000B inverted fluorescence microscope with Hamamatsu ImagEM ×2 camera.

Live-cell imaging of mammalian cells was performed at 37°C in CO_2-independent medium containing 10 % FBS and 2 mM L-glutamine. For immunofluorescence, cells were fixed in paraformaldehyde and permeabilized using 0.1 % Triton X-100 in PBS, followed by incubation with appropriate antibodies as specified. FLIP assays were performed using 30 or 50 iterations of a 488 nm laser light at full strength in a rectangular region of interest (ROI) repeatedly every 60 seconds. An image was taken immediately before and after each photobleaching session. FRAP assays were performed using a 488 nm laser light at full strength in a rectangular ROI, and 20 single scan images were collected following the photobleaching section. For measurement of peroxisome volume, Z-stacks series were collected.

To quantify the intracellular localization of the GFP-fused PEX16 constructs shown in Fig. 3.4 & 3.5, Volocity®5.0 software (Perkin Elmer) was used to measure the relative intensity of fluorescence attributable to GFP in individual cells. The maximal area of each cell enriched with GFP signal was selected as the ROI and the minimal threshold was adjusted accordingly to ensure that the background signal was eliminated from the measurement. The total GFP signal within each individual cell was obtained by measuring the total pixel intensity of the green channel in the ROI. Among all the cells expressing PEX16-GFP, the highest total GFP signal was chosen as the upper limit; the lowest total GFP signal was chosen as the lower limit. For all the PEX16 mutant constructs, only cells expressing the fusion protein at levels within the above range were selected for the localization analysis. To quantify the colocalization of Cer-PEX26 with the co-expressed GFP fusion proteins (Fig. 3.10), we used Volocity®5.0 software (Perkin Elmer) to measure the Manders' colocalization coefficient of

the GFP signal (M_{GFP}). The minimal threshold for the GFP and Cerulean channels was adjusted to ensure the maximal difference in the M_{GFP} values between the positive control (UB-GFP-SKL) and the negative control (ssGFP-KDEL). The same threshold for both channels was used for all cells examined.

For peroxisome diffusion analysis, Z stacks of single cells were acquired at 40 frames per min and projected to generate 2D videos. At each frame, individual peroxisomes were fit with multiple Gaussians to determine the center of the organelle with a positional accuracy of < 200 nm using the u-track analysis on MatLab software (185). Peroxisomes were tracked over 80 frames (2 mins) using u-track to determine the median diffusion coefficient of peroxisomes per cell.

The measurements of peroxisome volume, peroxisome area and Manders' colocalization coefficient were all performed using Volocity® 5.0 software (Perkin Elmer). All images were adjusted for brightness and contrast using ImageJ (NIH, Bethesda). Figure compositions and merged images were generated using Adobe Photoshop CS4 and Illustrator CS2 (Adobe Systems). Unless otherwise indicated, all statistical analysis was performed using a Student's t test.

2.10 Reagents

The antibodies used were rabbit monoclonal anti-PMP70 (Epitomics); rabbit polyclonal anti-Hsp60 (Abcam); mouse monoclonal anti-Myc (EMD Millipore); goat anti-rabbit Alexa Fluor 568 secondary antibody; goat anti-mouse Alexa Fluor 488 secondary antibodies (Invitrogen); goat anti-rabbit Alexa Fluor 488 secondary antibody (Invitrogen); rabbit polyclonal anti-VAPB(Sigma); rabbit polyclonal anti-VAPA (Novusbio); mouse anti-DLP1 (BD Biosciences), rabbit polyclonal anti-ACBD5 (Novusbio); monoclonal anti-mouse GAPDH (Novusbio); mouse anti-Myc antibodies in hybridoma medium (clone 9E10; Princeton University Monoclonal Antibody Facility); rabbit polyclonal anti-HA (Origene); goat anti-rabbit cottonseed catalase (186); goat anti-mouse or rabbit rhodamine red-X IgGs (Jackson ImmunoResearch Laboratories). To visualize mitochondria, mammalian cultured cells were incubated with media containing 20 nM MitoTracker®REDCMXRos (Invitrogen, M-7512)

for 15 min at 37°C prior to live-cell imaging. To visualize ER in plant suspension-cultured cells, ConA conjugated to Alexa 594 (Molecular Probes) was added to cells at a final concentration of 5 μg/mL during the final 20 min of incubation with secondary antibodies. The total cholesterol levels were measured using Amplex® Red Reagent (ThermoFisher Scientific).

Chapter 3

Multiple domains in PEX16 mediate its trafficking and recruitment of peroxisomal proteins to the ER

This chapter is adapted from an article originally published as:

- Hua R., Gidda S.K., Aranovich R.T., Mullen R.T., Kim P.K. 2015. Multiple Domains in PEX16 Mediate its Trafficking and Recruitment of Peroxisomal Proteins to the ER. *Traffic*. 16: 832-852.

Acknowledgement:

- The experiments in plant cells (Fig. 3.9A & B) were performed by Satinder K. Gidda.

3.1 Introduction

The direct targeting of PMPs to peroxisomes in mammalian cells relies on PEX19 and PEX3 (70, 90, 91, 101, 187). In addition, the direct targeting of PEX3 to peroxisomes in mammals involves PEX16, which serves as the integral membrane-bound receptor for PEX3 (96). Interestingly, PEX16 homologs are absent in most yeast species, suggesting that there are key differences in molecular mechanisms underlying peroxisome biogenesis in yeast and mammals, particularly with regards to the trafficking of PMPs (188). In terms of the trafficking of PEX16 itself, initially it was postulated that this PMP sorts directly from the cytosol to peroxisomes in a post-translational PEX19- and PEX3-dependent manner (70, 90, 91, 102, 187). However, more recent evidence has indicated that PEX16 targets indirectly to peroxisomes via the ER and does so in a co-translational manner (77, 78, 84). Moreover, based on analysis of the kinetics of PMP trafficking to peroxisomes, PEX3 and PMP34 were shown to also target to peroxisomes via the ER, and do so in a PEX16-dependent manner (78). As such, the most recent working model for the function of PEX16 and the role of ER in peroxisome maintenance in mammals is one in which all PMPs are considered to target to peroxisomes via the ER and that PEX16 functions as a PMP receptor at the ER. However, when PMP synthesis exceeds the capacity of PEX16 at the ER, such as exogenous (over)expression, they also target directly to peroxisomes (78).

Although the molecular mechanisms underlying the interplay of the ER and peroxisomes in terms of PMP trafficking are beginning to be understood, the precise role(s) that PEX16 serves in this process is still unclear. There is an especially limited information on the domain(s) within PEX16 that mediate its intracellular trafficking to the ER and then to peroxisomes, as well as the domain(s) that are involved in the recruitment of other PMPs to the ER. For instance, only two studies to date have been published on intracellular trafficking of human PEX16, whereby a distinct positively-charged-amino-acid containing sequence (residues 66-81) within the protein, along with the first of its two putative transmembrane (TM) domains, was shown to be necessary for what was considered at that time to be the direct targeting of PEX16 from the cytosol to peroxisomes (101, 102). Whether the same region and/or other region(s) within PEX16 is involved in its ER-to-peroxisome targeting has

not been investigated. Likewise, the ability of PEX16 to recruit PMPs to the ER has been only demonstrated for human PEX16 (77, 78, 96) and, thus, it remains an open question whether PEX16 in other species, wherein the protein is considered to also target to peroxisomes via the ER, performs the same function.

Here, we employed a comprehensive mutational analysis of human PEX16 in order to identify and characterize the targeting signals responsible for its initial sorting to the ER and then from the ER to peroxisomes, as well as the domain within the protein responsible for PMP recruitment to the ER. We also show that the ability of human PEX16 to recruit PMPs to the ER is shared by a plant (*Arabidopsis thaliana*) PEX16, which also targets to peroxisomes via the ER (174). Taken together, the implications of these results in terms of the role of PEX16 in the maintenance of peroxisomes from the ER are discussed.

3.2 The TM1 domain of PEX16 is both necessary and sufficient for its initial targeting to the ER

PEX16 is the only known mammalian peroxin that targets initially to the ER in a co-translational manner and does so in either the absence or presence of peroxisomes (77, 78). To identify the region(s) in PEX16 that mediate its ER targeting and/or other functions, we generated a series of fusion constructs consisting of PEX16 or portions thereof linked to the green fluorescent protein (GFP) (Fig. 3.1A). As illustrated in Fig. 3.1A, full-length PEX16 is predicted to contain two transmembrane (TM) domains, TM1 and TM2, resulting in the protein being orientated in membranes with both of its N and C termini facing the cytosol (102). PEX16 also lacks an N-terminal signal sequence and, thus, its co-translational targeting and insertion into ER membranes likely relies on at least one of its two TM domains serving as a so-called type II signal-anchor sequence (189, 190). To test this premise, we examined the subcellular localization of several of the PEX16 deletion mutants in a *pex3*-deficient cell line (i.e., PBD400) that is devoid of peroxisomes (81) and, thereby, provides a convenient means for assessing the initial ER targeting step in PEX16 biogenesis.

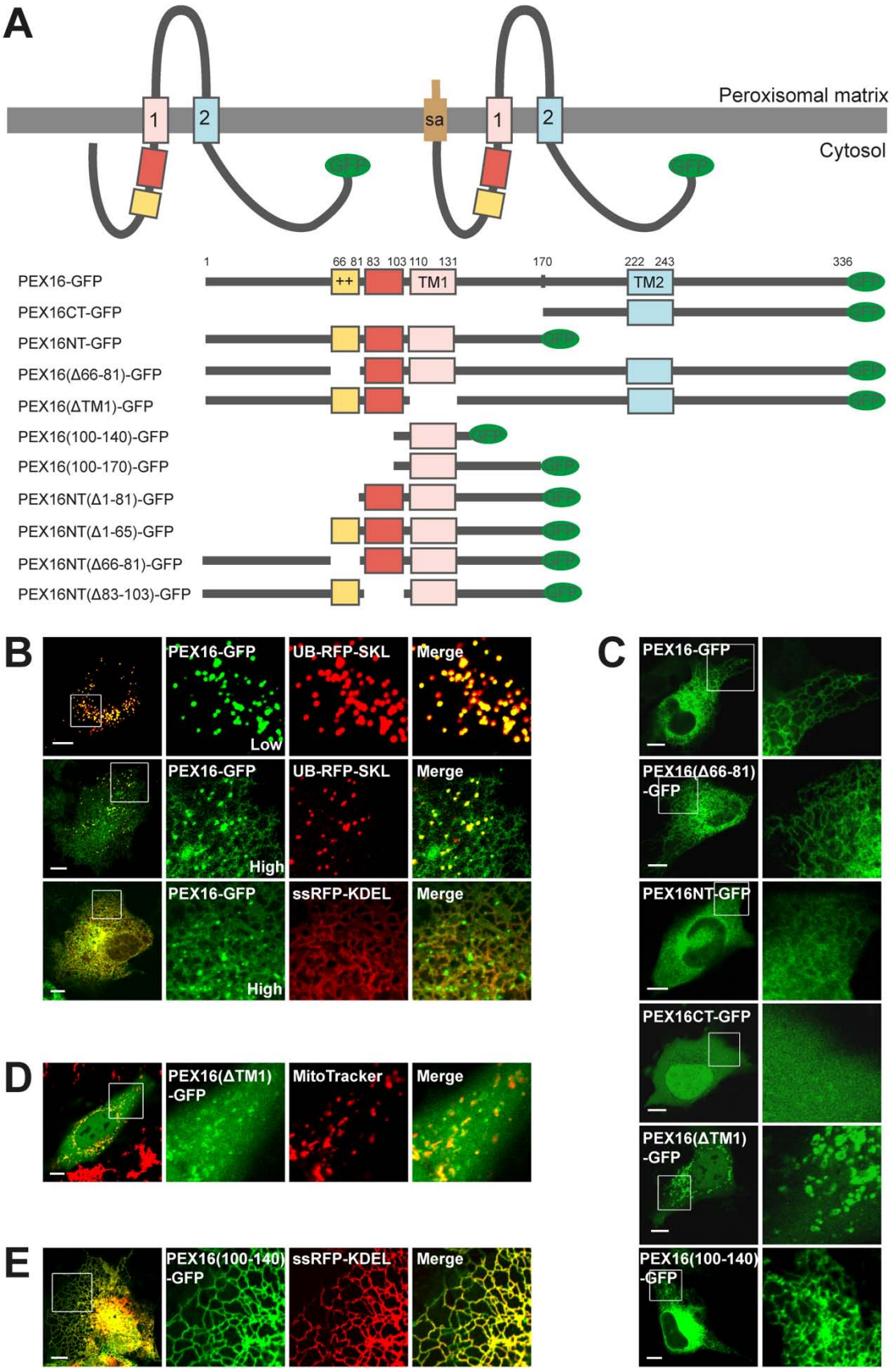
A
Peroxisomal matrix
Cytosol
1
2
sa
1
2
GFP
1
66 81 83 103 110 131
170
222 243
336
++
TM1
TM2
PEX16-GFP
PEX16CT-GFP
PEX16NT-GFP
PEX16(Δ66-81)-GFP
PEX16(ΔTM1)-GFP
PEX16(100-140)-GFP
PEX16(100-170)-GFP
PEX16NT(Δ1-81)-GFP
PEX16NT(Δ1-65)-GFP
PEX16NT(Δ66-81)-GFP
PEX16NT(Δ83-103)-GFP
B
PEX16-GFP
UB-RFP-SKL
Merge
Low
PEX16-GFP
UB-RFP-SKL
Merge
High
PEX16-GFP
ssRFP-KDEL
Merge
High
C
PEX16-GFP
PEX16(Δ66-81)
-GFP
PEX16NT-GFP
PEX16CT-GFP
PEX16(ΔTM1)
-GFP
PEX16(100-140)
-GFP
D
PEX16(ΔTM1)
-GFP
MitoTracker
Merge
E
PEX16(100-140)
-GFP
ssRFP-KDEL
Merge

Figure 3.1 The TM1 domain of PEX16 is both necessary and sufficient for its initial targeting to the ER.
(A) Cartoon of PEX16-GFP and saPEX16-GFP structure and topology in the peroxisomal membrane. Shown for both fusion proteins are the relative positions of the two transmembrane domains in PEX16 (TM1 and TM2), the C-terminal-appended GFP, and, for saPEX16-GFP, the N-terminal-appended type I signal anchor sequence (sa). Shown also are schematic representations of full-length and various truncation mutants of PEX16-GFP described in this study. Boxes represent specific regions of PEX16, including the putative peroxisomal targeting signal (i.e., residues 66-81), predicted TMs, i.e., TM1 (residues 110-131) and TM2 (residues 222-243), and a sub-region of the PMP recruitment domain (i.e., residues 83-103). Green circles represent the position of the C-terminal-appended GFP moiety. Numbers denote specific amino acid residues in full-length PEX16 (336 residues).
(B) Representative images of COS7 cells transiently-(co)expressing (as indicated by panel labels) PEX16-GFP and the peroxisomal or ER marker proteins, UB-RFP-SKL or ssRFP-KDEL, respectively. Note that, based on the relative intensity of its fluorescence, PEX16-GFP was considered to be expressed at low levels in the cell shown in the top row and at high levels in the cells shown in the middle and bottom two rows as indicated. Brightness has been adjusted for presentation.
(C) *pex3*-deficient peroxisome-less (PBD400) cells transiently-expressing PEX16-GFP or modified (truncated) versions thereof; refer to (A).
(D) PBD400 cells transiently-expressing PEX16(ΔTM1)-GFP and stained with MitoTracker® REDCMXRos.
(E) COS7 cells transiently-(co)expressing PEX16(100-140)-GFP and ssRFP-KDEL. The white box on each left side panel indicates the magnified area shown in the right side panels. The higher magnification panels show the individual micrographs including the corresponding merged image. Scale bars, 10 μm.

As shown previously (77), transiently-expressed PEX16-GFP localized in cells with pre-existing peroxisomes (i.e., COS7 cells) either to peroxisomes or to both the ER and peroxisomes, depending on its relative level of expression. At low expression levels, the fusion protein colocalized exclusively with the peroxisomal marker protein UB-RFP-SKL, consisting of the red fluorescent protein (RFP) fused to ubiquitin (UB) at its N terminus and a type I peroxisomal targeting signal tripeptide (i.e., Ser-Lys-Leu [SKL]) at its C terminus (77); whereas, at higher expression levels, PEX16-GFP localized to both peroxisomes and the ER as increased colocalization with the ER marker protein ssRFP-KDEL was readily observed (77) (Fig. 3.1B). In normal human fibroblast cells, PEX16-GFP targets to peroxisomes (191). In peroxisome-deficient PBD400 cells, PEX16-GFP localized to the ER as expected (Fig. 3.1C) (77), and at higher expression levels, also in the cytosol (data not shown). Similarly, both PEX16(Δ66-81)-GFP and PEX16NT-GFP localized to the ER and cytosol in PBD400 cells (Fig. 3.1C), indicating that deletion of either its putative

peroxisomal targeting signal (i.e., residues 66-81) (102) or the entire C-terminal half, including TM2 (refer to Fig. 3.1A), had no effect on the ability of PEX16 to target to the ER. By contrast, mutant constructs lacking either the entire N-terminal half of the protein (PEX16CT-GFP), including TM1, or TM1 only (PEX16(ΔTM1)-GFP) did not target to the ER in PBD400 cells (Fig. 3.1C). Instead, PEX16CT-GFP mislocalized to the cytosol and nucleus in these cells (Fig. 3.1C), while PEX16(ΔTM1)-GFP localized to mitochondria, as well as to the cytosol and nucleus (Fig. 3.1C&D), indicating that the TM1 domain of PEX16 is necessary for its targeting to the ER.

To further confirm that the TM1 domain of PEX16 is involved in its initial ER targeting, we tested whether TM1 is sufficient to target a passenger protein to the ER. Toward this end, TM1 (a.a. 110-131) and the adjacent N- and C-terminal 10-amino-acid sequences serving as linkers and providing the appropriate context were appended to GFP (refer to Fig. 3.1A PEX16(100-140)-GFP). As shown in Fig. 3.1C, similar to full-length PEX16-GFP, PEX16(100-140)-GFP localized to the ER in PBD400 cells. However, unlike PEX16-GFP, PEX16(100-140)-GFP localized only to the ER in COS7 cells and not to peroxisomes (Fig. 3.1E). Indeed, we confirmed that PEX16(100-140)-GFP did not target to peroxisomes in COS7 cells using a fluorescence-loss-in-photobleaching (FLIP) assay that depleted the ER of its fluorescent signals (Fig. 3.2). Since the ER is one large interconnected organelle, repetitive photobleaching a small region will deplete all the fluorescent signals in the ER, thus revealing less intense fluorescent signals such as those in peroxisomes. Compared to wild-type PEX16-GFP (Fig. 3.2A), depletion of the fluorescence attributable to ER-localized PEX16(100-140)-GFP by repetitive photobleaching revealed no obvious localization of the modified fusion protein to peroxisomes (Fig. 3.2B), reinforcing that the TM1 domain of PEX16 is sufficient for its targeting to the ER, but not its targeting to peroxisomes. Similar results were found with a PEX16 construct consisting of TM1 domain and a longer C-terminal luminal-facing region, i.e., PEX16(100-170)-GFP also localized exclusively to the ER (Fig. 3.3), suggesting that the lack of peroxisomal localization of PEX16(100-140)-GFP is not likely due to steric hindrance of the TM1 by the appended GFP moiety.

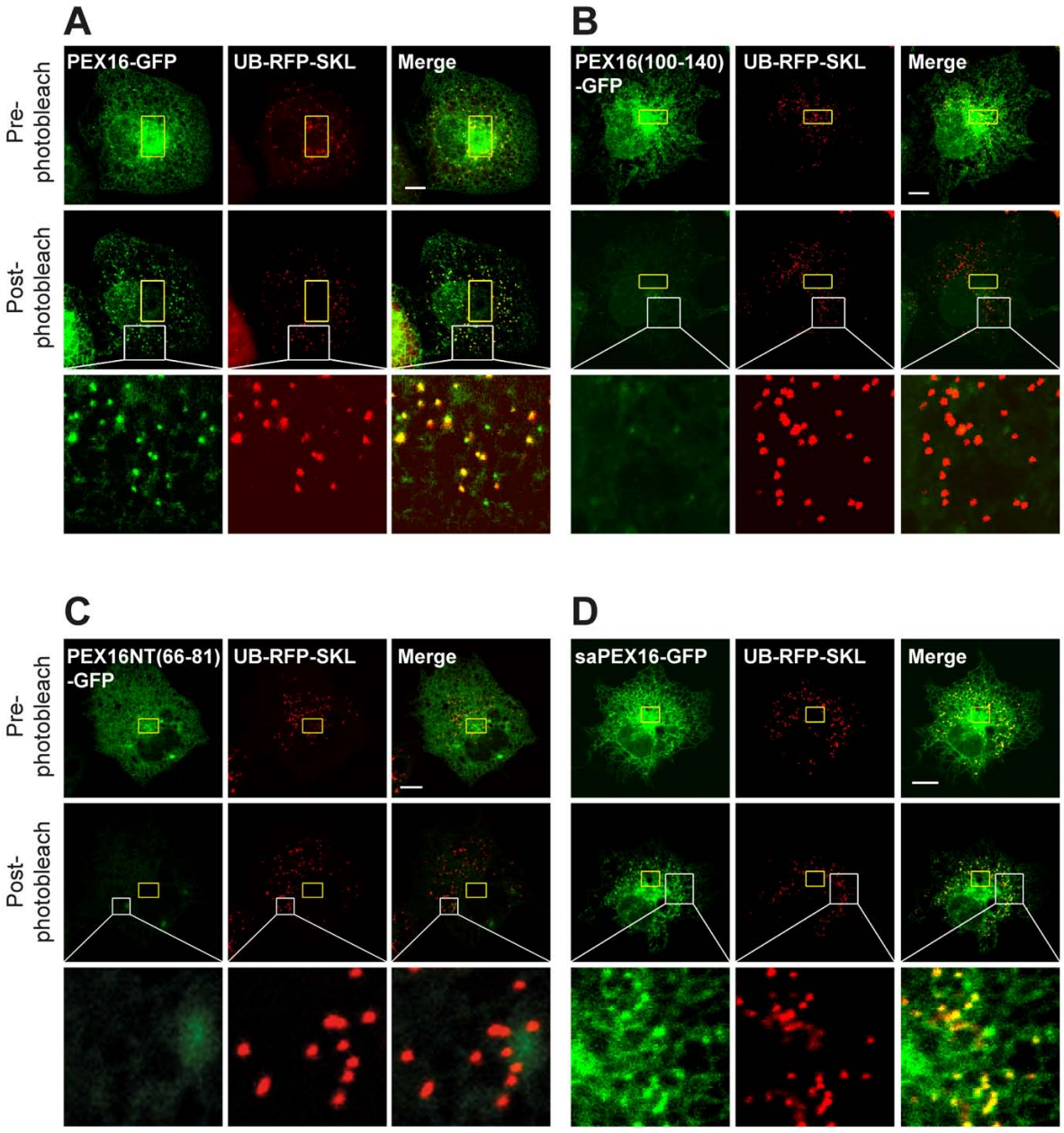

Figure 3.2 PEX16(100-140)-GFP and PEX16NT(Δ66-81)-GFP do not target to the peroxisomes. Representative images of FLIP assays performed with COS7 cells transiently-(co)expressing (as indicated by panel labels) (A) PEX16-GFP, (B) PEX16(100-140)-GFP, (C) PEX16NT(Δ66-81)-GFP or (D) saPEX16-GFP, along with the peroxisomal marker protein UB-RFP-SKL are shown. Each construct in pseudo color is shown along with the corresponding merged image. Yellow boxes represent the region of interest (ROI) in cell that was subjected to repeated photobleaching with 488-nm laser light. Both the first frame before photobleaching (Pre-photobleach) and the first image after repeated photobleaching (Post-photobleach) procedure are shown for all constructs. The white boxes are the regions magnified in the bottom panels. The images show that PEX16(100-140)-GFP and PEX16NT(Δ66-81)-GFP, unlike PEX16-GFP and saPEX16-GFP, do not colocalize to peroxisomes with the peroxisomal marker protein UB-RFP-SKL. Scale bars, 10 μm.

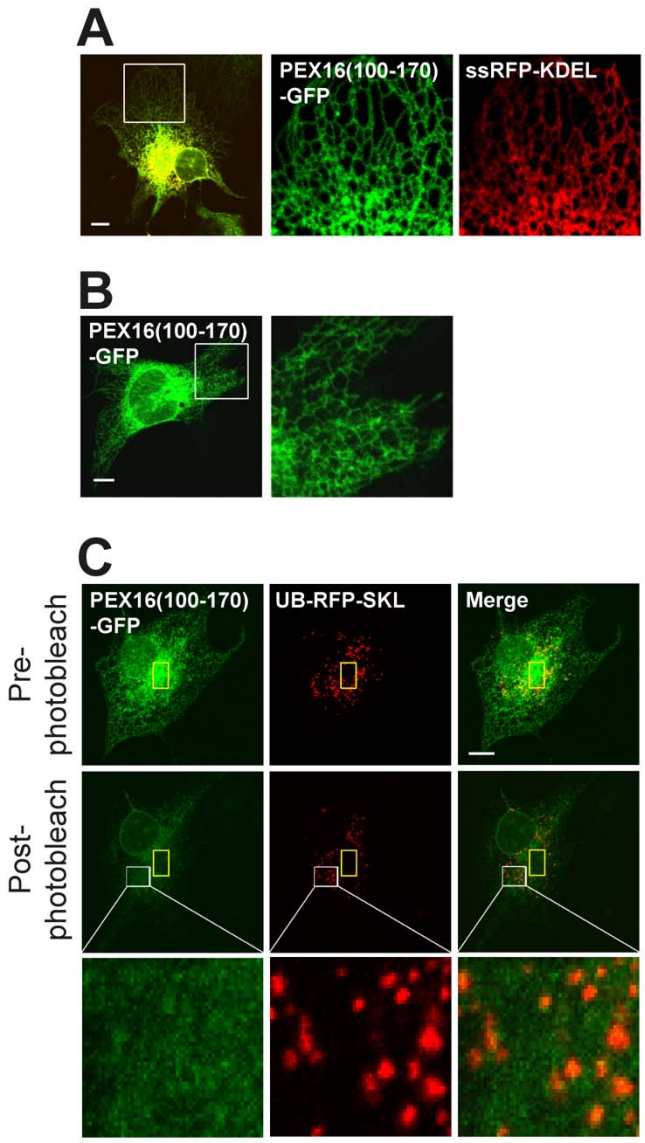

Figure 3.3 PEX16(100-170) targets only to the ER and not to peroxisomes.
(A) Representative images of COS7 cells transiently-(co)expressing PEX16(100-170)-GFP and the ER marker proteins, ssRFP-KDEL.
(B) Representative images of *pex3*-deficient peroxisome-less (PBD400) cells transiently-expressing PEX16(100-170)-GFP. The white box on each left side panel indicates the magnified area shown in the right side panels.
(C) Representative images of FLIP assay performed with COS7 cells transiently-(co)expressing PEX16(100-170)-GFP along with the peroxisomal marker protein UB-RFP-SKL. Yellow boxes represent the region of interest (ROI) in cell that was subjected to repeated photobleaching with 488-nm laser light. Both the first frame before photobleaching (Pre-photobleach) and the first image after repeated photobleaching (Post-photobleach) procedure are shown. The white boxes are the regions magnified in the bottom panels. Scale bars, 10 μm.

3.3 Identification of the ER-to-peroxisome targeting signal of PEX16

Given that PEX16 targets to peroxisomes via the ER (77, 78), we next assessed which region(s) of the protein mediates its ER-to-peroxisome trafficking. Toward this end, we developed a microscopy-based assay to quantify the intracellular distribution of PEX16. More specifically, full-length or selected mutant versions of PEX16-GFP (Fig. 3.1A) were co-expressed in COS7 cells with the peroxisome marker UB-RFP-SKL or the ER marker ssRFP-KDEL. The intracellular distribution of GFP fluorescence in transfected cells ($n \geq 50$) was quantified as either exclusively peroxisomes or ER, or a combination of both organelles (Fig. 3.4).

In agreement with previous findings (77, 78) and those described above (Fig. 3.1B), PEX16-GFP in COS7 cells was observed and quantified to be localized most often exclusively to peroxisomes, less often to both peroxisomes and ER, and never exclusively to the ER (Fig. 3.4A and Fig. 3.2A). Also as mentioned above (Fig. 3.1B), the dual localization of PEX16-GFP to peroxisomes and ER was typically observed only in cells expressing the fusion protein at relatively high levels, which was likely due to the saturation of sorting machinery responsible for trafficking PEX16 from the ER to peroxisomes (77). Therefore, to ensure that any differences in the observed localization of the corresponding PEX16-GFP mutants examined were not simply due to differences in their relative expression levels, only those cells that exhibited GFP fluorescence signals within the range of intensities measured for wild-type PEX16-GFP either exclusively at peroxisomes or at both peroxisomes and the ER were imaged and quantified (see Chapter 2 for details). Based on this range, PEX16NT-GFP localized exclusively to peroxisomes in almost all cells examined, with only a few cells displaying localization to both peroxisomes and ER (Fig. 3.4B). These data indicate that the peroxisomal targeting signal(s) of PEX16 is located within the N-terminal half (i.e., residues 1-170) of the protein.

Consistent with this conclusion and also with previous results (102), deletion of the putative peroxisomal targeting signal in PEX16 (i.e., residues 66-81) completely abolished its ability to target to peroxisomes (Fig. 3.4C) and instead, PEX16NT(Δ66-81)-GFP localized exclusively to the ER, as verified by a FLIP assay (Fig. 3.2C). Furthermore, deletion of the first 65 amino acid residues from the N terminus of PEX16NT-GFP resulted in the modified mutant protein being localized in a similar manner as PEX16-GFP, i.e., PEX16NT(Δ1-65)-GFP localized most often exclusively to peroxisomes and less so to both peroxisomes and ER (compare Fig. 3.4A&D). On the other hand, the PEX16NT(Δ1-81)-GFP construct, where the N-terminal 81 residues were deleted from PEX16NT-GFP, localized exclusively to the ER in all cells examined (Fig. 3.4E). Taken together, these results indicate that amino acid residues 66-81 in PEX16 are required for its targeting from the ER to peroxisomes.

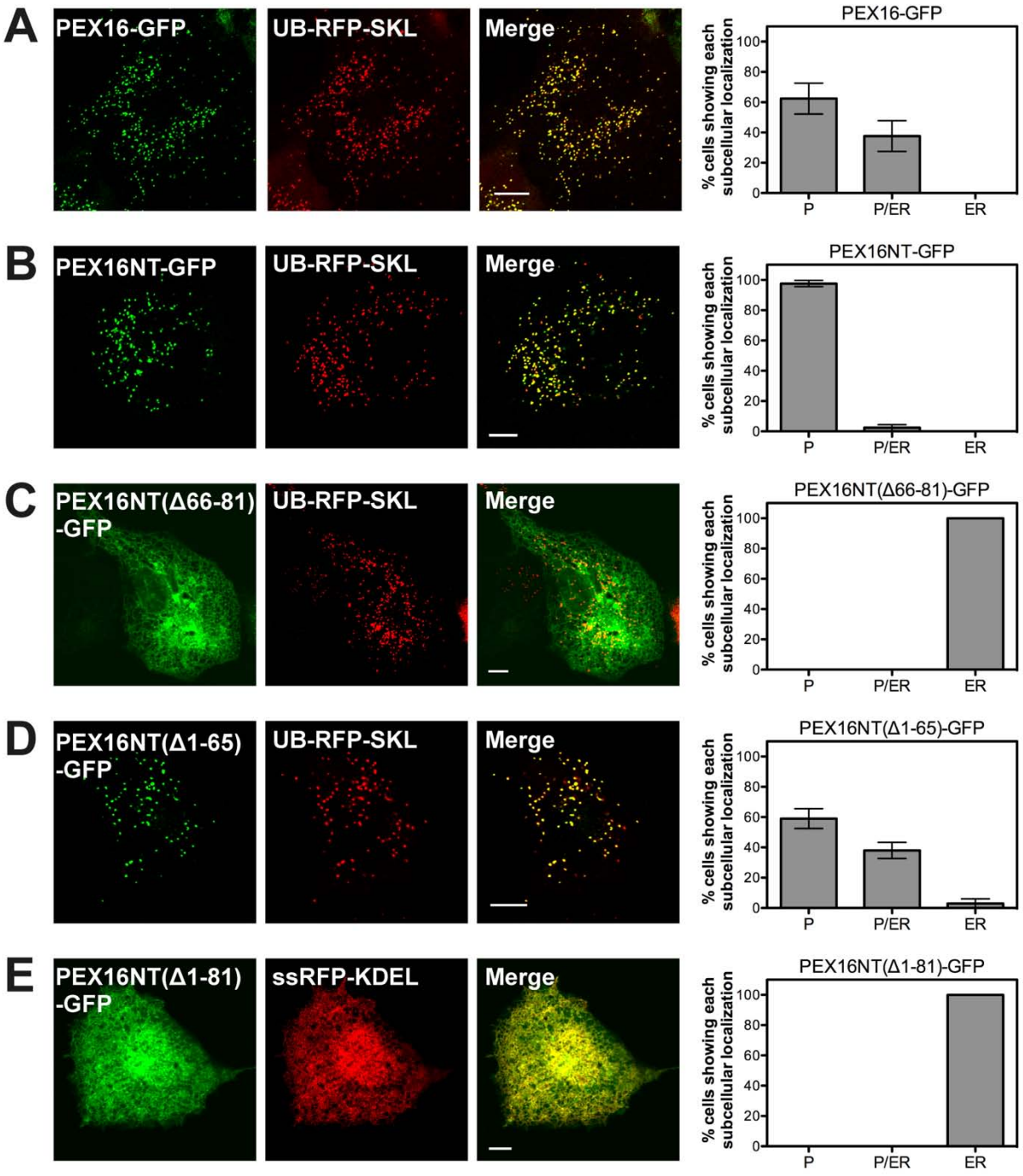

Figure 3.4 Amino acid residues 66-81 in PEX16 are necessary for its ER-to-peroxisome targeting.

Representative images of COS7 cells transiently-coexpressing (A) PEX16-GFP, (B) PEX16NT-GFP, (C) PEX16NT(Δ66-81)-GFP, (D) PEX16NT(Δ1-65)-GFP, and (E) PEX16NT(Δ1-81)-GFP, along with the peroxisomal marker protein, UB-RFP-SKL. Shown to the right of each set of images is a bar graph depicting the percentage of transfected cells displaying intracellular localization of the corresponding PEX16-GFP fusion protein either exclusively to peroxisomes (P) or ER, or to a combination of both organelles (P/ER). Each graph represents the analysis of ≥150 cells from three separate transfections (N=3 ± standard deviation). Scale bars, 10 μm.

3.4 Characterization of the PEX16 ER-to-peroxisome targeting signal

In order to further characterize the putative ER-to-peroxisome targeting signal in PEX16, we performed a mutagenic analysis of amino acids 66-81 (Fig. 3.5). We focused initially on whether the conspicuous enrichment of positively-charged residues within this sequence (refer to Fig. 3.1A and Fig. 3.5A) is an essential feature of the targeting signal, as it is a common characteristic in the peroxisomal targeting signals of other PMPs (63, 66, 67). As shown in Fig. 3.5B, the mutant PEX16(66-81Ala)-GFP, where all of the lysine and arginine residues in the 66-81 amino acid sequence were replaced with alanine readily localized to peroxisomes (Fig. 3.5A). These results indicate that the positively-charged residues within the 66-81 amino acid sequence are not required for sorting PEX16 from the ER to peroxisomes and that the putative peroxisomal targeting signal of PEX16 may be distinct from that present in other PMPs, including those that utilize an ER-to-peroxisome targeting pathway.

We tested next whether any other specific residues within the 66-81 amino acid sequence of PEX16 are required for its proper targeting from the ER to peroxisomes by replacing all of the amino acids in this sequence with random amino acids (Fig. 3.5A). As shown in Fig. 3.5C, the resulting construct, PEX16(66-81random)-GFP, localized exclusively to the ER in almost all cells examined (Fig. 3.5C). We also generated three modified versions of the PEX16(66-81random)-GFP mutant whereby five/six-amino-acid-long regions within the 66-81 amino acid sequence were restored back to their corresponding wild-type sequence (Fig. 3.5A). As shown in Fig. 3.5E&F, re-introduction of either -KKLPV- (PEX16(66-81randomB)-GFP) or -SLSQQK- (PEX16(66-81randomC)-GFP) within the 66-81 amino acid sequence restored its peroxisomal targeting. By contrast, re-introduction of -RKELR- did not restore its peroxisomal targeting, i.e., PEX16(66-81randomA)-GFP, similar to PEX16(66-81random)-GFP, localized in most cells exclusively to the ER (Fig. 3.5D). Collectively, these results suggest that residues 71-81 in PEX16 represent the most essential region of the ER-to-peroxisome targeting signal.

A

PEX16(66-81WT)	RKELRKKLPVSLSQQK
PEX16(66-81Ala)	AAELAAALPVSLSQQA
PEX16(66-81random)	QMYRNRLESVWVEAQI
PEX16(66-81randomA)	**RKELR**RLESVWVEAQI
PEX16(66-81randomB)	QMYRN**KKLPV**WVEAQI
PEX16(66-81randomC)	QMYRNRLESV**SLSQQK**

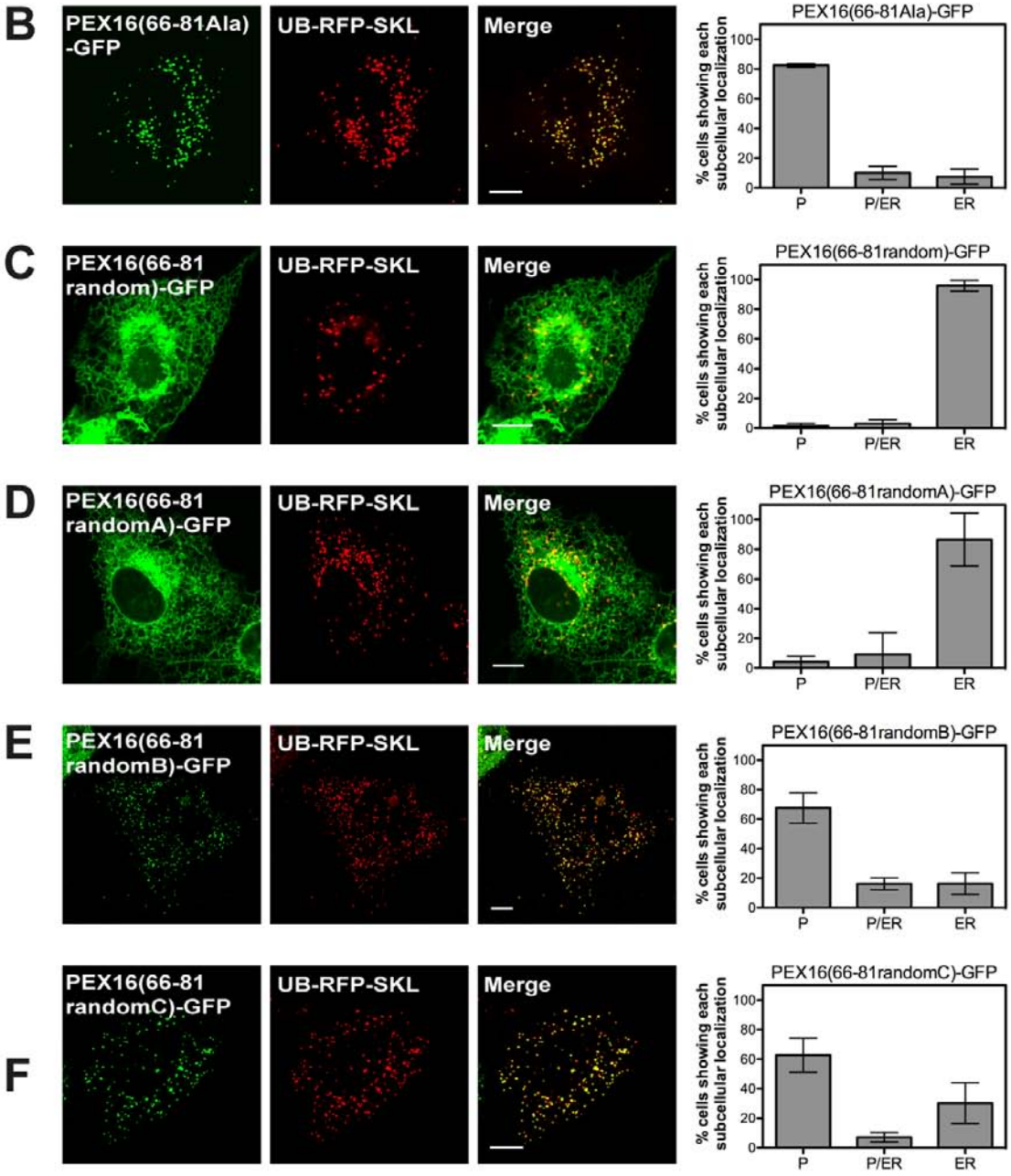

Figure 3.5 Characterization of the PEX16 ER-to-peroxisome targeting signal.
(A) Overview of 66-81 amino acid sequences in either wild-type (WT) PEX16-GFP or various modified versions. Alanine substitution of wild-type lysine and arginine residues within the 66-81 amino acid sequence in PEX16(66-81Ala)-GFP is underlined. PEX16(66-81random)-GFP is a mutant where residues 66-81 have been replaced with randomly selected residues as shown. The mutants with restored (wild-type) residues in PEX16(66-81randomA)-GFP, PEX16(66-81randomB)-GFP and PEX16(66-81randomC)-GFP are bolded.
(B-F) Representative images of COS7 cells transiently-(co)expressing (as indicated by panel labels) (B) PEX16(66-81Ala)-GFP, (C) PEX16(66-81random)-GFP, (D) PEX16(66-81randomA)-GFP, (E) PEX16(66-81randomB)-GFP, and (F) PEX16(66-81randomC)-GFP, along with the peroxisomal marker protein, UB-RFP-SKL. Shown to the right of each set of images is a bar graph depicting the percentage of transfected cells displaying intracellular localization of the corresponding PEX16-GFP fusion protein either exclusively to peroxisomes (P) or ER, or to a combination of both organelles (P/ER). Each graph represents the analysis of ≥150 cells from three separate transfections (N=3 ± standard deviation). Scale bars, 10 μm

3.5 A specific TM1 domain is not necessary for the ER-to-peroxisome targeting of PEX16

We next asked whether the TM1 domain in PEX16 is required not only for its initial targeting to the ER (Fig. 3.1), but also for its subsequent ER-to-peroxisome targeting. To test this premise, we generated a hybrid fusion protein construct, PEX16(1-109)-Vamp1A(TM)-GFP (Fig. 3.6A), whereby the amino acid sequence corresponding to the C-terminal end of PEX16NT, including TM1, was replaced with the C-terminal ER-targeting domain of Vamp1A (192-194). As shown in Fig. 3.6, Vamp1A-GFP localized to the ER as expected (Fig. 3.6B) (192-194), but not to peroxisomes (Fig. 3.6C). On the other hand, PEX16(1-109)-Vamp1A(TM)-GFP localized to both the ER (Fig. 3.6D) and peroxisomes (Fig. 3.6E). These results indicate that the TM1 domain of PEX16 is not specifically necessary for its trafficking from the ER to peroxisomes since a TM sequence from another (non-peroxisomal) membrane protein can serve this function.

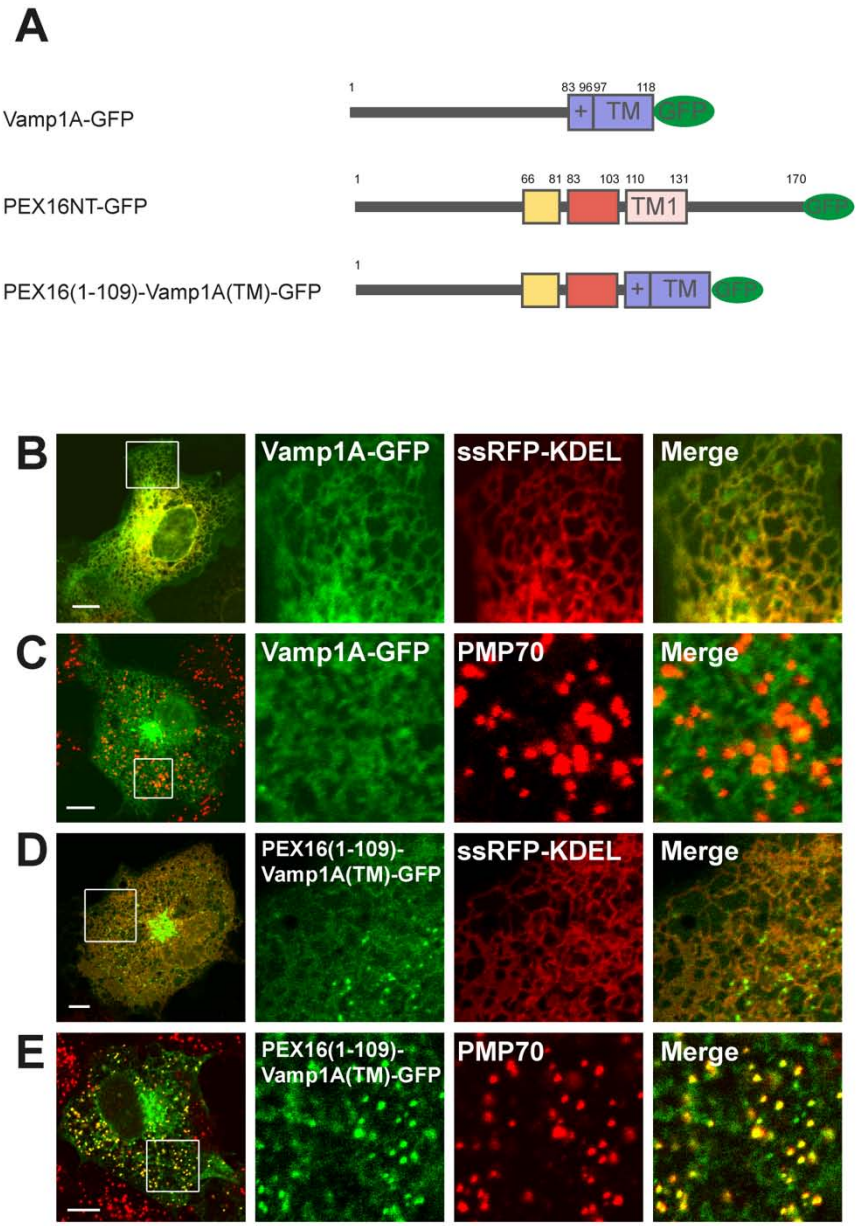

Figure 3.6 A specific TM1 domain is not necessary for the ER-to-peroxisome targeting of PEX16.

(A) Schematic presentation of Vamp1A-GFP, PEX16NT-GFP, and PEX16(1-109)-Vamp1A(TM)-GFP. Purple boxes represent the C-terminal ER-targeting domain of Vamp1A (i.e., resides 83-118), including its single TM domain and adjacent upstream sequences. The yellow and pink boxes represent specific regions of PEX16, including the putative peroxisomal targeting signal (i.e., residues 66-81) and its first transmembrane (TM1) domain (i.e., residues 110-131). Numbers denote specific amino acid residues in either full-length Vamp1A (118 residues) or full-length PEX16 (336 residues). (B and D) Representative images of COS7 cells transiently-(co)expressing (as indicated by panel labels) (B) Vamp1A-GFP or (D) PEX16(1-109)-Vamp1A(TM)-GFP, along with the ER marker protein, ssRFP-KDEL. (C and E) Representative images of COS7 cells transiently-expressing (C) Vamp1A-GFP or (E) PEX16(1-109)-Vamp1A(TM)-GFP, and immunostained for endogenous peroxisomal PMP70. Shown in the panels on the left in (B - E) are the low magnification merged images of fluorescence attributable to the (co)expressed fusion proteins or PMP70 immunostaining; boxes represent the portions of the cells shown at higher magnification and as individual fluorescence micrographs in the panels to the right, including the corresponding merged image. Scale bars, 10 μm.

3.6 PEX16 is capable of recruiting a wide range of PMPs to the ER

Previously, we showed that PEX16 is capable of recruiting two other PMPs, namely PEX3 and PMP34, to the ER, from where they are subsequently transported to pre-existing peroxisomes, and that this may be the default pathway for the trafficking of these proteins (77, 78). This suggests that PEX16 may serve as a general PMP receptor at the ER. To further test this premise, we assessed whether a variety of other PMPs can also be recruited to the ER by PEX16. Specifically, we co-expressed several different PMPs with a well-characterized modified version of PEX16-GFP known as saPEX16-GFP (see Fig. 3.1A). This fusion protein is appended to an N-terminal type I signal anchor sequence (sa) that, compared to wild-type PEX16-GFP, serves to retain it longer in the ER after its co-translational synthesis (Fig. 3.2D), while also preserving the native membrane topology of PEX16 (77). Moreover, saPEX16-GFP has been previously shown to complement *pex16*-deficient cells, confirming that this modified fusion protein functions in a similar manner as its wild-type counterpart (77).

We first examined whether saPEX16-GFP can recruit PEX26 to the ER. As shown in Fig. 3.7A, Cer-PEX26$_{TM}$, consisting of the Cerulean fluorescent protein fused to the C-terminal half of the tail-anchored PMP PEX26 (the portion that contains its membrane targeting TM sequence), localized exclusively to peroxisomes and not to the ER when expressed on its own, as expected (92, 195). Notably, in cells where Cer-PEX26$_{TM}$ was expressed at relatively high levels, the fusion protein localized to both peroxisomes and mitochondria (Fig. 3.7A). By contrast, co-expression of Cer-PEX26$_{TM}$ with saPEX16-GFP, resulted in both proteins colocalized at the ER (Fig. 3.7A), indicating that PEX26, similar to PEX3 and PMP34 (77, 78), can be recruited to the ER by PEX16.

We also examined three other PMPs that differ in their membrane topology and function, namely PEX10, PEX11β and FIS1. Similar to PEX26, they were also recruited to the ER by PEX16. That is, both the multi-spanning PMPs, PEX10-Cer and PEX11β-Cer, localized exclusively to peroxisomes when expressed on their own (196, 197), but co-localized at the ER when co-expressed with saPEX16-GFP (Fig. 3.7B). Likewise, Myc-FIS1, a tail-anchored membrane protein that localizes and functions at both peroxisomes and mitochondria (29),

partially colocalized with both the endogenous peroxisomal and mitochondrial marker proteins, PMP70 and Hsp60, respectively (Fig. 3.7C). However, when co-expressed with saPEX16-GFP, Myc-FIS1 localized to the ER (Fig. 3.7C). On the other hand, Cer-OMP25$_{TM}$, a mitochondrial outer membrane protein (198, 199), localized exclusively to mitochondria and not to peroxisomes or the ER when either expressed on its own or co-expressed with saPEX16-GFP (Fig. 3.7D), indicating that the ability of PEX16 to recruit proteins to the ER is specific for PMPs.

While the mechanism of how PEX16 recruits PMPs to the ER is not yet known, it is generally thought that, at the peroxisomes, PEX16 acts in cooperation with PEX3 and PEX19 to mediate the recruitment of nascent PMPs in the cytosol into peroxisomal membranes (77, 96). To test whether PEX3 and/or PEX19 are also required in PEX16-mediated recruitment of PMPs to the ER, Cer-PEX26$_{TM}$ was co-expressed with saPEX16-GFP in *pex3*- or *pex19*-deficient cells (i.e., PBD400 and PBD399, respectively), which are devoid of peroxisomes (18, 81). As shown in Fig. 3.7E&F, Cer-PEX26$_{TM}$ colocalized with saPEX16-GFP at the ER in both PBD400 and PBD399 cells. When expressed on its own in these cells, Cer-PEX26$_{TM}$ did not localize to the ER (ssGFP-KDEL), but instead localized to mitochondria. Similar results were observed with PMP34 when co-expressed with PEX16 in PBD400 and PBD399 cells (Fig. 3.8B&C). Taken together, these results indicate that at the ER, PEX16-mediated recruitment of PMPs does not depend on PEX3 or PEX19.

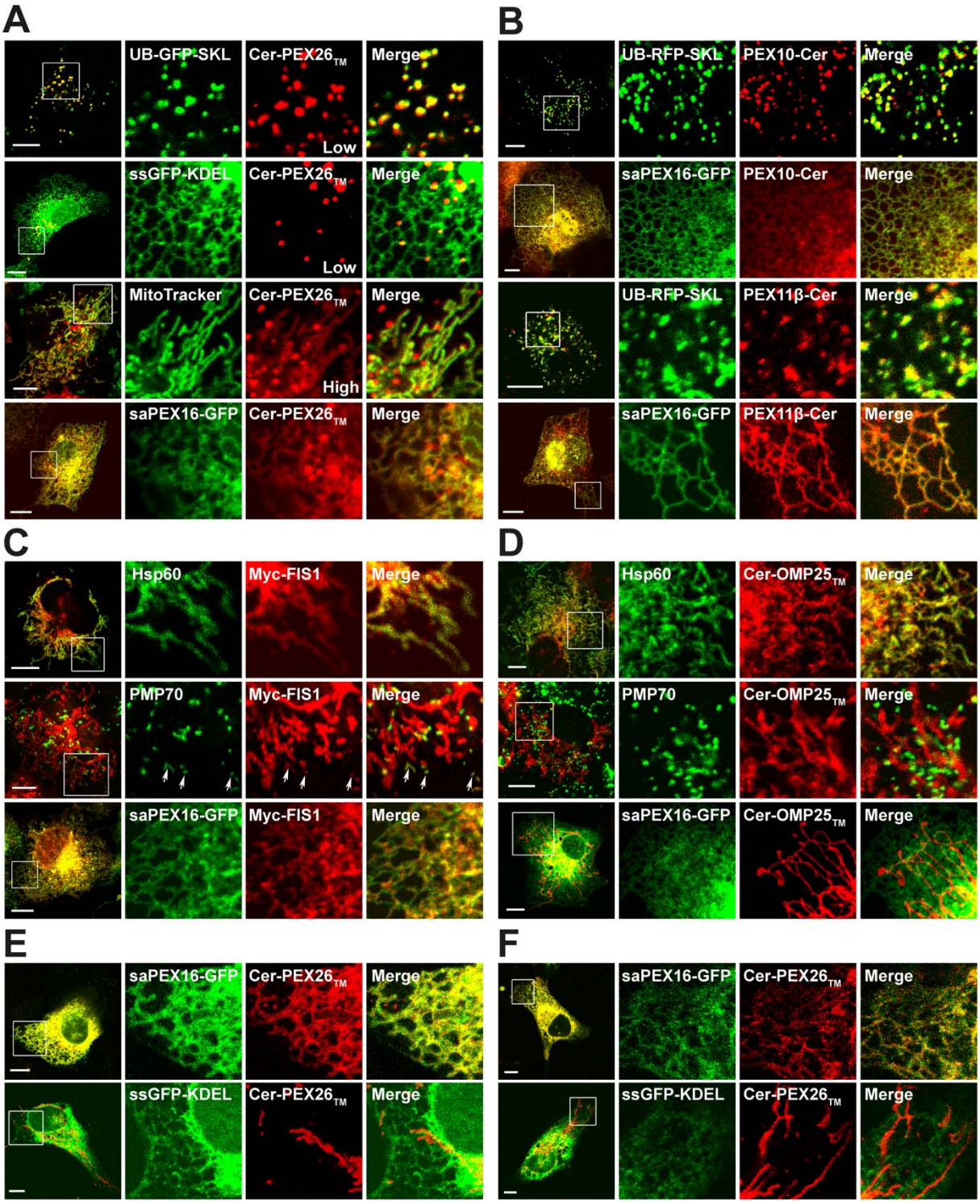

Figure 3.7 PEX16 is capable of recruiting a wide range of PMPs to the ER.
(A-D) Representative images of COS7 cells transiently-(co)expressing (A) Cer-PEX26$_{TM}$ and either UB-GFP-SKL, ssGFP-KDEL or saPEX16-GFP (as indicated by panel labels), or immunostained with MitoTracker® REDCMXRos, (B) PEX10-Cer or PEX11β-Cer and UB-GFP-SKL or saPEX16-GFP, (C) Myc-FIS1 and saPEX16-GFP, or Myc-FIS1 expressing cells immunostained for endogenous mitochondrial Hsp60 or peroxisomal PMP70, (D) Cer-OMP25$_{TM}$ and saPEX16-GFP, or Cer-OMP25$_{TM}$ expressing cells immunostained for endogenous Hsp60 or PMP70. Note in (A) that, based on the relative intensity of its fluorescence, Cer-PEX26$_{TM}$ was considered to be expressed at low levels in the cells shown in the top two rows and at high level in the cell shown in the third row as indicated.

(E) Representative images of *pex3*-deficient (PBD400) cells transiently-(co)expressing Cer-PEX26$_{TM}$ and saPEX16-GFP or ssGFP-KDEL.
(F) Representative images of *pex19*-deficient (PBD399) cells transiently-(co)expressing Cer-PEX26$_{TM}$ and saPEX16-GFP or ssGFP-KDEL. Shown in the panels on the left in (A-F) are the low magnification merged images; boxes represent the portions of the cells shown at higher magnification and as individual micrographs in the panels to the right, including the corresponding merged image. Scale bars, 10 μm.

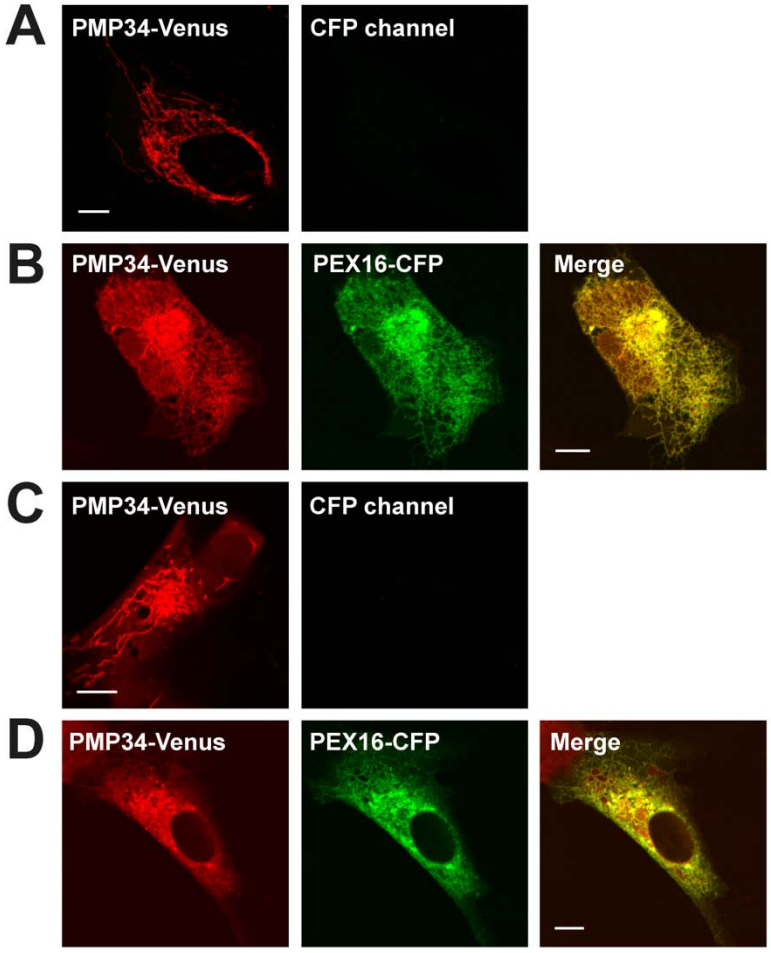

Figure 3.8 PEX16 recruits PMP34 to the ER independently of PEX3 or PEX19.
(A and B) pex3-deficient (PBD400) or (C and D) pex19-deficient (PBD399) cells were transfected with plasmids encoding for PMP34-Venus (A and C), or co-transfected with PEX16-CFP (B and D). Scale bars, 10 μm.

3.7 The recruitment of PMPs to the ER by PEX16 is conserved in plant cells

Like human PEX16, plant (*A. thaliana*) PEX16 (AtPEX16) is considered to target to peroxisomes via the ER and participate in multiple processes in peroxisome biogenesis in plant cells depending on its localization (188). For instance, deletion of the *AtPEX16* gene leads to complete loss of peroxisomes (200). Hence, like its human counterpart, AtPEX16 is also thought to function at the ER in the early stages of *de novo* peroxisome biogenesis, and perhaps as a general PMP receptor (26).

To begin to confirm whether PEX16 function is conserved among evolutionarily diverse organisms, we tested whether plant PEX16, similar to human PEX16, can recruit PMPs to the ER. As shown in Fig. 3.9A and consistent with previous observations (174), wild-type AtPEX16 (AtPEX16-GFP) localized to peroxisomes and not to the ER in plant suspension-cultured cells, presumably because its transit through the ER to peroxisomes is rapid (174). By contrast, AtPEX16-GFP with an N-terminal-appended sa sequence (i.e., saAtPEX16-GFP) localized primarily to the ER and only at later time points following transformation (i.e., 8 h versus 4 h) did the fusion protein localize also to peroxisomes (Fig. 3.9A). These data are consistent with the notion that, similar to human PEX16, plant PEX16 targets to peroxisomes via the ER and that an appended signal anchor sequence serves to retain the protein longer in the ER. Indeed, mutation in the peroxisomal targeting signal of AtPEX16 (174) resulted in the modified fusion protein, i.e., saAtPEX16(mut)-GFP, localized exclusively to the ER (Fig. 3.9A).

As shown in Fig. 3.9B and again consistent with human PEX16 (Fig. 3.7), co-expression of saAtPEX16-GFP with two other plant PMPs, namely AtPEX3 and AtPMP36 (*A. thaliana* homologs of mammalian PEX3 and PMP34, respectively), resulted in both proteins being localized to the ER, whereas they localized exclusively to peroxisomes when expressed on their own (201, 202). Interestingly, plant PEX16 was also capable of recruiting PMPs to the ER in mammalian cells. That is, saAt^{Hs}PEX16-GFP, which consists of a human codon-optimized version of saAtPEX16, localized to the ER in COS7 cells and also recruited Cer-PEX26$_{TM}$ to the ER when both proteins were co-expressed (Fig. 3.9C). Collectively, these

results support the notion that the ability of PEX16 to serve as a general PMP receptor at the ER is conserved between plants and mammals.

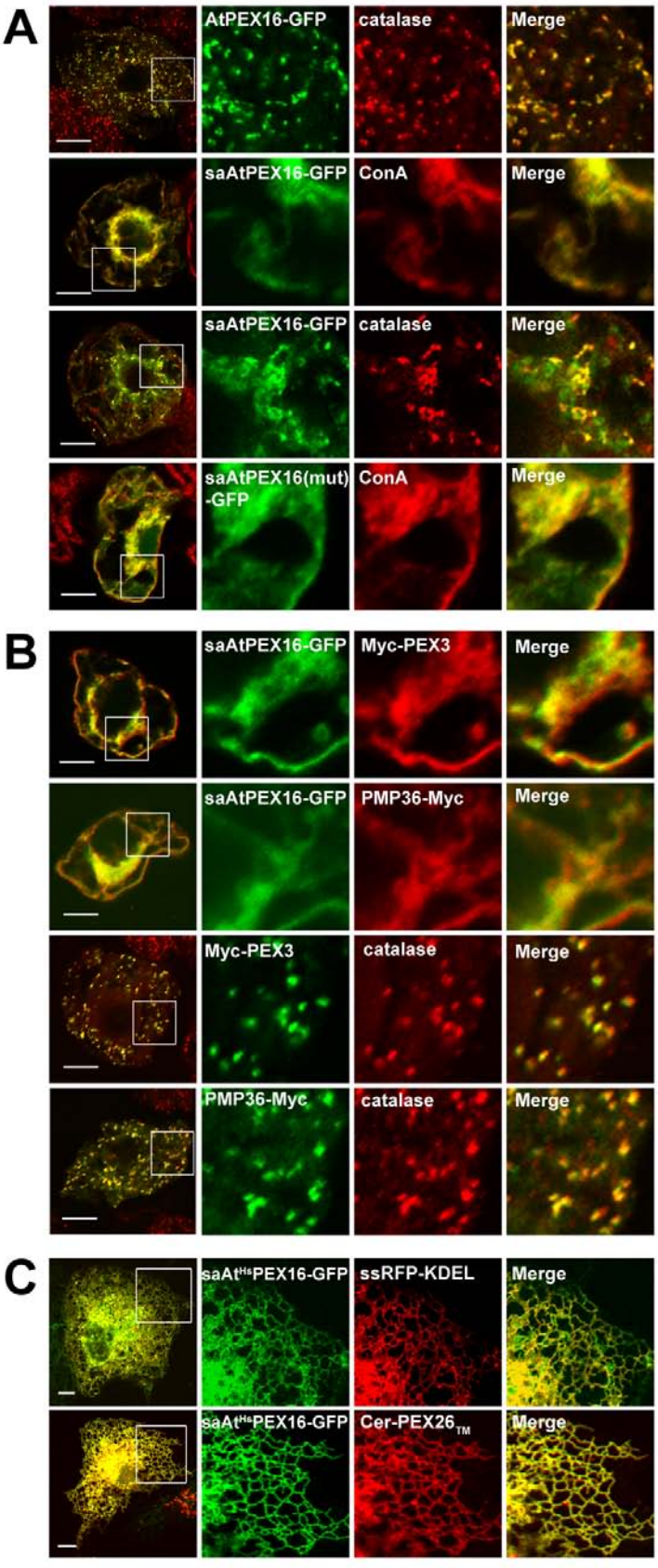

Figure 3.9 PEX16 recruits PMPs to the ER in plant cells.
(A and B) Representative images of plant (*Nicotiana tabacum*) suspension-cultured cells transiently-(co)expressing (as indicated by panel labels) (A) AtPEX16-GFP, saAtPEX16-GFP, or saPEX16(mut)-GFP and either immunostained for endogenous peroxisomal catalase or stained with fluor-conjugated ConA serving as an ER marker. (B) saAtPEX16-GFP and/or Myc-PEX3 or PMP36-Myc, or immunostained for endogenous catalase. All cells in (A and B) were formaldehyde fixed and processed for immunostaining 4 h after transformation, with the exception of the cells shown in the bottom two rows of (A) which were fixed and immunostained 8 h after transformation.
(C) Representative images of COS7 cells transiently-(co)expressing saAt^{Hs}PEX16-GFP, and ssRFP-KDEL or Cer-PEX26$_{TM}$. Cells in (C) were imaged 24 h after transfection. Shown in the panels on the left in (A-C) are the low magnification merged images; boxes represent the portions of the cells shown at higher magnification and as individual micrographs in the panels to the right, including the corresponding merged image. Scale bars, 10 μm.

3.8 Amino acid residues 66-103 in PEX16 mediate the recruitment of PMPs to the ER

Next, to search for the specific region(s) in human PEX16 responsible for recruiting PMPs to the ER, we co-expressed selected mutant versions of PEX16 (see Fig. 3.1A) in the context of saPEX16-GFP along with Cer-PEX26$_{TM}$ in COS7 cells. Then we quantified protein colocalization at the ER using the Manders' colocalization coefficient of the GFP signal (M_{GFP}), which represents the fraction of the intensities of GFP pixels that coincide with Cerulean pixels attributable to the co-expressed saPEX16-GFP mutant protein and Cer-PEX26$_{TM}$, respectively. As such, our expectation was that the recruitment of Cer-PEX26$_{TM}$ to the ER by wild-type saPEX16-GFP would yield a high degree of colocalization and hence a high M_{GFP} value. However, disruption in the recruitment of Cer-PEX26$_{TM}$ to the ER by mutating the region(s) in saPEX16-GFP responsible for PMP recruitment would yield a low degree of colocalization and a correspondingly low M_{GFP} value.

When Cer-PEX26$_{TM}$ (which localizes readily to peroxisomes [Fig. 3.7A]) was co-expressed with the peroxisomal marker UB-GFP-SKL, the two peroxisome-localized proteins yielded an average M_{GFP} value of 0.52 ± 0.02 (Fig. 3.10B). By contrast, co-expression of Cer-PEX26$_{TM}$ with the ER marker ssGFP-KDEL yielded an average M_{GFP} value of 0.05 ± 0.01 (Fig. 3.10B). As shown also in Fig. 3.10 and consistent with results presented above (Fig. 3.7A), Cer-PEX26$_{TM}$ readily colocalized with saPEX16-GFP at the ER (Fig. 3.10A) and yielded an average M_{GFP} value of 0.59 ± 0.05 (Fig. 3.10B). Taken together, these results confirm that measurements of the M_{GFP} value are a reliable and quantifiable indicator of not only protein colocalization in COS7 cells, but also the recruitment of Cer-PEX26$_{TM}$ to the ER by saPEX16-GFP.

Based on Manders' coefficient M_{GFP} values, we observed that saPEX16NT-GFP recruited Cer-PEX26$_{TM}$ to the ER to the same extent as full-length saPEX16-GFP (Fig. 3.10), indicating that the N-terminal half of PEX16 (i.e., amino acids 1-170 [see Fig. 3.1A]) is sufficient for recruiting PMPs to the ER. We next co-expressed Cer-PEX26$_{TM}$ with one of the two saPEX16NT-GFP mutants whereby its TM1 domain was either deleted (i.e., saPEX16NT(ΔTM1)-GFP) or replaced with the TM domain of Vamp1A (i.e., saPEX16(1-

109)-Vamp1A(TM)-GFP). As shown in Fig. 3.10, Cer-PEX26$_{TM}$ did not colocalize with saPEX16NT(ΔTM1)-GFP (M_{GFP} = 0.10 ± 0.06), but did colocalize with saPEX16(1-109)-Vamp1A(TM)-GFP (M_{GFP} = 0.62 ± 0.01), indicating that TM1 of PEX16 is not specifically necessary for PMP recruitment to the ER. As expected, Cer-PEX26$_{TM}$ did not colocalize with Vamp1A-GFP at the ER (M_{GFP} = 0.08 ± 0.02) (Fig. 3.10). Furthermore, PEX16(100-170)-GFP, which includes the region within PEX16 responsible for its initial targeting to the ER, i.e., residues 100-170 (Fig. 3.1E), did not recruit Cer-PEX26$_{TM}$ to the ER (M_{GFP} = 0.08 ± 0.01) (Fig 3.10).

Based on the results above for saPEX16(1-109)-Vamp1A(TM)-GFP and PEX16(100-170)-GFP, we reasoned that the region(s) within PEX16 responsible for recruitment of PMPs to the ER is located within its N-terminal, cytosolic-facing 109 amino-acid-long sequence. To test this possibility, we deleted three specific stretches of amino acid residues from this region in saPEX16NT-GFP, yielding saPEX16NT(Δ1-65)-GFP, saPEX16NT(Δ66-81)-GFP, and saPEX16NT(Δ83-103)-GFP (see Fig. 3.1A). As shown in Fig. 3.10, deletion of residues 66-81 or 83-103 from saPEX16NT-GFP significantly diminished its ability to recruit Cer-PEX26$_{TM}$ to the ER, whereas the deletion of the first 65 residues from saPEX16NT-GFP had no apparent effect as compared to saPEX16NT-GFP, suggesting that amino acid residues 66-103 in PEX16 are responsible for recruiting PMPs to the ER. Interestingly, the relatively high average M_{GFP} attributable to saPEX16NT(Δ66-81) (M_{GFP} = 0.23 ± 0.05) and saPEX16NT(Δ83-103) (M_{GFP} = 0.24 ± 0.01) compared to the negative controls (i.e., ssGFP-KDEL and Vamp1A-GFP), suggested that the putative PMP recruitment domain in PEX16 overlaps somewhere between residues 66-81 and 83-103. To test this premise, we generated another mutant version of saPEX16NT-GFP whereby all the amino acids within the 66 to 103 sequence in PEX16 were replaced with a random series of residues. As shown in Fig. 3.10, saPEX16NT(66-103R)-GFP did not recruit Cer-PEX26$_{TM}$ to the ER (M_{GFP} = 0.08 ± 0.02), reinforcing the notion that the 66-103 amino acid sequence in PEX16 contains the region necessary for PMP recruitment to the ER.

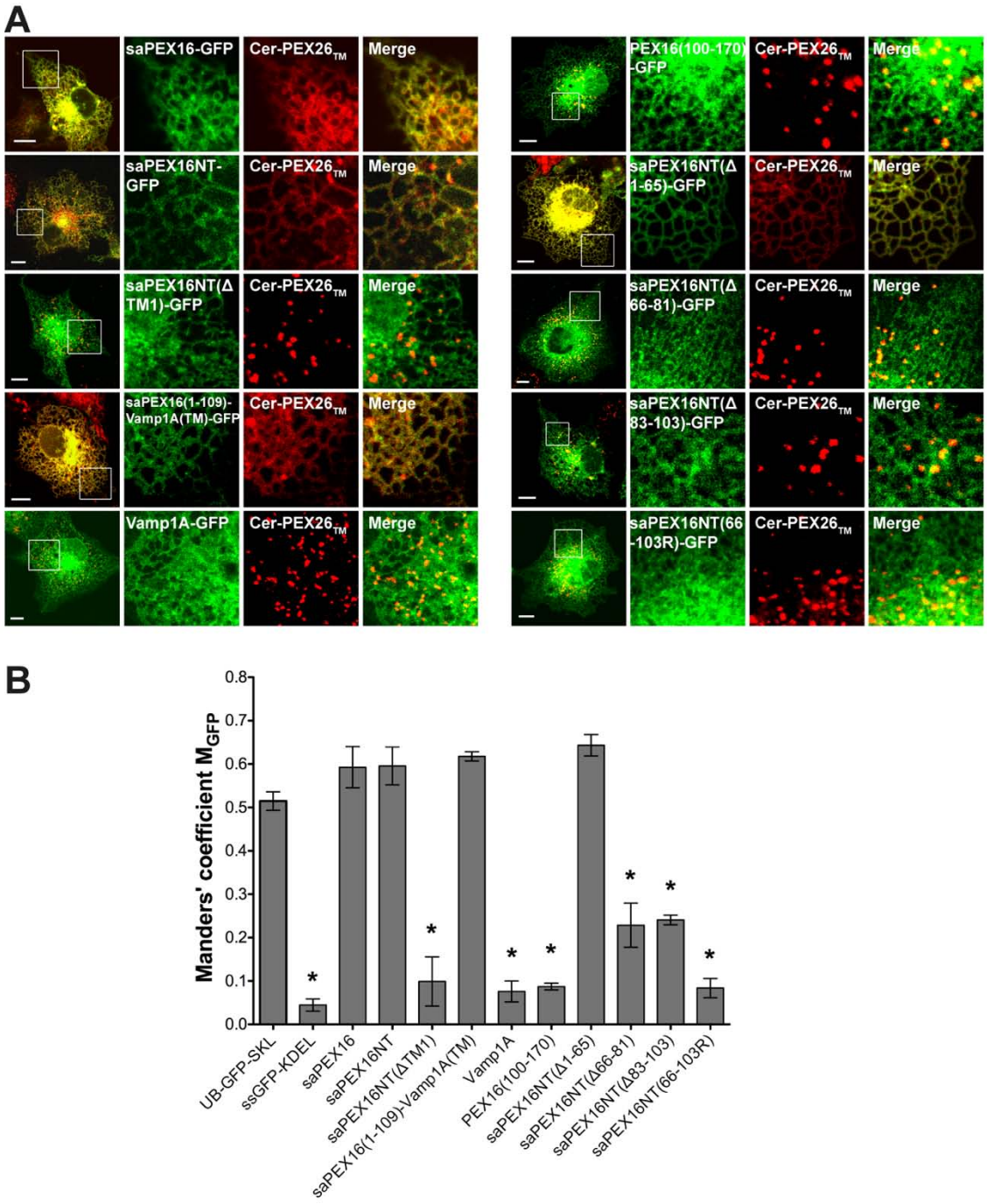

Figure 3.10 Residues 66-103 in PEX16 participate in the recruitment of PMPs to the ER.
(A) Representative images of COS7 cells transiently-(co)expressing Cer-PEX26$_{TM}$ and either full-length saPEX16-GFP or a mutant version thereof, or full-length Vamp1A-GFP. Shown in the panels on the left are the low magnification merged images; boxes represent the portions of the cells shown at higher magnification and as individual micrographs in the panels to the right, including the corresponding merged image. Scale bars, 10 μm.
(B) Bar graph illustrating the Manders' colocalization coefficient M_{GFP} values for Cer-PEX26$_{TM}$ and each of the above mentioned GFP fusion proteins from (A), as well as UB-GFP-SKL and ssGFP-KDEL, serving as positive and negative controls, respectively. M_{GFP} values for each set of co-expressed proteins were based on analysis of 60 cells from three separate transfections (N=3 ± standard deviation). Student's t-test. * P<0.01 as compared to M_{GFP} value of full-length saPEX16-GFP.

3.9 Discussion

In *S. cerevisiae*, the role of the ER in peroxisome biogenesis in wild-type cells is unclear. While one current model suggests that the ER plays a role in providing lipids and at least a subset of PMPs to pre-existing peroxisomes, allowing them to grow and divide (203), another model suggests that the ER is solely responsible for the formation of all peroxisomes *de novo* without communicating with pre-existing peroxisomes (73). Whatever the situation is in *S. cerevisiae*, results to date suggest that, in mammalian cells, most PMPs can sort to pre-existing peroxisomes via the ER (78). Furthermore, the ER-to-peroxisome trafficking of PMPs in mammals appears to be dependent on PEX16, whereby PEX16 itself targets initially to the ER and does so in a co-translational manner. Thereafter, at the ER, PEX16 appears to recruit other PMPs and together they traffic to peroxisomes in a yet-to-be identified manner (78). Here, we extend the role of PEX16 and the ER in peroxisome biogenesis in mammalian cells by identifying the regions within human PEX16 that are required for its intracellular trafficking and the recruitment of other PMPs to the ER.

3.9.1 Targeting signals involved in the intracellular trafficking of PEX16

Using deletion and replacement mutagenesis in combination with CLSM imaging of living cells, we identified the targeting signals within PEX16 that are responsible for its localization to the ER and subsequent localization to peroxisomes from the ER. More specifically, we found that the first of the two putative TM domains within PEX16 is both necessary and sufficient for its initial targeting to the ER (Fig. 3.1). Based on the membrane topology of PEX16, which exposes both its N- and C-termini towards the cytosol (102), and the fact that PEX16 targets to the ER in a co-translational manner (77, 78), TM1 likely serves as a type II signal-anchor sequence, and its second TM domain (i.e., TM2) likely serves as an internal stop-transfer sequence (204).

Previously, amino acid residues 66-81 in human PEX16, which include a distinct cluster of positively-charged residues, along with the adjacent TM1, were reported to be responsible for the direct targeting of PEX16 to peroxisomes from the cytosol (101, 102). Here, we further delineated the peroxisomal targeting signal within this region of PEX16 to residues 71-81 (Fig. 3.4 and 3.5). However, we propose that this refined targeting signal within PEX16 is

not a so-called type 1 peroxisomal membrane targeting signal (mPTS1) that is responsible for targeting PMPs directly to peroxisomes from the cytosol as suggested previously for PEX16 (66). Instead, residues 71-81 in PEX16 appear to serve as an mPTS2, which requires the PMP to be targeted first to the ER (via an ER targeting signal) before it can be directed to peroxisomes (63, 66). Support for this conclusion comes in part from our observation that the targeting of PEX16 to peroxisomes requires its ER targeting signal. As mentioned above, we showed that deletion of its ER targeting information (i.e., TM1) results in PEX16 being mislocalized to the cytosol and mitochondria (Fig. 3.1C&D), while replacing its TM1 with the ER targeting sequence of Vamp1A did not affect the peroxisomal localization of PEX16 (Fig. 3.6). Furthermore, we previously showed that the rate at which PEX16 targets to peroxisomes is similar to that of a modified PMP (via an appended N-terminal signal sequence) that utilized the ER-to-peroxisome targeting pathway and had a slower rate as compared to a PMP that targets directly to peroxisomes from the cytosol (78). We also showed previously, using an *in vitro* targeting assay, that PEX16 targets to the ER in a co-translational manner, which is distinct from other PMPs that target in a strictly post-translational manner (57). Together, these findings suggest that PEX16 targets to peroxisomes exclusively via the ER.

Interestingly, the peroxisomal targeting signal of PEX16 appears to be conspicuously distinct from those found in other PMPs. That is, one of the defining features of other mPTS2s and most mPTS1s characterized to date is a cluster of positively-charged amino acid residues adjacent to a TM domain that are essential for peroxisomal targeting (63, 65-67). However, we found that replacement of the positively-charged residues within the PEX16 peroxisomal targeting signal (i.e., residues 71-81) with non-charged alanines did not affect its peroxisomal targeting (Fig. 3.5B). This implies that PEX16, compared to other mPTS2-bearing PMPs, might rely on a unique trafficking pathway for sorting from the ER to peroxisomes. The nature of this pathway, as well as the precise physicochemical features within the peroxisomal targeting signal of PEX16, are important open questions, and which may be addressed through comparative analysis of the peroxisomal targeting signals in other PEX16 homologs that also sort to peroxisomes via the ER, particularly plant (*A. thaliana*) and yeast (*Yarrowia lipolytica*) PEX16 (72, 174).

3.9.2 PEX16-mediated PMP recruitment to the ER

Previously, we reported that human PEX16 recruits both PEX3 and PMP34 to the ER (77, 78). Consistent with these results, here we showed that PEX16 is capable of recruiting a wide range of other PMPs to the ER, including PEX26, PEX10 and PEX11β, as well as FIS1, a PMP that also localizes to mitochondria (29) (Fig. 3.7). Similarly, we showed that *A. thaliana* PEX16, which targets to peroxisomes via the ER (31), is also capable of recruiting at least two PMPs, i.e., PEX3 and PMP36, to the ER in plant cells (Fig. 3.9), suggesting that the PMP recruitment function of PEX16 at the ER is evolutionarily conserved at least between mammals and plants.

Based on a comprehensive mutational analysis of human PEX16 (Fig. 3.10), we further showed that a specific domain within the protein (i.e., residues 66-103) is necessary for its PMP recruitment function at the ER. Interestingly, this region alone is not sufficient for recruiting PMPs to the ER. Instead, PEX16 also requires a TM domain adjacent to residues 66-103 for it to properly function in PMP recruitment at the ER. In fact, it appears that any TM domain adjacent to residues 66-103 is sufficient as part of the PMP recruitment domain, since replacing TM1 in PEX16 with the TM domain of Vamp1A was also sufficient to recruit PMPs. Taken together, this suggests that the TM domain serves a role in the ability of the PMP recruitment domain to function properly by providing the necessary structural context and/or ensuring the proper membrane topology of PEX16.

We also found that PMP recruitment to the ER by PEX16 does not appear to require PEX3 and/or PEX19 (Fig. 3.7E&F). We showed that Cer-PEX26$_{TM}$ mislocalized to the mitochondria in cells absent of peroxisomes, but localized to the ER when co-expressed with ER-localized PEX16 in both *pex3*- and *pex19*- deficient cell lines (Fig. 3.7E&F). Similar results were observed for PMP34 (Fig. 3.8A&B). This suggests that the molecular mechanisms underlying PEX16 recruitment of PEX3 and other PMPs to the ER differs from that at peroxisomes. Similarly, the apparent lack of involvement of PEX19 in PMP targeting to the ER suggests that other cytosolic component(s) either serves as the chaperone, or is able to compensate for PEX19, similar to how HSP70s participate in the import of peroxisomal matrix proteins (205).

3.9.3 Future directions

Currently, it remains unclear how PEX16 recruits other PMPs from the cytosol to the ER and how PEX16 along with other PMPs are eventually transported from the ER to peroxisomes. Recently, Sec16B was reported to play a role in the latter process (84). However, overall how Sec16B operates in this regard and, thus, participates in the interrelationship of the ER and peroxisomes is not yet known. This question might begin to be addressed through detailed analysis of the putative PEX16 interactome. Such information will provide the framework to understand the molecular mechanism of the ER-to-peroxisome pathway, as the cell likely employs a highly regulated network of proteins in addition to PEX16 to constitutively provide pre-existing peroxisomes with proteins, lipids and metabolites for their functions and maintenance.

Chapter 4

VAPs and ACBD5 tether peroxisomes to the ER for peroxisome maintenance and lipid homeostasis

This chapter is adapted from an article originally published as:

- Hua R., Cheng D., Coyaud É., Freeman S., Pietro E.D., Wang Y., Vissa A., Yip C.M., Fairn G.D., Braverman N., Brumell J.H., Trimble W.S., Raught B., Kim P.K. 2017. VAPs and ACBD5 tether peroxisomes to the ER for peroxisome maintenance and lipid homeostasis. *Journal of Cell Biology*. 216(2): 367-377.

Acknowledgements:

- The PEX16 BioID analysis (Fig. 4.1A) was performed by Étienne Coyaud.
- The SIM images (Fig, 4.1F) were acquired by Adrian Vissa.
- The peroxisome mobility analysis (Fig. 4.4D-E and 4.6A) was performed by Peter Kim and Spencer Freeman.
- The measurement of plasmalogens and VLCFAs (Fig. 4.6B-E and 4.8A-B) was performed by Erminia Di Pietro.
- The western blots in Fig. 4.5C were performed by Derrick Cheng.

4.1 Introduction

Peroxisomes are unique among the endomembrane organelles due to their semi-autonomous nature. They are capable of importing newly synthesized peroxisomal matrix (lumen) proteins directly from the cytosol, and multiply in numbers by the growth and division of existing peroxisomes (206-208). However, like other organelles of the endomembrane system, peroxisomes depend on the ER for their lipid composition and also receive some of their membrane proteins from the ER (40). Similarly, the ER receives lipid precursors required for the biosynthesis of specialized lipids from peroxisomes. For example, the synthesis of plasmalogens, a class of ether phospholipids that represent about 20 % of the total phospholipid mass in humans, is initiated in the peroxisomes and completed in the ER (41). Furthermore, cholesterol is not only trafficked through peroxisomes, but peroxisomes may also synthesize precursors for cholesterol biosynthesis (42, 146).

Several models have been proposed as to how lipids and/or proteins are exchanged between the ER and peroxisomes (See Sections 1.3 and 1.4.2 for more detail). The earliest model is the shuttling of specific lipids to peroxisomes through the cytosol by lipid binding proteins such as carnitine transporters (209, 210). A vesicular model has recently been popularized with the discovery of peroxisomal protein-containing vesicles in various yeast (211, 212) that transport proteins from the ER to peroxisomes (207). Another mechanism of how peroxisomes interface with the ER may be through the ER-peroxisome membrane contact sites (MCSs) or tethers (38, 137). In budding yeast *S. cerevisiae* and the filamentous *Ascomycetes*, ER-peroxisome tethers are required for proper peroxisome inheritance (117, 213). Contact sites mediated by two proteins, Pex30p and Pex31p, are reported to play a role in peroxisome growth in a number of yeast (43-45). However, no known homologue of Pex30p and Pex31p have been identified in mammalian cells. In mammalian cells, contacts between peroxisomes and lysosomes were shown to be necessary for cholesterol trafficking from lysosomes to peroxisomes (146). However, whether peroxisomes and the ER exchange lipids in mammalian cells is not known.

Previously (See Chapter 3), we have shown that a key peroxisomal biogenesis protein, PEX16, initially targets to the ER before being trafficked to peroxisomes (77-79). We also

showed that PEX16 recruits peroxisomal membrane proteins to the ER before being trafficked to existing peroxisomes, suggesting that PEX16 may be interacting with components involved in trafficking of proteins and lipids between the two organelles. To understand the mechanism(s) by which the ER and peroxisomes communicate with each other, we carried out a screen to identify both proximal and interacting proteins of PEX16. Along with peroxisomal membrane proteins, we identified the VAMP-associated proteins A and B (VAPA and VAPB), which are ER resident proteins involved in organelle tethering to the ER. Here, we show that the VAPs serve to tether peroxisomes to the ER through their interaction with the peroxisomal membrane protein acyl-CoA binding domain containing 5 (ACBD5). Furthermore, we present evidence of the importance of this ER-peroxisome tether for both peroxisome maintenance and lipid homeostasis.

4.2 A proximity interaction network for PEX16

As PEX16 recruits other peroxisomal membrane proteins to the ER and subsequently transports them to peroxisomes (188), we reasoned that identifying PEX16 interacting partners could allow us to discover other polypeptides that are important for ER-peroxisome communication. To this end, we conducted BioID (proximity-dependent biotinylation coupled with mass spectrometry) analysis on PEX16 (177, 214, 215). Briefly, BioID is a newly developed method for the identification of protein-protein interactions in living cells. It utilizes a mutant biotin conjugating enzyme (BirA*) in *E. coli*. that is fused to a protein of interest (bait), in our case PEX16 (i.e., FlagBirA*-PEX16). When expressed in living cells and stimulated by excess biotin, the BirA* moiety will efficiently activate biotin, so that biotinoyl-AMP diffuses away and reacts with nearby amine groups including those present on lysine residues in neighboring proteins. In other words, BirA* will promiscuously biotinylated proteins in a proximity-dependent manner. Following cell lysis, the biotinylated proteins will be purified using streptavidin and analyzed by mass spectrometry (176, 177).

By using the BioID assay, we identified 70 high confidence proximal interactors for PEX16, including 17 of the 25 known peroxisomal membrane proteins (103) (Fig. 4.1A and Table 4.1), suggesting that the dataset comprises biologically relevant polypeptides. Notably, the interactors also include the organelle tethering proteins VAPA and VAPB. The VAPs form

Table 4.1 High confidence FlagBirA*-PEX16 interacting proteins. (Summary Tab) High confidence interacting partners identified in BioID conducted on 293 T-REx cells expressing FlagBirA*-PEX16 (BFDR <0.01 and identified with >2 unique peptides). (Raw data Tab) Raw spectral counts for control and PEX16 BioID analyses (TPP>0.90). Bait data highlighted in yellow.

							PEX16 BioID					
							pool A		pool B			
Gene ID	Protein ID	Gene Name		Category	Control runs		tech#1	tech#2	tech#1	tech#2	Total	SAINT
9409	4758898	**PEX16**	*peroxisomal biogenesis factor 16*	*BAIT*			403	447	431	418	**1699**	**NA**
5825	4506341	**ABCD3**	*ATP binding cassette subfamily D member 3*	*peroxisome*	5	4	487	500	675	648	**2310**	**1.00**
23344	14149680	**ESYT1**	*extended synaptotagmin 1*	*ER*	2		228	226	171	177	**802**	**1.00**
3326	20149594	**HSP90AB1**	*heat shock protein 90 alpha family class B member 1*	*Other*	56	53	162	172	166	163	**663**	**1.00**
5824	302370946	**PEX19**	*peroxisomal biogenesis factor 19*	*peroxisome*			142	137	148	147	**574**	**1.00**
91452	203098629	**ACBD5**	*acyl-CoA binding domain containing 5*	*peroxisome*			110	120	145	137	**512**	**1.00**
10726	5729953	**NUDC**	*nuclear distribution C, dynein complex regulator*	*Other*	18	17	131	140	114	124	**509**	**1.00**
5195	4758896	**PEX14**	*peroxisomal biogenesis factor 14*	*peroxisome*			105	114	130	136	**485**	**1.00**
5830	196259776	**PEX5**	*peroxisomal biogenesis factor 5*	*peroxisome*			105	105	134	132	**476**	**1.00**
10059	171460914	**DNM1L**	*dynamin 1 like*	*peroxisome*			89	92	148	145	**474**	**1.00**
60	4501885	**ACTB**	*actin beta*	*Vesicle*			107	111	106	109	**433**	**1.00**
8504	4505727	**PEX3**	*peroxisomal biogenesis factor 3*	*peroxisome*			88	83	101	103	**375**	**1.00**
27101	60218913	**CACYBP**	*calcyclin binding protein*	*Vesicle*			68	68	54	49	**239**	**1.00**
54940	269914128	**OCIAD1**	*OCIA domain containing 1*	*Mitochondrion*			56	59	56	59	**230**	**1.00**
54839	312222716	**LRRC49**	*leucine rich repeat containing 49*	*Other*			50	58	61	57	**226**	**1.00**
91978	123173766	**TPGS1**	*tubulin polyglutamylase complex subunit 1*	*Other*			57	55	57	56	**225**	**1.00**
9352	4759274	**TXNL1**	*thioredoxin like 1*	*Mitochondrion*			68	61	41	36	**206**	**1.00**
224	73466520	**ALDH3A2**	*aldehyde dehydrogenase 3 family member A2*	*peroxisome*			49	50	51	55	**205**	**1.00**
10963	5803181	**STIP1**	*stress induced phosphoprotein 1*	*Other*	3		54	52	47	46	**199**	**1.00**
55968	20149635	**NSFL1C**	*NSFL1 cofactor*	*Other*			50	43	33	32	**158**	**1.00**
2010	4557553	**EMD**	*emerin*	*ER*	4	3	42	44	31	34	**151**	**1.00**
488	24638454	**ATP2A2**	*ATPase sarcoplasmic/endoplasmic reticulum Ca2+ transporting 2*	*ER*	7	4	30	32	40	46	**148**	**1.00**
3930	37595750	**LBR**	*lamin B receptor*	*Other*	13	10	38	38	37	35	**148**	**1.00**
79096	51558748	**C11orf49**	*chromosome 11 open reading frame 49*	*Other*	9	9	37	38	27	37	**139**	**1.00**
8471	4504733	**IRS4**	*insulin receptor substrate 4*	*Other*	3	3	25	28	42	44	**139**	**1.00**
10652	5730120	**YKT6**	*YKT6 v-SNARE homolog (S. cerevisiae)*	*Mitochondrion*			35	38	25	32	**130**	**1.00**
8165	4502015	**AKAP1**	*A-kinase anchoring protein 1*	*Mitochondrion*	3	2	27	28	36	36	**127**	**1.00**
7415	6005942	**VCP**	*valosin containing protein*	*ER*			32	30	23	24	**109**	**1.00**
5770	4506289	**PTPN1**	*protein tyrosine phosphatase, non-receptor type 1*	*ER*			31	23	27	26	**107**	**1.00**
57650	190194355	**KIAA1524**	*KIAA1524*	*Other*	2		29	21	27	25	**102**	**1.00**
6836	19557691	**SURF4**	*surfeit 4*	*ER*	6	5	24	21	24	28	**97**	**1.00**
10985	54607053	**GCN1L1**	*GCN1, eIF2 alpha kinase activator homolog*	*Other*	4	4	21	21	28	25	**95**	**1.00**
10424	291621647	**PGRMC2**	*progesterone receptor membrane component 2*	*Other*	5	4	39	29	12	15	**95**	**0.84**
23386	122939165	**NUDCD3**	*NudC domain containing 3*	*Other*			27	30	19	16	**92**	**1.00**
65084	281182571	**TMEM135**	*transmembrane protein 135*	*peroxisome*			16	15	31	28	**90**	**1.00**
5194	4505723	**PEX13**	*peroxisomal biogenesis factor 13*	*peroxisome*			17	22	26	22	**87**	**1.00**
5189	4505725	**PEX1**	*peroxisomal biogenesis factor 1*	*peroxisome*			12	14	31	24	**81**	**1.00**
9217	4759302	**VAPB**	*VAMP associated protein B and C*	*ER*			23	26	15	12	**76**	**1.00**
57506	83776598	**MAVS**	*mitochondrial antiviral signaling protein*	*peroxisome*			20	13	25	17	**75**	**1.00**
9218	94721252	**VAPA**	*VAMP associated protein A*	*ER*			18	26	19	12	**75**	**1.00**
6767	19923193	**ST13**	*suppression of tumorigenicity 13 (colon carcinoma) (Hsp70 interacting protein)*	*Vesicle*			18	20	16	16	**70**	**1.00**
10273	56181387	**STUB1**	*STIP1 homology and U-box containing protein 1*	*ER*			18	19	18	14	**69**	**1.00**
10910	195963398	**SUGT1**	*SGT1 homolog, MIS12 kinetochore complex assembly cochaperone*	*Other*	3		22	19	15	13	**69**	**0.99**

2288	4503729	**FKBP4**	*FK506 binding protein 4*	*Mitochondrion*	4		23	16	13	17	**69**	**0.97**
10890	256222019	**RAB10**	*RAB10, member RAS oncogene family*	*Vesicle*	6		14	14	19	19	**66**	**0.87**
64786	226342869	**TBC1D15**	*TBC1 domain family member 15*	*Vesicle*	3	3	19	17	13	15	**64**	**1.00**
9524	24475816	**TECR**	*trans-2,3-enoyl-CoA reductase*	*ER*	3		16	18	17	13	**64**	**0.99**
23190	24307965	**UBXN4**	*UBX domain protein 4*	*ER*			20	16	14	13	**63**	**1.00**
11140	5901922	**CDC37**	*cell division cycle 37*	*Vesicle*			16	16	16	14	**62**	**1.00**
8799	296317239	**PEX11B**	*peroxisomal biogenesis factor 11 beta*	*peroxisome*			13	17	17	14	**61**	**1.00**
51337	7706200	**C8orf55**	*thioesterase superfamily member 6*	*Other*			12	11	16	18	**57**	**1.00**
55161	224589127	**TMEM33**	*transmembrane protein 33*	*ER*			10	8	16	13	**47**	**1.00**
56947	31377607	**MFF**	*mitochondrial fission factor*	*peroxisome*			11	9	13	12	**45**	**1.00**
3843	24797086	**IPO5**	*importin 5*	*Other*			10	11	10	11	**42**	**1.00**
5190	194018488	**PEX6**	*peroxisomal biogenesis factor 6*	*peroxisome*			9	4	15	14	**42**	**1.00**
134492	21687129	**NUDCD2**	*NudC domain containing 2*	*Vesicle*			11	11	10	9	**41**	**1.00**
23197	24797106	**FAF2**	*Fas associated factor family member 2*	*ER*			10	11	9	10	**40**	**1.00**
5757	151101404	**PTMA**	*prothymosin, alpha*	*Vesicle*			8	10	12	10	**40**	**1.00**
4747	105990539	**NEFL**	*neurofilament, light polypeptide*	*Other*			11	7	11	10	**39**	**1.00**
79777	13376029	**ACBD4**	*acyl-CoA binding domain containing 4*	*peroxisome*			9	9	9	9	**36**	**1.00**
7265	4507711	**TTC1**	*tetratricopeptide repeat domain 1*	*peroxisome*			9	10	9	7	**35**	**1.00**
8878	214830438	**SQSTM1**	*sequestosome 1*	*ER*			10	11	6	7	**34**	**1.00**
7266	221219056	**DNAJC7**	*DnaJ heat shock protein family (Hsp40) member C7*	*Vesicle*			6	7	10	10	**33**	**1.00**
2166	166795287	**FAAH**	*fatty acid amide hydrolase*	*ER*			9	10	5	9	**33**	**1.00**
9532	4757834	**BAG2**	*BCL2 associated athanogene 2*	*Other*			9	7	8	8	**32**	**1.00**
10476	51479152	**ATP5H**	*ATP synthase, H+ transporting, mitochondrial Fo complex subunit D*	*Mitochondrion*			5	6	6	7	**24**	**1.00**
29097	7661824	**CNIH4**	*cornichon family AMPA receptor auxiliary protein 4*	*ER*			10	7	5	2	**24**	**0.99**
11260	8051636	**XPOT**	*exportin for tRNA*	*Other*			7	2	4	8	**21**	**0.99**
10113	7019503	**PREB**	*prolactin regulatory element binding*	*ER*			8	6	3	2	**19**	**0.98**
60412	82546830	**EXOC4**	*exocyst complex component 4*	*Vesicle*			5	4	4	5	**18**	**1.00**
5707	25777600	**PSMD1**	*proteasome 26S subunit, non-ATPase 1*	*Vesicle*			7	4	4	3	**18**	**1.00**
55627	102467484	**SMPD4**	*sphingomyelin phosphodiesterase 4*	*ER*			4	2	4	6	**16**	**0.99**

homodimers or heterodimers on the ER, and are found at the MCSs between the ER and many other organelles, including the plasma membrane (161), the Golgi apparatus (107), mitochondria (155), and endosomes (153, 154) (see Section 1.5 for more detail). To date, it is not known whether VAPs are also required for the formation of an ER-peroxisome tether.

4.3 VAPs are juxtaposed to peroxisomes on the ER

To determine whether the VAPs are localized at or near the site of ER-peroxisome contact, we first examined their subcellular localization in mammalian cells. When expressed in COS7 cells, both VAPB-GFP (Fig. 4.1B) and VAPA-GFP (Fig. 4.2A) displayed ER localization as seen by their colocalization with the ER marker ssRFP-KDEL. Interestingly, despite the strong co-localization, the VAPs appeared more punctate. Examination of endogenous VAPB in COS7 cells showed that most VAPB is localized to punctate structures (Fig. 4.1C). To determine whether these VAP puncta colocalized with peroxisomes, we co-expressed VAPB-GFP (Fig. 4.1D) or VAPA-GFP (Fig. 4.2A) with the peroxisomal marker UB-RFP-SKL, and found that some of the VAP puncta colocalized with peroxisomes. Similar colocalization of punctate structures with peroxisomes was also observed when we immunostained for endogenous VAPB (Fig. 4.1E). Remarkably, using a structured illumination super-resolution approach, we observed that most endogenous VAPB puncta do not perfectly overlap with the peroxisomal marker, but are in juxtaposition to peroxisomes (Fig. 4.1F).

As VAPs are reported to be ER resident proteins, we reasoned that the VAPs might be concentrating on the ER in juxtaposition to peroxisomes rather than being localized on peroxisomes. To test this, we performed a fluorescence recovery after photobleaching (FRAP) assay in COS7 cells co-expressing VAPB-GFP (Fig. 4.3A) or VAPA-GFP (Fig. 4.2C) with UB-RFP-SKL. We expected that if the peroxisome-localized VAP-GFP punctate structure is on the ER, then its fluorescence should rapidly recover upon photobleaching due to the influx of fluorescent molecules from other portions of the ER. However, those on peroxisomes will not recover during the short recovery time (~30 s). In this assay, the high 488 laser power used to photobleach the GFP also partially photobleached the UB-RFP-SKL signal (Fig. 4.3A and 4.2C). This served as an internal control for a fluorescence signal on

peroxisomes that should not recover during the duration of the FRAP assay. Consistent with our hypothesis, the signal for both VAPs on the punctate structures recovered to ~80 % of their initial levels in about 30 s after photobleaching, whereas the UB-RFP-SKL signal did not recover (Fig. 4.3B and 4.2D).

To validate this observation, we performed a fluorescence loss in photobleaching (FLIP) assay in COS7 cells co-expressing either VAPB-GFP (Fig. 4.3C) or VAPA-GFP (Fig. 4.2B) with UB-RFP-SKL. Here, we repeatedly photobleached a small region of the ER to deplete the entire ER of VAP-GFP signal. As the ER is inter-connected, the photobleaching should result in the loss of VAP-GFP signal on the entire ER, whereas VAP-GFP not localized to the ER will be protected. As seen in Fig. 4.3C and Fig. 4.2B, depleting the respective VAPB-GFP or VAPA-GFP signal from the ER resulted in the loss of the GFP fluorescence signal from the punctate structures colocalized with peroxisomes. However, the rate of depletion of VAPB-GFP signal associated with peroxisomes was slower than those in other portions of the ER (Fig. 4.3D&E), suggesting that the mobility of VAPB-GFP fluorescent molecules juxtaposed to peroxisomes was more constrained.

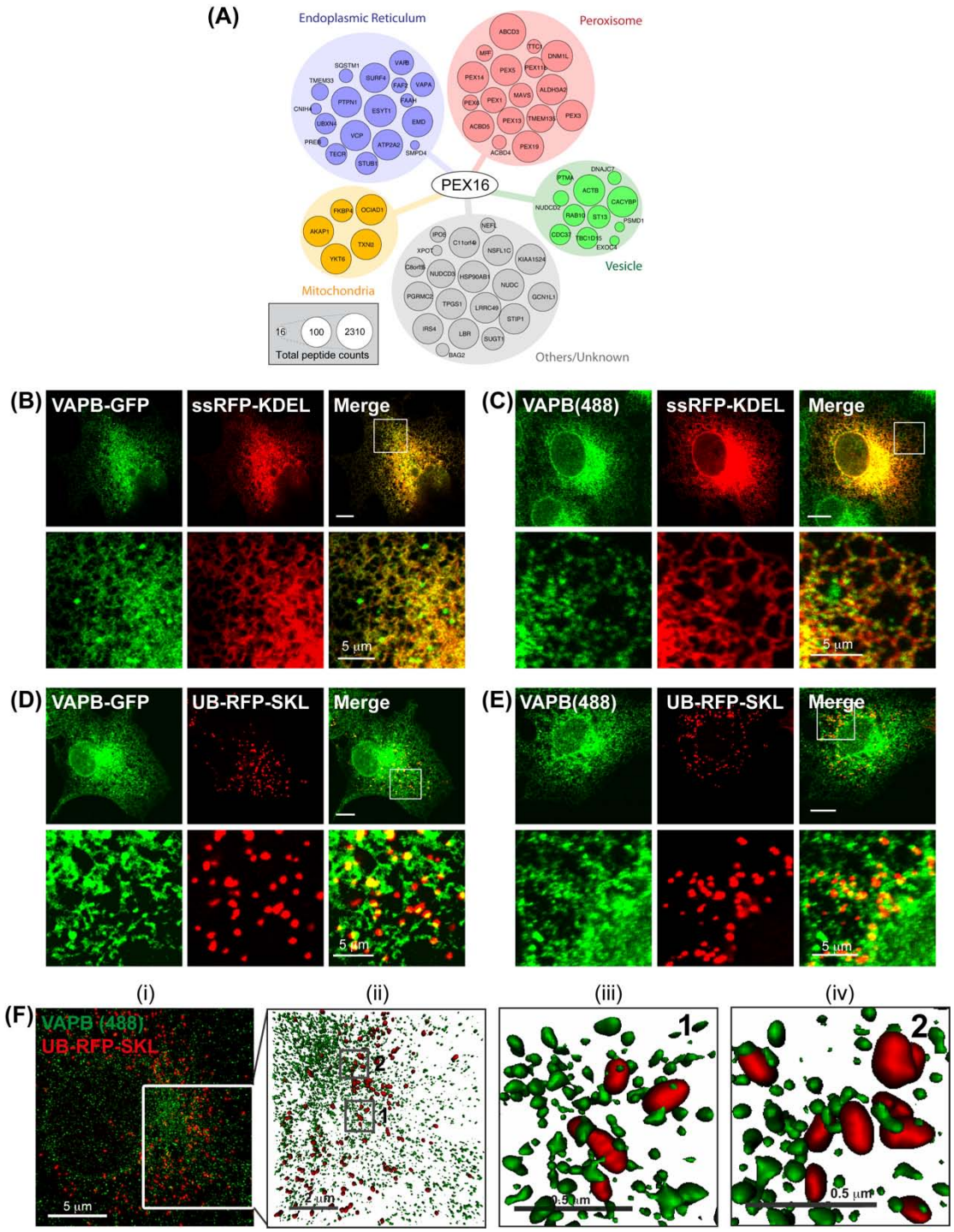

Figure 4.1 VAPB punctate structures colocalize with peroxisomes.

(A) PEX16 interactome. *In vivo* proximity-dependent biotinylation (BioID) was conducted on PEX16. High confidence interactors are displayed, categorized according to intracellular localization. Node size is proportional to peptide counts detected.

(B-E) COS7 cells transiently expressing ssRFP-KDEL (B,C) or UB-RFP-SKL (D,E) and either (co)expressing VAPB-GFP (B,D) or immunostained for endogenous VAPB (C,E). The white box indicates the magnified area shown below each panel. Scale bar, 10 μm or as indicated.

(F) From left to right: *(i)* Maximum intensity projection of VAPB-Alexa 488 (green) and UB-RFP-SKL (red) acquired via structured illumination microscopy. *(ii)* Surface projection of the region denoted in (i). Green: VAPB. Red: UB-RFP-SKL. Box denoted by 1 and 2 in (ii) are magnified in *(iii)* and *(iv)*. The surface projections demonstrate the apposition of the two organelles in 3D space.

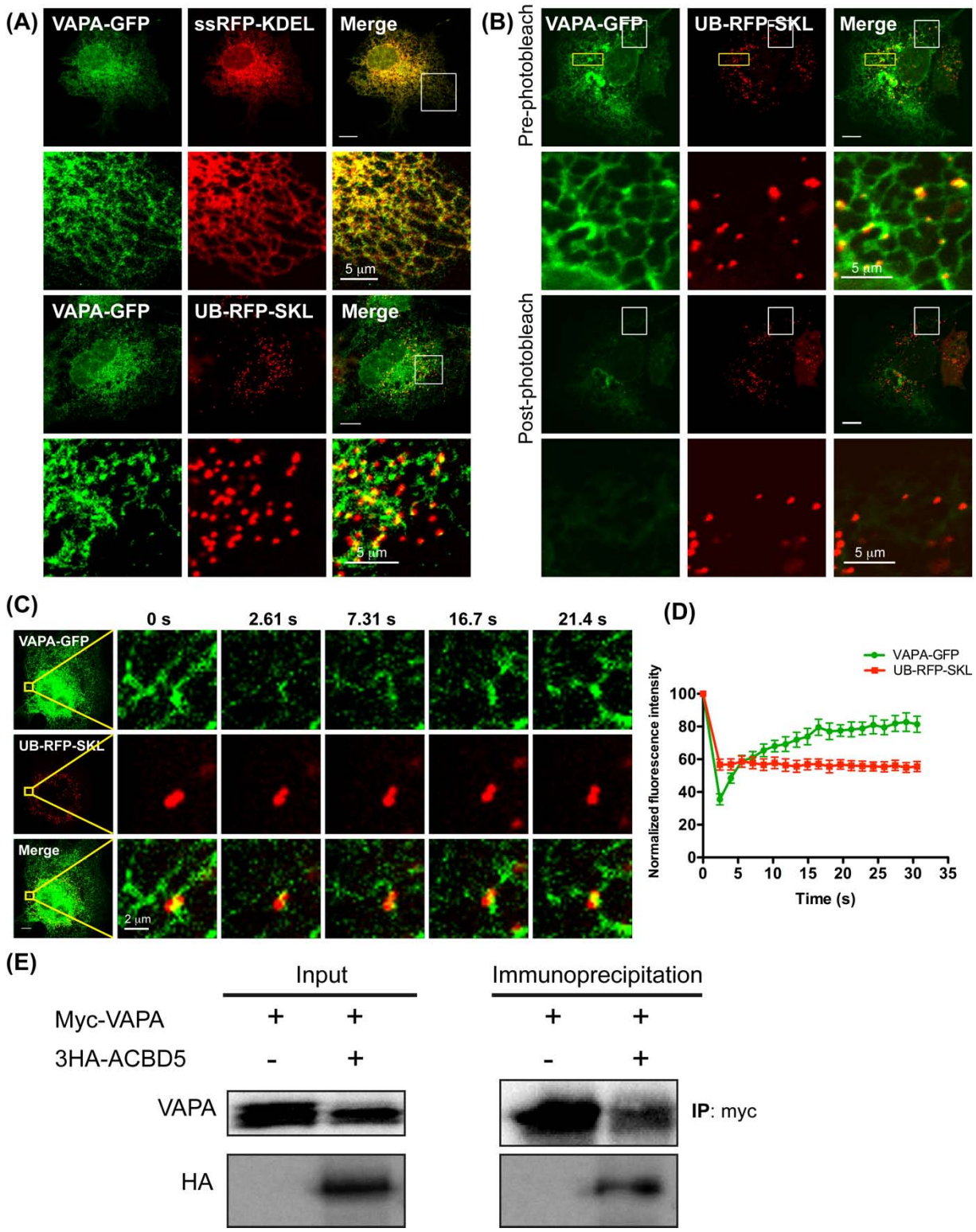

Figure 4.2 VAPA localizes in juxtaposition to peroxisomes on the ER and interacts with the peroxisomal protein ACBD5.

(A) Representative images of COS7 cells transiently (co)expressing VAPA-GFP, along with the ER or peroxisomal marker proteins, ssRFP-KDEL or UB-RFP-SKL.

(B) Representative images of FLIP assays performed with COS7 cells transiently (co)expressing VAPA-GFP and UB-RFP-SKL. Yellow box represents the region of interest (ROI) in the cell that was subjected to repeated photobleaching with a 488-nm laser light. Both the first frame before photobleaching (pre-photobleach) and the first image after repeated photobleaching (post-photobleach)

procedure are shown. (A and B) The white box indicates the magnified area shown below each panel. (C) FRAP assay was performed in a COS7 cell transiently (co)expressing VAPA-GFP and UB-RFP-SKL using a 488 nm laser light at full strength in a yellow rectangular region of interest (ROI). (D) FRAP curve. Shown is the normalized fluorescence intensity of VAPA-GFP and UB-RFP-SKL punctate structures within each ROI. All values are mean ± SD (n = 9). Scale bar, 10 μm. (E) Myc-VAPA and 3HA-ACBD5 co-immunoprecipitated in transfected HEK293T cells.

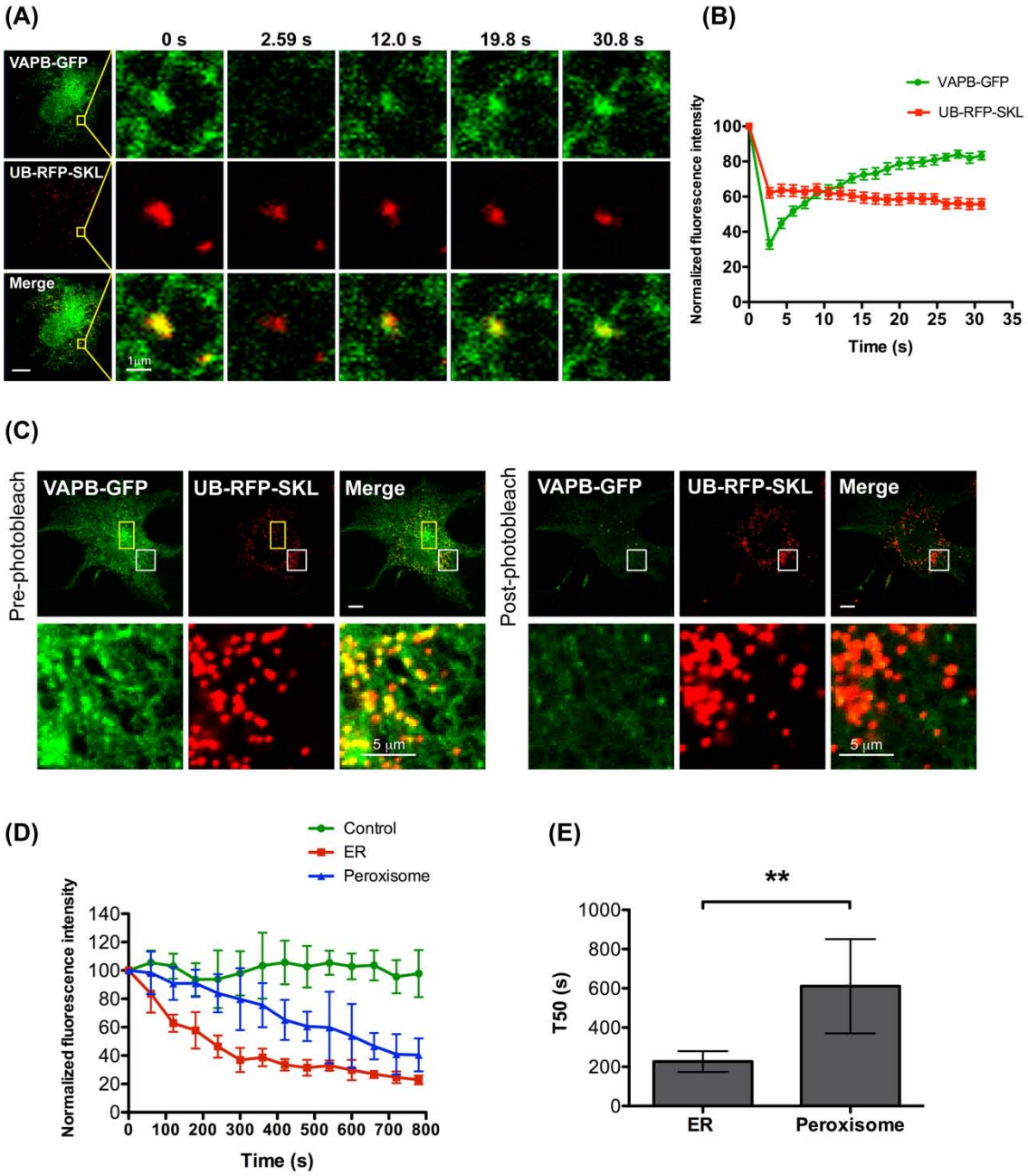

Figure 4.3 VAPB localizes in juxtaposition to peroxisomes on the ER.
(A) FRAP assay performed in a COS7 cell transiently (co)expressing VAPB-GFP and UB-RFP-SKL. Yellow rectangular indicates the photobleached ROI.
(B) FRAP curves. Shown is the normalized fluorescence intensity of VAPB-GFP and UB-RFP-SKL punctate structures within each ROI. Mean ± SD (n = 12).
(C) FLIP assay performed in a COS7 cell transiently coexpressing VAPB-GFP and UB-RFP-SKL in a yellow rectangular ROI. Shown is the first frame before photobleaching (pre-photobleach) and the first image after repeated photobleaching (post-photobleach). Scale bar, 10 μm or as indicated.
(D) FLIP curves. Shown is the normalized fluorescence intensity of VAPB-GFP punctate structure juxtaposed to a peroxisome (blue curve: peroxisome), and that of ER-localized VAPB-GFP (red curve: ER). The fluorescence intensity of VAPB-GFP in an adjacent cell from the same image serves as a control for imaging induced photobleaching (green curve: control). Mean ± SD (n = 6).
(E) Bar graph illustrating the time taken by the ER localized VAPB-GFP and peroxisomal VAPB-GFP in (D) to drop to 50 % of its original level. Mean ± SD (n = 6). **p < 0.01.

4.4 VAPs interact with ACBD5

We hypothesized that the constrained VAPs juxtaposed to peroxisomes was due to their interaction with a peroxisomal protein. VAPs are membrane-anchored proteins on the ER that are known to interact with proteins containing a 'two phenylalanines in an acidic tract' (FFAT) motif through their Major Sperm Protein (MSP) domain (158, 159). As PEX16 does not contain a FFAT domain, we examined the PEX16 BioID dataset (Fig. 4.1A) for a peroxisomal protein that possessed a FFAT domain. In the screen, we only found ACBD5 to contain a FFAT domain (216). Co-immunoprecipitation analysis of VAPs and ACBD5 in HEK293T cells showed that ACBD5 co-immunoprecipitated with both VAPB (Fig. 4.4A) and VAPA (Fig. 4.2E), but not with the FFAT mutant form of ACBD5, ACDB5(FFATmut) (Fig. 4.4A).

We next examined whether ACBD5 was responsible for the juxtaposition of VAPB to peroxisomes. In cells depleted of ACBD5, VAPB-GFP puncta juxtaposed to peroxisomes were no longer observed (Fig. 4.4B). Quantification of UB-RFP-SKL that colocalized with VAPB-GFP by Mander's coefficient showed a significant decrease in colocalization between VAPB-positive puncta and peroxisomes in cells depleted of ACBD5 (Fig. 4.4C). Interestingly, the expression of endogenous ACBD5 appears to depend on the VAPs as the depletion of both VAPs resulted in a significant decrease in ACBD5 level, suggesting that the VAPs may stabilize ACBD5 (Fig. 4.5A&B).

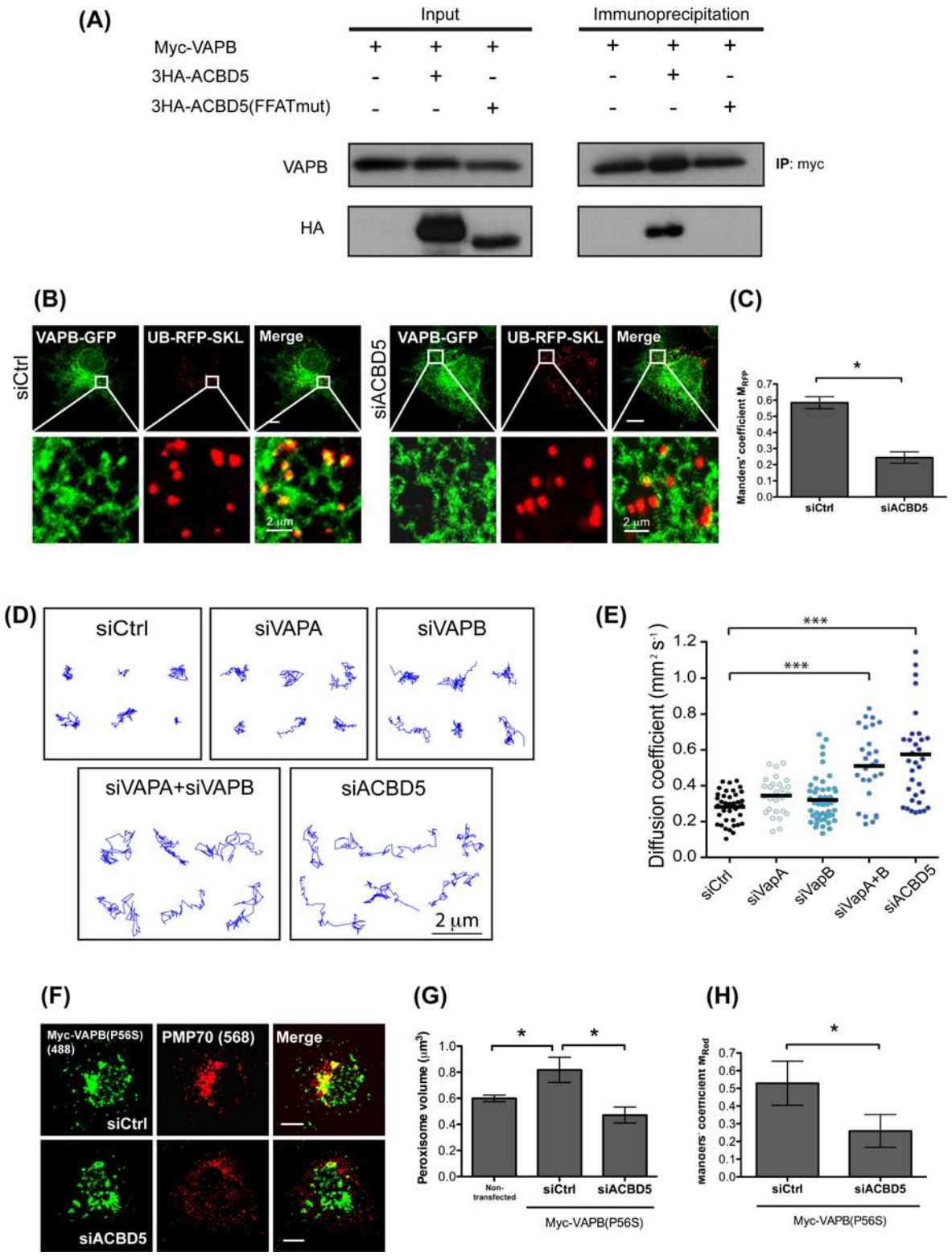

Figure 4.4 VAPB-ACBD5 tethers peroxisomes to the ER.

(A) Co-immunoprecipitation performed in HEK293 cells transiently expressing Myc-VAPB with WT or FFAT-motif mutant ACBD5.

(B) COS7 cells treated with indicated siRNAs, and co(expressing) VAPB-GFP and UB-RFP-SKL. Scale bar, 10 μm or as indicated.

(C) Bar graph illustrating the Manders' colocalization coefficient M_{RFP} for UB-RFP-SKL and VAPB-GFP in (B). Mean ± SD (n =3; 20 cells per trial). *$p < 0.05$

(D) Representative trajectories of HeLa cells treated with indicated siRNAs and expressing UB-RFP-SKL. Z stacks of single cells were acquired at 40 frames per min and the centers of peroxisomes were tracked over 2 min.
(E) The median diffusion coefficient of >27 cells from 3 experiments are graphed (dots) along with the mean (bars). Each video analyzed contained >30 trajectories and each condition >6000 trajectories. ***P < 0.001.
(F) COS7 cells treated with indicated siRNAs and expressing Myc-VAPB(P56S). Cells were immunostained for the Myc tag and endogenous peroxisomal PMP70. Scale bar, 10 μm.
(G and H) Quantification of average peroxisome volume (G) and the Manders' colocalization coefficient M_{RFP} for PMP70 and Myc-VAPB(P56S) in (F). Mean ± SD (n = 3; 20 cells per trial). *p < 0.05.

4.5 The VAP-ACBD5 interaction tethers peroxisomes to the ER

We next asked whether the VAP-ACBD5 interaction acts as a tether for peroxisomes to the ER. To test this hypothesis, we reasoned that if VAP-ACBD5 is indeed a tether for peroxisomes to the ER, then disrupting this interaction should result in an increase in peroxisome mobility. To evaluate peroxisome mobility, we determined the diffusion coefficient of peroxisomes in cells depleted of VAPs or ACBD5 in COS7 cells expressing UB-RFP-SKL. Cells depleted with either VAPA or VAPB did not show a visual change in the peroxisome mobility (Fig. 4.4D&E and 4.6A). However, a significant increase in both peroxisome mobility and diffusion coefficient was observed in cells depleted of both VAPs, or ACBD5 alone. Together with the localization and immunoprecipitation data, our results suggest that ACBD5 tethers peroxisomes to the ER through its interaction with the VAPs.

4.6 An ALS-associated VAPB mutant requires ACBD5 to induce peroxisome clustering

The proline-to-serine mutation in VAPB at position 56 (P56S) is linked to amyotrophic lateral sclerosis (ALS) (165, 217). Over-expressing mutant VAPB(P56S) has been shown to induce ER clustering with mitochondria, the Golgi and endosomes inside cells, and this clustering is thought to cause defects in the functions of these organelles (218). Similarly, we found that over-expression of this VAPB mutant resulted in peroxisome aggregation (Fig. 4.4F). The peroxisome clustering was validated by the increase in peroxisome volume compared to non-transfected cells (Fig. 4.4G). However, the clustering of peroxisomes (Fig. 4.4F&G) and colocalization between peroxisome and VAPB(P56S) aggregates (Fig. 4.4H) were not observed in cells depleted of ACBD5. These results further indicate that peroxisomes are tethered to the ER through ACBD5 interaction with VAPs.

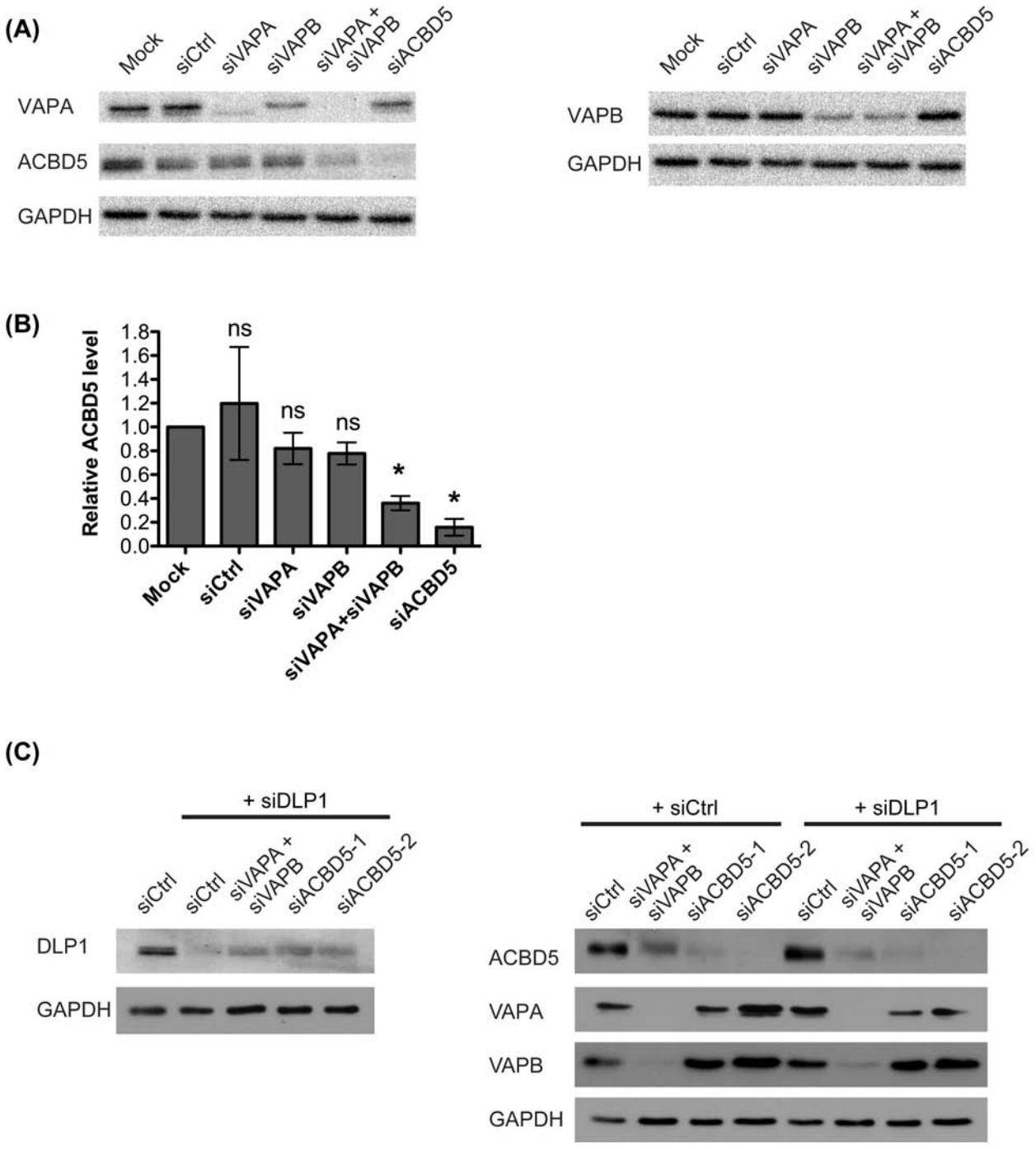

Figure 4.5 Validation of siRNA-mediated knockdowns.
(A) Western blots confirming the knockdowns of indicated proteins in HeLa cells
(B) Densitometry of ACBD5 protein level. The relative ACBD5 protein levels (normalized to the loading control, GAPDH) are based on analysis of three separated transfections (mean ± SD). *$p < 0.05$ as compared to relative ACBD5 levels in mock cells.
(C) Western blots confirming the knockdowns of indicated proteins in Fig. 4.7A.

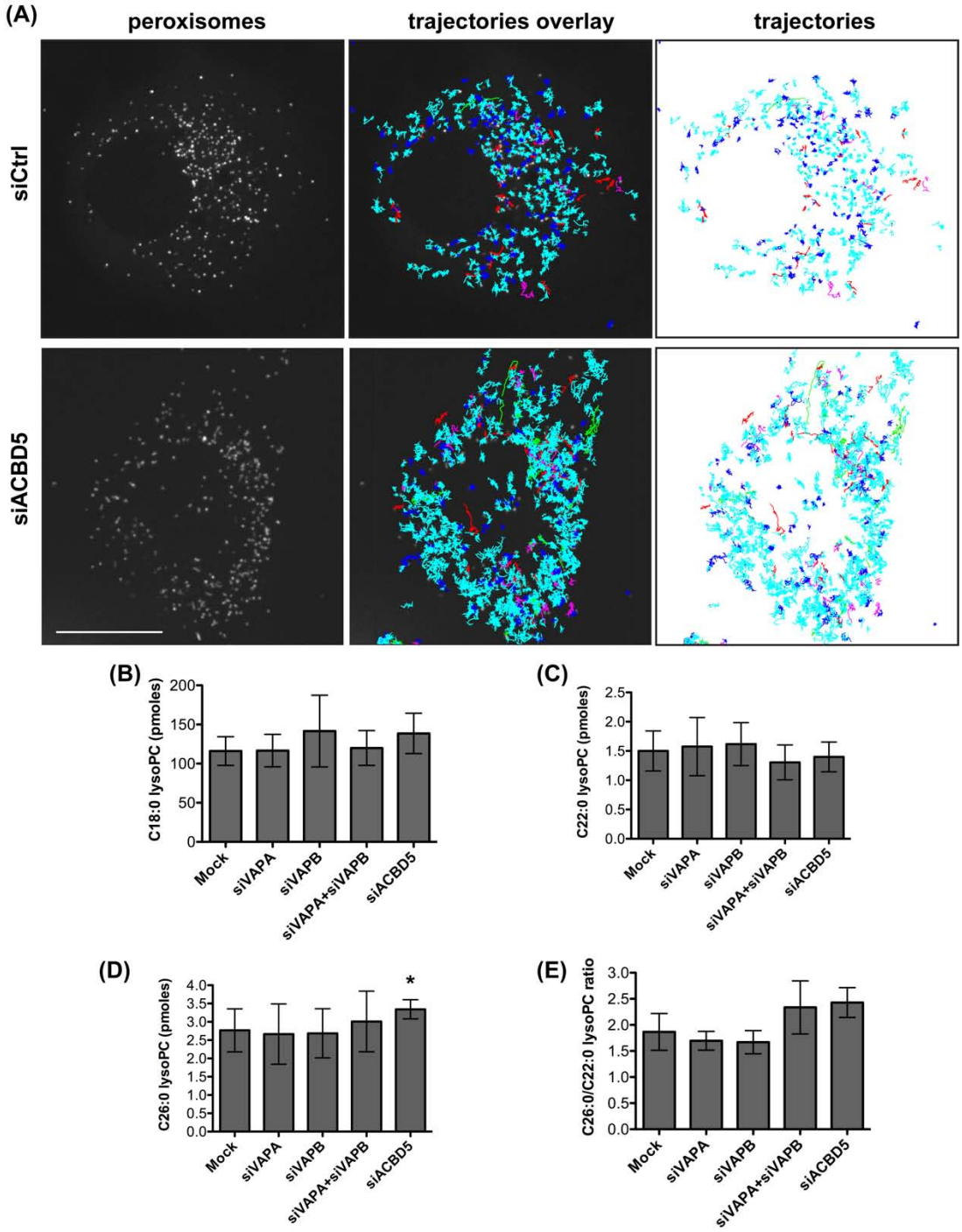

Figure 4.6 Loss of VAP-ACBD5 tether affect peroxisome mobility and cellular lipid homeostasis.
(A) VAP-ACBD5 interaction limits the mobility of peroxisomes. HeLa cells expressing UB-RFP-SKL to label peroxisomes, were transfected with indicated siRNAs. Z stacks of single cells were acquired at 40 frames per min and the centers of peroxisomes were tracked over 2 min. Frame 1 from the video (left panels), generated trajectories (right panels), or an overlay of the two (middle panels) are shown. Scale bar, 20 μm.
(B-E) An increasing trend in VLCFAs levels was observed in VAPs or ACBD5 depleted cells, but the changes are not statistically significant. Bar graph of C18:0 lysoPC (A), and C22:0 lysoPC (B), C26:0 lysoPC (C), and C26:0/C22:0 lysoPC ratio (D) in HeLa cells treated with indicated siRNAs. Mean ± SD (n = 4). *$p < 0.1$ as compared to mock cells.

4.7 The VAP-ACBD5 tether is required for peroxisome growth

The multiplication of peroxisomes by growth and division first requires the expansion of the lipid bilayer leading to elongation followed by fission. Peroxisome fission is mediated by FIS1, MFF and DLP1/DRP1, and depleting any of these proteins was shown to result in elongated peroxisomes (208, 219). However, the manner in which peroxisomes obtain membrane lipids for their growth is not known.

To test whether the VAP-ACBD5 tether is required for lipid transport from ER to peroxisomes for membrane expansion during peroxisome elongation, we depleted the tethering components in cells where peroxisomal elongation was induced. We found that depleting VAPs or ACBD5 prevented elongation of peroxisomes in cells predisposed to have elongated peroxisomes due to lack of DLP1 activity (Fig. 4.7A and Fig. 4.5C). The quantification of average peroxisome area showed that individual peroxisome was no longer elongated upon DLP1 knockdown (Fig. 4.7B). A decrease in the total peroxisome area was also observed (Fig. 4.7C&D), suggesting that VAPs and ACBD5 are required for peroxisomal membrane expansion. We also examined the impact of ACBD5 overexpression on peroxisome size. We observed that over-expressing wild-type ACBD5 induced peroxisomal elongation in a VAP-dependent manner, but not in cells expressing the FFAT-motif mutant ACBD5 (Fig. 4.7E-G). Together these results suggest that the VAP-ACBD5 tether is required for peroxisome growth.

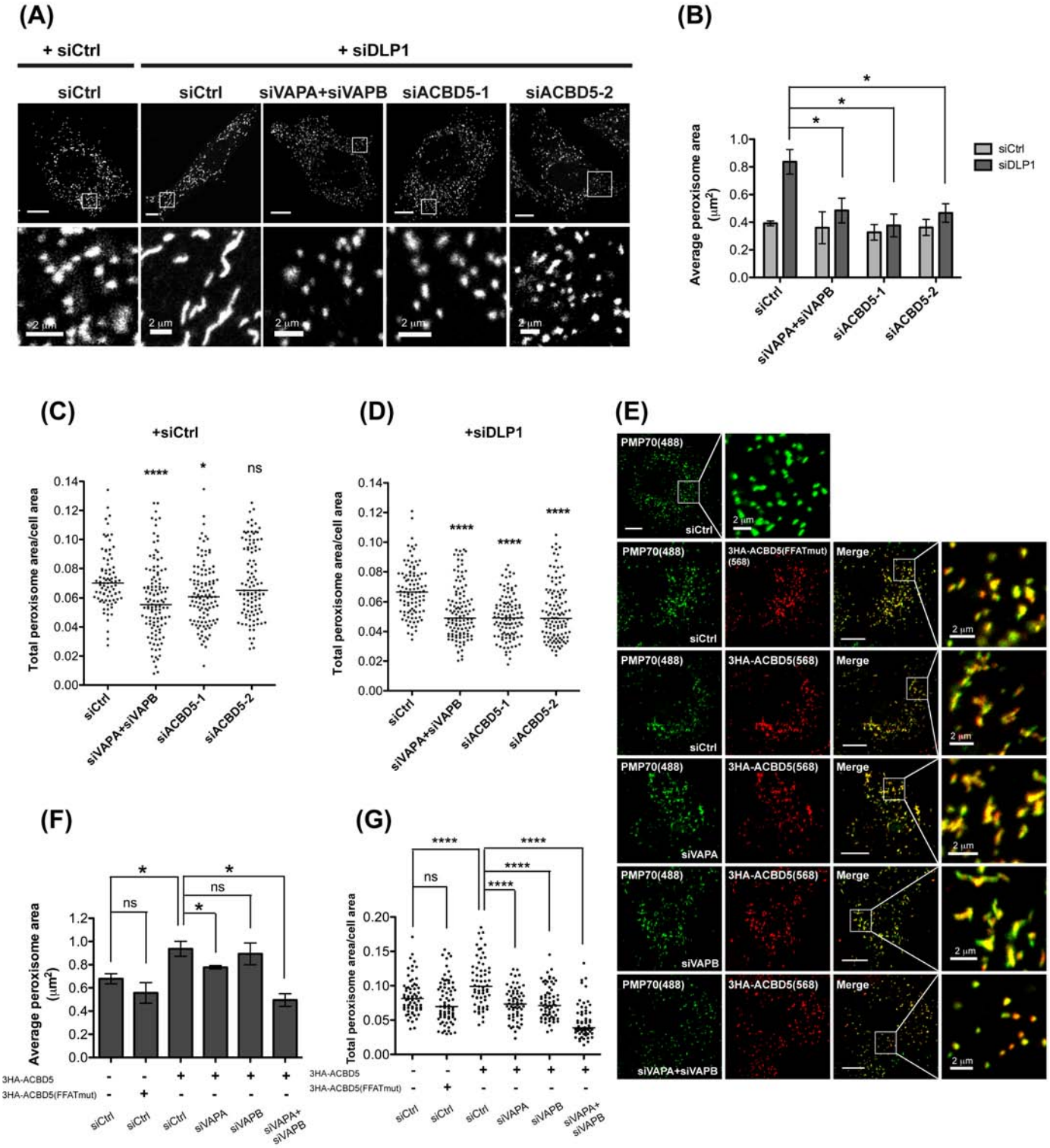
(A)
+ siCtrl
+ siDLP1
siCtrl
siCtrl
siVAPA+siVAPB
siACBD5-1
siACBD5-2
2 μm
(B)
Average peroxisome area (μm²)
siCtrl
siDLP1
siCtrl
siVAPA+siVAPB
siACBD5-1
siACBD5-2
(C)
+siCtrl
Total peroxisome area/cell area
(D)
+siDLP1
Total peroxisome area/cell area
(E)
PMP70(488)
3HA-ACBD5(FFATmut) (568)
3HA-ACBD5(568)
Merge
siCtrl
siVAPA
siVAPB
siVAPA+siVAPB
(F)
Average peroxisome area (μm²)
3HA-ACBD5
3HA-ACBD5(FFATmut)
(G)
Total peroxisome area/cell area

Figure 4.7 Loss of VAP-ACBD5 tether prevents peroxisomal membrane expansion.
(A) HeLa cells treated with indicated siRNAs and immunostained for PMP70. Scale bar, 10 μm or as indicated.
(B) Quantification of average peroxisome area in HeLa cells treated with indicated siRNAs. Mean ± SD (n = 3; 30 cells per trial). *p < 0.05.
(C & D) Quantification of total peroxisome area in HeLa cells either in the absence (C) or in the presence (D) of DLP1 knockdown, and treated with indicated siRNAs. The total peroxisome area of >90 cells from 3 experiments for each siRNA condition are graphed (dots) along with the medium (bars). One-way ANOVA with Bonferroni Correction. *p < 0.05, ****p < 0.0001.
(E) COS7 cells treated with indicated siRNAs, and expressing WT or the FFAT-motif mutant ACBD5. Cells were immunostained for HA tag and endogenous PMP70. Scale bar, 10 μm or as indicated. (F) Quantification of average peroxisome area in COS7 cells in (E). Mean ± SD (n = 3: 30 cells per trial). *p < 0.05.
(G) Quantification of total peroxisome area in COS7 cells in (E). Quantification similar to C. ****p < 0.0001.

4.8 VAP-ACBD5 interaction plays a role in lipid synthesis

To determine whether lipids are transported from peroxisomes to the ER through the VAP-ACBD5 tether, we examined the cellular levels of two peroxisomal lipids, plasmalogens and cholesterol. The synthesis of plasmalogens is initiated in peroxisomes and subsequently completed in the ER (41). Similarly, precursors of cholesterol are synthesized in peroxisomes (220, 221). Moreover, peroxisomes have recently been shown to be involved in trafficking of cholesterol from lysosomes and eventually to the plasma membrane (PM) (146). However, it is not known whether the ER is an intermediate compartment for the trafficking of cholesterol from peroxisomes to the PM. Here, we tested whether the VAP-ACBD5 tether is required for the maintenance of both plasmalogens and cholesterol levels. We found that depleting both VAPs or ACBD5 alone resulted in a decrease in phosphatidylethanolamine (PE) plasmalogens (Fig. 4.8A&B) and total cholesterol levels (Fig 4.8C). However, non-peroxisomal lipids were not affected (Fig. 4.6B-C).

The impact of siRNA treatment on plasmalogen synthesis was modest when compared to prior studies of fibroblast cell lines from patients with constitutional defects in plasmalogen synthesis (i.e. AGPS and GNPAT) where plasmalogen levels are barely detectable (222). We attribute our observed phenotypes to i) the short-term nature of the siRNA experiment; ii) the turnover rate of plasmalogen phospholipid fraction; and iii) alternative pathways of lipid exchange between the ER and peroxisomes (e.g. vesicular intermediates, see Introduction).

In summary, we conclude that the VAP-ACBD5 tether is required for the optimal biosynthesis of plasmalogens.

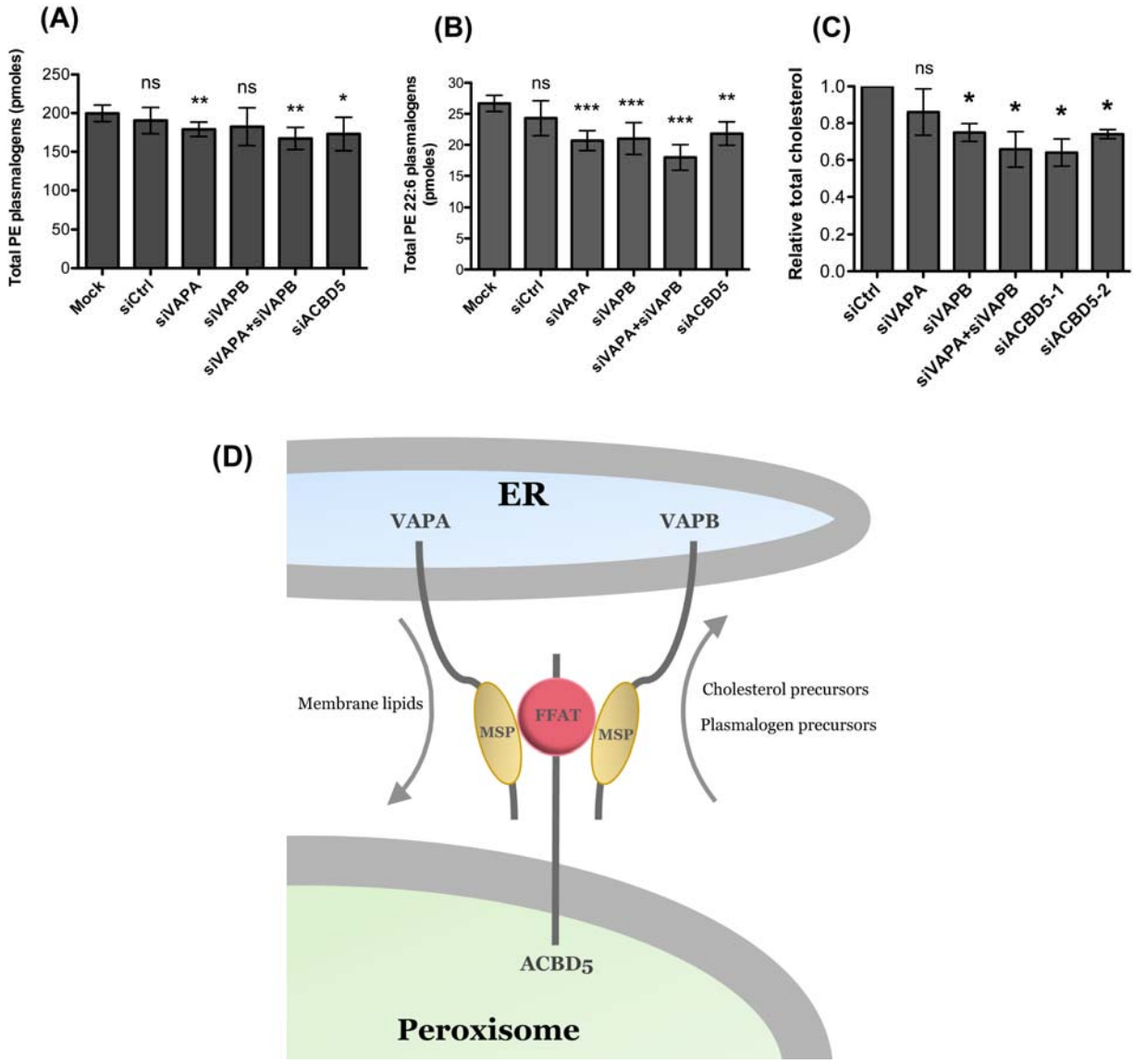

Figure 4.8 Loss of VAPs-ACBD5 tether affects cellular plasmalogen and cholesterol levels.
(A & B) Bar graphs of total PE plasmalogens (A), and total PE 22:6 plasmalogens (B) in HeLa cells treated with indicated siRNAs. Mean ± SD (n=4). *p < 0.1, **p < 0.05, ***p < 0.01 as compared to mock cells, and ns=not significant.
(C) Quantification of total cholesterol levels in HeLa cells treated with indicated siRNAs using the Amplex® Red Cholesterol Reagent. The total cholesterol level for each siRNA treatment (n=3; mean ± SD) was normalized to that in siCtrl-treated cells. *p < 0.05 as compared to siCtrl-treated cells.
(D) Model for ER-peroxisome contact sites**.** The ER-anchored VAPs bind directly to the FFAT motif containing peroxisomal protein ACBD5 via their MSP domains to allow for peroxisome tethering and lipid exchange.

4.9 Discussion

Like any organelles, peroxisomes need to communicate with their surroundings and other cellular compartments to properly perform various functions. Particularly, peroxisomes have long been seen in close opposition to the ER in which the ER is thought to provide lipids and proteins for peroxisome biogenesis. The ER-peroxisome interplay is also important for various metabolic pathways including the biosynthesis of specialized lipids, such as plasmalogens, cholesterol, and bile acids. However, how peroxisomes communicate with the ER, in particular, the mechanism(s) by which lipids and proteins are exchanged between them, is not fully understood. Here, we provide evidence for the first identification of a tether between the ER and peroxisomes in the mammalian system. The physiological functions of this novel ER-peroxisome tether in peroxisome maintain and lipid homeostasis were also examined here.

By using the proximity-dependent BioID, we have identified in total 70 high confidence proximal interactors of PEX16, and grouped them based on their known cellular localizations. Several proteins with known functions in vesicular trafficking (e.g., Ykt6 and Rab10) are identified to be interacting/proximal to PEX16 in our screen. Since PEX16 is demonstrated to recruit other PMPs to the ER and mediate their subsequent trafficking to peroxisomes, it is possible that these vesicular proteins may work cooperatively with PEX16 in PMP targeting (See Section 5.4 for more detailed discussion). Notably, the most well documented ER contact site proteins VAPA and VAPB are also identified in our screen. VAPs are anchored to the ER through their C-terminal TM domain and their MSP domains in the cytosol are shown to bind to proteins containing the FFAT motif (158, 159). The interaction between ER-resident VAPs and the FFAT-motif containing protein in the other membrane bridges the two respective membranes, thereby mediating the contact between the two organelles. Our confocal microscopy and SIM data show that VAPs localize to specific loci on the ER, and indeed some of the VAP-positive puncta are found to be juxtaposed to peroxisomes. Furthermore, we also showed that the targeting of VAPs to these specific loci in juxtaposition to peroxisomes depends on their interaction with the peroxisomal protein ACBD5 that contains a FFAT motif. These results raise a possibility that VAPs may bind to ACBD5 in the peroxisomal membranes to form a tether between the two organelles.

Recently, several prerequisites have been proposed for how to categorize a protein as a tether (223). Our results show that the VAP-ACBD5 tether fulfills the minimal criteria to be defined as a real tether. 1) Defined location — by using confocal microscopy and SIM, we showed that VAPs are juxtaposed to peroxisomes in the ER (Fig. 4.1B-F, 4.2A-C, and 4.3). Moreover, the rate of depletion of the VAPB-GFP signal associated with peroxisomes was shown to be slower than those in other portions of the ER (Fig. 4.3D&E) in the FLIP assay, suggesting that the mobility of VAPB-GFP fluorescent molecules juxtaposed to peroxisomes was more constrained. In other words, this data also suggests that VAPB is enriched at these specific loci. 2) Structural capability to tether the two opposing membranes — both VAPA and VAPB were shown to immunoprecipitate with the peroxisomal protein ACBD5 in a FFAT-motif–dependent manner (Fig. 4.4A & 4.2E). Disruption of this VAP-ACBD5 interaction also accelerated the mobility of peroxisomes, implying the involvement of VAP-ACBD5 interaction in anchoring peroxisomes to the ER. 3) Functional activity — our data showed that disruption of the VAP-ACBD5 interaction affects peroxisomal membrane expansion (Fig. 4.7) and cellular plasmalogen and cholesterol levels (Fig. 4.8A-C). Taken together, we conclude that the complex consisting of ER resident VAPs and peroxisomal ACBD5 is a tether between peroxisomes and the ER.

Recently, two groups independently reported that patients with mutations in ACBD5 show elevated levels in very long chained fatty acids (VLCFAs) (224, 225). Although we did observe an increasing trend in VLCFA levels in ACBD5 or VAPs depleted cells in our system, the changes are not statistically significant (Fig. 4.6B-E). Since much of the VLCFAs are incorporated in phospholipids, the relatively short nature of the transient siRNA knockdown was likely not sufficient for the measurement of a robust change in VLCFAs.

In conclusion, our new insight into ER-peroxisome tethering advances our understanding of communication between the ER and peroxisomes. We show that peroxisomes are tethered to the ER through the interaction between peroxisomal ACBD5 with ER resident VAPs, and this tether is required for the exchange of lipids between them (Fig. 4.8D). More work is required to further characterize this VAP-ACBD5 tether. For example, VAPA and VAPB are shown to form homo- and/or hetero-dimers via their TM domains. It is not known whether VAPA and VAPB work simultaneously with ACBD5 in the same tethering complex, or there

exist two different types of tethers mediated by VAPA and VAPB respectively. Moreover, whether this VAP-ACBD5 tether acts only to provide a tethering force to bridge the two membranes or if it is directly involved in the lipid transfer between them is also not clear. Identification of other molecular components associated with this complex is crucial for understanding the underlying mechanism for lipid exchange between peroxisomes and the ER. Finally, as ALS patients carrying the VAPB(P56S) mutation are reported to have increased cholesterol levels (226), it is tempting to speculate that this increase in cholesterol levels may be due to increased ER-peroxisome contact. Further studies on patient cells carrying the VAPB(P56S) mutant will help to illustrate a possible role of the ER-peroxisome tethering in the pathogenesis of ALS.

Chapter 5

Discussion and Future directions

Part of this chapter is adapted from a review originally published as:

- Hua R., and Kim P.K. 2016. Multiple paths to peroxisomes: Mechanism of peroxisome maintenance in mammals. *Biochim Biophys Acta*. 1863(5): 881-891.

5.1 Evolutionary significance of PEX16 in peroxisome maintenance

In this thesis, we have provided evidence for a function of PEX16 as a general PMP receptor at the ER. We also have identified specific domains in PEX16 that are required for its targeting and PMP recruitment function. Interestingly, a homologue of the mammalian PEX16 is not found in most yeast, but is present in higher eukaryotes where its function appears to vary depending on the organism (188). That is, while the loss of PEX16 results in the complete absence of peroxisomes in both human and *Arabidopsis* (227, 228); *Drosophila pex16* mutant cells possess peroxisome-like structures (229), suggesting a difference in function of PEX16 among these organisms. In *Y. lipolytica*, the *PEX16* gene differs from its mammalian homolog in that it is a peripheral membrane protein located at the matrix side of peroxisomal membranes, and is required for the division of pre-existing peroxisomes (85, 99, 100). Overall, these studies suggest that PEX16 proteins perform a wide diversity of functions in different organisms.

These functional differences among PEX16 homologs may explain the evolutionary need for this gene in higher eukaryotes. For example, both human and *Arabidopsis* PEX16 are involved in the recruitment of PMPs to the ER (79) and, at least in mammalian cells, PEX16 is also required for the subsequent transport of PMPs to peroxisomes from the ER (78). By contrast, in *S. cerevisiae*, which does not have a PEX16 homologue, Pex3p instead acts to mediate the trafficking of PMPs to peroxisome from the ER (98). A possible explanation for the existence of PEX16 gene in higher eukaryotes is that mammalian PEX3 may have lost its ability to target directly to the ER. That is, unlike ScPex3p, which contains an ER targeting TM domain and an ER-to-peroxisome targeting signal (65), mammalian PEX3 does not have any ER targeting signal within the protein (91, 96). Instead, in the absence of any peroxisomes, mammalian PEX3 targets to mitochondria (77, 78, 91). It is possible that PEX3 at the mitochondria is targeted to peroxisomes, as mitochondria-derived vesicles (MDVs) have been shown to fuse with pre-existing peroxisomes (230). However, as these vesicles only fuse with a subset of peroxisomes (128), the PEX16/ER pathway likely plays a more dominant role in maintaining peroxisomes. This is further supported by the recent finding in *S. cerevisiae* where the expression of Tom20p-Pex3p, a Pex3p construct where its mPTS was replaced with the mitochondrial targeting transmembrane sequence of Tom20p, led to the

formation of new peroxisomes in *pex3* deficient cells (132). However, these new peroxisomes were not fully functional, as Tom20p-Pex3p expression did not complement the growth defect on oleic acid (132). Based on the recent structural and functional studies, the juxtaposition of the cytosolic domain of Pex3p to the lipid bilayer may play a critical role in the efficient import of PMPs to membranes (94, 231, 232). Therefore, the lack of complementation by Tom20p-Pex3p may be due to the length of the Tom20p transmembrane domain in respect to the Pex3p import region. Hence, it is not all together inconceivable that peroxisomes may form *de novo* from mitochondria under the appropriate conditions in mammalian cells. Moreover, the relatively higher numbers of peroxisomes in mammalian and plant cells as compared to most yeast (233, 234) also imply the importance of the existence of PEX16 gene in higher eukaryotes, as the PEX16/ER pathway may be an essential mean for providing both the protein and lipid components required for maintaining the steady-state number of peroxisomes (See Section 5.3 for detailed discussion).

5.2 Model for *de novo* peroxisome biogenesis

Conceptually, *de novo* formation of peroxisomes requires the action of three groups of peroxins involved in (i) membrane modulation, (ii) peroxisomal membrane assembly/PMP import, and (iii) matrix protein import (Fig. 5.1). In this model of *de novo* formation of peroxisomes, peroxisome biogenesis starts with the membrane modulator(s) that remodel the ER, leading to membrane curvature and the formation of specialized subdomains on the ER. The molecular components involved in this process are not known. Based on our findings that PEX16 is capable of recruiting a wide variety of PMPs to the ER, it is a likely candidate involved in this process (77, 79). Other factors that may be involved in modulating membranes at the ER are the PEX11 family proteins that function to elongate peroxisomes and mediate the formation of indention where fission components FIS1 and MFF are recruited for peroxisome division (26, 29, 30, 33, 34). Pex25p, a member of the PEX11 family in *S. cerevisiae* is required for the *de novo* biogenesis of peroxisomes from the ER (71). Since we showed that PEX16 recruits various PMPs including PEX11β to the ER (Fig. 3.7B), it is conceivable that a member of the PEX11 family may be recruited early to the ER to mediate the formation of the specialized peroxisomal/ER subdomains. This is in line with previous findings that peroxisomes appeared to be lower in number and enlarged in size in

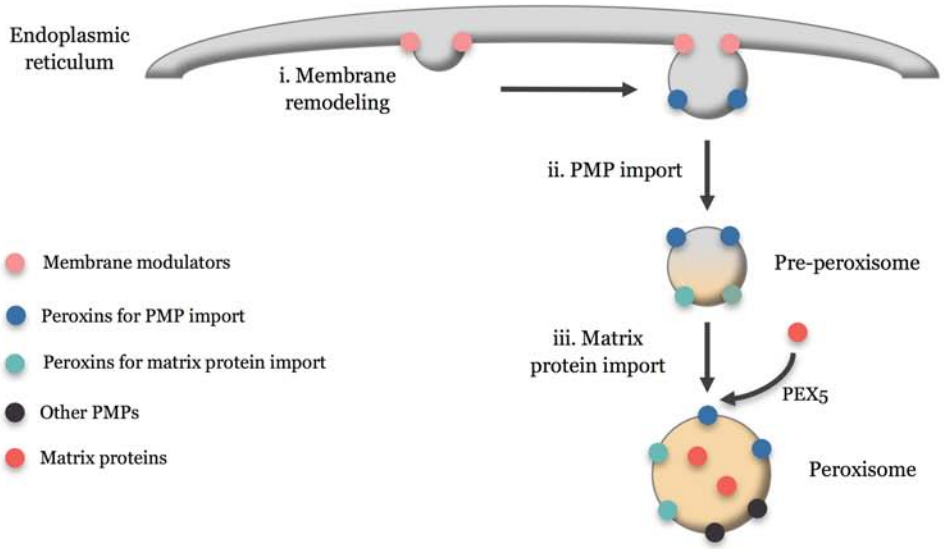

Figure 5.1 Model for *de novo* biogenesis of peroxisomes
(i) Membrane modulation: *de novo* formation of peroxisomes starts with the recruitment of membrane modulating factors that induce membrane curvature and the assembly of pre-peroxisomal vesicles/structures at the specialized subdomains of the ER. Although the molecular components involved are not known, PEX16 is one of the most likely candidates that may play a role in this process. After being cotranslationally inserted into the ER membranes, PEX16 recruits a variety of PMPs, including PEX3, which is an early-stage peroxin, as well as the PEX11 family proteins, to the ER. The PEX11 family proteins act as the membrane modulators that induce membrane elongation, resulting in the formation of indention where they recruit fission components FIS1 and MFF to their site of action for subsequent growth and division. These PMPs together with PEX16 will concentrate in a specialized subdomain on the ER, leading to the formation of the pre-peroxisomal vesicles/structures. (ii) *Peroxisomal membrane assembly/PMP import*: once released from the ER, these pre-peroxisomal structures can continuously import PMPs via the action of the PEX3-PEX19 complex, leading to the assembly of the matrix protein import machinery. PEX19 acts as a soluble receptor that binds to the mPTS of the newly synthesized PMPs, stabilizes them in a soluble state in the cytosol. The cargo-loaded PEX19 complex will then be guided to peroxisomal membranes via the direct interaction between PEX19 and the docking factor PEX3, while PEX16 acts as the membrane receptor for PEX3-PEX19 complex on the peroxisomal membranes. (iii) *Matrix protein import*: once the matrix protein import machinery comprising the docking complex (PEX14/PEX13), the RING complex (PEX2/PEX10/PEX12), and the AAA-type ATPase complex (PEX1/PEX6/PEX16) is fully assembled, these pre-peroxisomal structures subsequently uptake peroxisomal matrix enzymes from the cytosol and eventually give rise to the formation of new mature peroxisomes. The soluble receptor PEX5 (or PEX7) recognizes the PTS1 (or PTS2) on the newly synthesized proteins, and the cargo-loaded receptors will be guided to peroxisomes via their interaction with the docking complex at the peroxisomal membranes. After being translocated across the membranes, the cargo is then released into the peroxisomal matrix and the receptor is recycled back to the cytosol.

patient fibroblasts with a non-sense mutation in the PEX11β gene (235). The peroxisome division defect in these patient fibroblasts could be rescued or partially rescued by over-expression of wild-type PEX11β or PEX11γ respectively, suggesting potential functions of the PEX11 family proteins in both the growth and division and the *de novo* pathways for peroxisome biogenesis (235). Another group of proteins that may be involved in membrane modulation are the reticulon-like domain containing proteins, Pex30p and Pex31p (236). In yeast *S. cerevisiae*, Pex30p was shown to tubulate membrane both in cells and *in vitro*, indicating that this reticulon-like protein is a novel ER-shaping protein. Pex30p was found to be enriched at subdomains of the peripheral ER where preperoxisomal vesicles (PPVs) are generated. Moreover, deletion or overexpression of Pex30p or Pex31p not only altered the number of PPVs, but also resulted in a change in the morphology of these PPVs, suggesting a possible role of these proteins in shaping PPVs. However, what remains unclear is whether Pex30p and Pex31p directly mediate PPV budding from the ER, or they help to generate subdomains in which PPVs are generated by modulating the ER membranes. Since no homologue of Pex30p or Pex31p has been found in mammalian cells, identification of peroxisomal proteins with reticulon-like domains will help to uncover and enhance our understanding about the mechanism of the *de novo* peroxisomes formation from the ER.

Our data also suggests that the ER recruitment of various PMPs by PEX16 is independent of either PEX3 or PEX19 (Fig. 3.7E-F), suggesting that PEX16 may utilize other cytosolic chaperone(s), and/or another ER membrane bound receptor. However, as these experiments were carried out using an ER-localized PEX16 construct, it is not certain whether PEX16 is also required for recruiting PMPs to pre-peroxisomes and mature peroxisomes. Recent *in vitro* evidence showed that PEX16 can function as a receptor for the targeting of PEX3 to pre-existing peroxisomes (96), suggesting that PEX16 may be involved in the recruitment of various PMPs at both the ER and peroxisomes. This also suggests that PEX16 may be responsible for transporting various PMPs to pre-peroxisomal structures, such as the components of the matrix protein import machinery, which include the docking complex (PEX14/PEX13), the RING complex (PEX2/PEX10/PEX12), and the AAA-type ATPase complex (PEX1/PEX6/PEX26) (11, 13, 62-64). The assembly of the matrix protein machinery will allow for the import of matrix proteins, thus allowing for the maturation of these pre-peroxisomal structures into functional peroxisomes (Fig. 5.1). Alternatively,

PEX16 may recruit PMPs to a specialized subdomain of the ER, where pre-peroxisomal vesicles are being formed and released into the cytosol. Similar to those described in *Y. lipolytica* and *S. cerevisiae* (72, 73), these ER-derived vesicles may contain subsets of PMPs such that fusion with each other will allow for the formation of peroxisomal structures with the full complement of peroxins necessary for maturation. These structures would subsequently uptake peroxisomal matrix enzymes from the cytosol, and eventually give rise to the formation of new mature peroxisomes. Whether similar pre-peroxisomal vesicles exist in the mammalian system is not clear at this moment.

5.3 Contribution of *de novo* biogenesis versus fission in the formation of new peroxisomes

It is generally accepted that the ER contributes to the *de novo* formation of peroxisomes, especially in cells without pre-existing peroxisomes. However, the role that the ER pathway plays in normal, dividing cells with pre-existing peroxisomes is not clear. Conflicting evidence has been reported as to the extent that the two mechanisms, *de novo* formation and fission from pre-existing peroxisomes, are utilized in normal mammalian cells. By using a photoactivatable GFP (PAGFP), Kim et al. were able to distinguish between the pre-existing and newly synthesized peroxisomal protein content (77). The assumption made by these authors is that the two daughter peroxisomes that are formed by fission will receive equal protein content from the mother peroxisome, while those derived *de novo* from the ER will only receive the newly synthesized proteins. By quantifying the number of the newly formed peroxisomes that receive the pre-existing protein content (i.e., formed by fission of pre-existing peroxisomes) and those receive only the newly synthesized proteins (i.e., formed *de novo* from the ER), the authors interpreted their work to suggest that ER-derived *de novo* formation represents the major pathway for the biogenesis of peroxisomes in mammalian cells.

An alternative view was recently put forth by Marc Fransen's group, who used a novel HaloTag technology to label peroxisomes in cultured mammalian cells (237). In their study, the authors demonstrated an age-related heterogeneity of peroxisomes with respect to their capability to import newly synthesized proteins. The authors also provided evidence showing

that 1) mammalian peroxisomes do not fuse and exchange their protein content; 2) the newly synthesized PMPs, including PEX16, could be imported to the pre-existing peroxisomes; 3) the matrix protein content is not evenly distributed between the two daughter peroxisomes that are formed by fission of the pre-existing one. Generalizing the above findings, these authors argued that peroxisomes in mammalian cells multiply primarily by growth and non-symmetrical division from pre-existing ones. Hence, this concept contrasts sharply with the view presented by Kim et al.

At this point, it is not clear which pathway plays a dominant role in the formation of new peroxisomes. The possibility that both pathways exist in mammalian cells cannot be excluded. Also, with the knowledge gained from the latest studies and data presented in this thesis, some of the results in these earlier studies need to be re-interpreted. The main argument raised by Huybrechts et al. against the model of *de novo* formation is that the assumption made by Kim et al. that peroxisomes divide evenly may be inaccurate (77, 237). This is supported by the observation in *H. polymorpha* and *S. cerevisiae* that matrix content of a pre-existing peroxisome was unevenly distributed between the two daughter peroxisomes upon fission (117, 238). In mammalian cells, however, this uneven division was only observed in cells with overexpression of PEX11 proteins, which induces peroxisome elongation/tubulation (239, 240). Here, peroxisomes form tubular structures that are devoid of matrix proteins, and new matrix proteins will be imported into these tubular structures. However, this phenomenon has only been shown in cells when peroxisome proliferation was induced by the over-expression of the PEX11 family proteins. Hence, it is not known whether similar structures would be formed in normal dividing cells. In *S. cerevisiae*, it was shown that normal dividing cells were able to divide their matrix content between the two daughter peroxisomes (203). Therefore, it is possible that PAGFP-SKL used by Kim et al. (77) can be passed from pre-existing peroxisomes to the daughter peroxisomes in constitutively dividing cells.

Furthermore, based on the assumption that mammalian peroxisomes do not exchange their protein content and that the newly synthesized PMPs can be imported to pre-existing peroxisomes, Huybrechts et al. argued that peroxisomes in mammalian cells are unlikely to multiply by *de novo* formation from the ER or other pre-peroxisomal structures (237).

However, an alternative interpretation of the above results could be that the ER may contribute to the maintenance of peroxisomes by providing both lipids and PMPs to pre-existing peroxisomes. We have recently tested this hypothesis by quantifying the kinetics of PMP import to pre-existing peroxisomes (78). We showed that PMPs can be imported into peroxisomes with two distinct rates, suggesting the existence of two PMP import pathways: the Group I pathway (the indirect pathway via the ER with slower kinetics) and the Group II pathway (the direct pathway from the cytosol with faster kinetics) (Fig. 1.1) (78). The Group I was exemplified by a PEX3 construct with an ER targeting signal sequence, ssPEX3, which rapidly targeted to pre-existing peroxisomes but at a slower rate as compared to the wild type PEX3 (78). In fact, any accumulation of ssPEX3 on the ER was observed only upon an extended period of over-expression in cells (78). Human PEX16 has a similar rate of import into peroxisomes as the ER targeting ssPEX3 (78). As mentioned earlier, our data show that PEX16 can recruit various PMPs to the ER, and this ER recruitment of PMPs is independent of PEX3 or PEX19. Interestingly, over-expressing PEX16 with PEX3 or PMP34 decreased the import rates of both PEX3 and PMP34 into peroxisomes, but silencing PEX16 significantly increased the import rates of both proteins (78). Taken together, we interpreted these finding to suggest that the ER may constitutively provide PMPs to pre-existing peroxisomes and that in the presence of PEX16, PMPs target to peroxisomes via the ER (Group I pathway).

On the other hand, the ER may also contribute to peroxisome maintenance by providing essential lipids for their membrane expansion during growth and division as supported by the data presented in Chapter 4. We showed that disruption of the ER-peroxisome tether by depleting VAPs or ACBD5 prevented elongation of peroxisomes in cells predisposed to have elongated peroxisomes due to lack of DLP1 activity (Fig. 4.7A&B). A decrease in the total peroxisome area was also observed (Fig. 4.7C&D), indicating that the ER-peroxisome tether mediated by VAP-ACBD5 interaction is required for peroxisomal membrane expansion. Interestingly, no change in peroxisome number was observed in cells depleted of these tether proteins (data not shown), suggesting that the VAP-ACBD5 tether is only required for peroxisome membrane expansion (i.e., peroxisome growth), but does not play a role in the fission step. Another possible mechanism as to how the ER could provide peroxisomes with lipids for their growth is via the ER-derived preperoxisomal vesicles. Although the exact

mechanism by which the ER targeted PMPs are transported to the pre-existing peroxisomes is not known, it is likely that this protein targeting pathway is mediated by vesicular transport between the two organelles (See Section 5.4 for detailed discussion). Once released from the ER, these pre-peroxisomal vesicles can either mature into newly formed peroxisomes, or fuse with pre-existing ones to provide essential proteins and at the same time, a bulk amount of lipid content for their steady-state maintenance.

One possible reason for the existence of these specialized ER-to-peroxisome protein and lipid trafficking pathways in the mammalian system, as well as perhaps in plants (79, 174, 188, 241, 242), is that these organisms need to maintain a relatively large population of peroxisomes as compared to most yeast. Mammalian and plant cells, for instance, typically contain 100-1000 peroxisomes compared to the 2-10 peroxisomes found in most yeast, although the numbers can vary widely within each of these organisms depending on the metabolic state of the cell (233, 234). Regardless, the relatively lower number of peroxisomes in yeast implies that there is less demand on the ER in terms of providing the protein (PMPs) and lipid components required for maintaining the steady-state number of peroxisomes. On the other hand, the relatively high number of peroxisomes in mammals and plants suggests that a specialized mechanism involving PEX16 underlies the role in which the ER provides peroxisomes with their constituents.

5.4 Mechanism for ER-to-peroxisome protein targeting

One aspect of PMP targeting that remains largely unknown is how the ER targeted PMPs are transported to the existing peroxisomes. It is likely that this protein targeting pathway is mediated by vesicular transport between the two organelles (Fig. 5.2), as the vesicle forming protein Sec16B is required for the transport of PEX16 to peroxisomes (84). However, the exact mechanism underlying this protein trafficking pathway is not known. It is possible that PEX16 could recruit other essential PMPs to the ER and concentrate them at specialized subdomains on the ER to form pre-peroxisomal structures. However, it is unknown what defines these specialized domains on the ER. More specifically, it is unclear whether these specialized subdomains are pre-existing on the ER and PEX16 is being specifically targeted there after its cotranslational insertion into the ER, or whether PEX16 itself recruits certain

factors to the ER and thus generates these specialized subdomains. Furthermore, the nature of these pre-peroxisomal structures and the mechanism of their release from the ER remain undefined. In yeast, it has been shown that distinct types of pre-peroxisomal vesicles with different PMP composition bud from the ER in a Pex3p- and Pex19p-dependent manner, and undergo heterotypic fusion followed by a series of maturation processes to form new peroxisomes (72, 73). The reticulon-like domain containing Pex30p and Pex31p were also

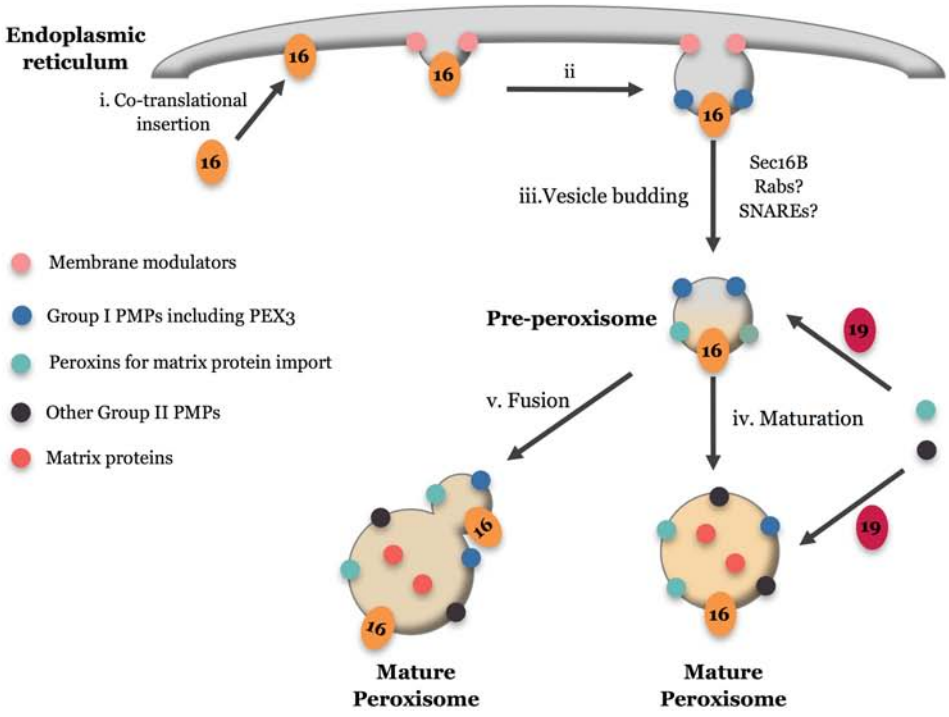

Figure 5.2 Mechanism for ER-to-peroxisome protein targeting and roles of PEX16.
Although the exact mechanism underlying the ER-to-peroxisome protein trafficking pathway is not known, it is like that this protein targeting pathway is mediated by vesicular transport between the two organelles. Once cotranslationally inserted into the ER membranes (i), PEX16 could recruit other essential PMPs including PEX3 and membrane modulators to the ER, and concentrate them at specialized subdomains on the ER to form pre-peroxisomal structures (ii). However, the nature of these pre-peroxisomal structures and the mechanism of their release from the ER remain undefined (iii). Candidate proteins that may be involved in generating these pre-peroxisomal vesicles/structures and facilitating their release from the ER include the reticulon-like domain containing Pex30p and Pex31p in yeast and the ER exit site protein Sec16B in mammalian cells. The Rab proteins (Rab10, Rab6, Rab14 and Rab18) and the SNARE Ykt6 that have been identified to be proximal to PEX16 in our BioID analysis are also potential candidates involved in this PMP targeting pathway. (iv) On the other hand, PEX16 works cooperatively with PEX3 and PEX19 to mediate the targeting of various PMPs to pre-peroxisomal structures, allowing for the maturation of these pre-peroxisomal structures into functional peroxisomes. (v) At the same time, these pre-peroxisomal structures can also fuse with pre-existing peroxisomes to provide both lipid and protein contents for their maintenance.

shown to help to shape and generate subdomains of the ER where preperoxisomal vesicles are originated (236). In mammalian cells, Sec16B, a vesicular factor that defines the ER exit sites, was shown to be essential for the exit of PEX16 from the ER (84). Also, over-expression of the protein interferes with the peroxisomal targeting of PEX3 (84). Based on the above data, one plausible hypothesis is that PEX16 recruits the membrane modifying proteins such as PEX11, and the early-stage peroxin PEX3, to the ER, where they are packaged into pre-peroxisomal vesicles/structures. Once these pre-peroxisomal structures are released from the ER, they can either mature into new functional peroxisomes similarly to the yeast system, or fuse with pre-existing peroxisomes in a similar way as how MDVs fuse with mature peroxisomes. One aspect worth mentioning is that these pre-peroxisomal vesicles are unlikely to follow the secretory pathway upon budding from the ER, since neither COPI or COPII is required for the targeting of PEX3 to peroxisomes (81). Hence, identification of other key factors in this pathway is essential for the study of this interrelationship between the ER and peroxisomes. Since PEX16 is demonstrated to recruit other PMPs to the ER (77, 79) and mediate their subsequent trafficking to peroxisomes (78), we speculate that proteins involved in the ER-to-peroxisome PMP targeting pathway are likely to be interacting with or proximal to PEX16. Therefore, searching for proteins in our PEX16 BioID screen that have known functions in vesicular trafficking would allow us to discover other important factors in this process.

As mentioned in Chapter 4, several proteins with known functions in vesicular trafficking have been identified to be interacting/proximal to PEX16 in our PEX16 BioID screen (Table 4.1). It is possible that one or some of these proteins may be required for the vesicular transport of PMPs to peroxisomes from the ER. Notably, Rab10 together with three other Rab proteins (i.e., Rab6, Rab14, and Rab18) have been previously demonstrated to associate with peroxisomal membranes in a proteomics immunofluorescence study (243). Interestingly, Rab10 has been identified as an ER-specific GTPase that regulates ER dynamics and morphology. The Rab10-mediated formation of dynamic domains at the leading edge of ER tubules leads to the extension and fusion of ER tubules. Moreover, these dynamic domains are also enriched in enzymes that are required for phospholipid synthesis (244). Since Rab10 is shown to be associated with peroxisomal membranes and it is also a candidate protein that may be interacting or proximal to PEX16, it is reasonable to postulate

that this protein may be involved in the formation of pre-peroxisomal vesicles/structures from the ER, thereby mediating the ER-to-peroxisome PMP trafficking. Also, the Rab10-mediated dynamic domains at the leading edge of the ER tubule may be the sites where pre-peroxisomal vesicles are derived/released from the ER. Therefore, examining the effect of Rab10 on PMP targeting in particular PEX16 is crucial for our understanding about its potential role(s) in peroxisome biogenesis and maintenance. The SNARE Ykt6 that is involved in multiple membrane fusion reactions in the secretory pathway (245, 246) is another likely candidate protein. Its potential involvement in PMP targeting and peroxisome biogenesis is also worth examining in the future. Specifically, the localization of these candidate proteins to peroxisomes needs to be examined. Whether any of them affects the distribution of PMPs and the export of PMPs from the ER to peroxisomes also need be tested.

Another area that remains an enigma is the biophysical and molecular mechanism of PMPs insertion into the lipid bilayer. Recently, Gregory Jedd's group proposed a model for the mechanism of tail-anchored PMP (TA-PMP) insertion by PEX3/PEX19 into peroxisomal membranes (232). By using an *in vitro* assay, they showed that a hydrophobic segment of amphipathic helices in PEX19 work together with a hydrophobic region of PEX3 to insert the transmembrane domain (TMD) of a TA-PMP into the peroxisomal membranes. For the actual insertion of the TMD, the hydrophobic region of PEX3 near the lipid bilayer promotes an unconventional membrane intercalation that may promote the insertion of the TMD into the bilayer. This model is attractive as it addresses the lack of a translocon for the insertion of a TMD across the peroxisomal lipid bilayer. However, whether a similar mechanism can be utilized to insert multi-spanning PMPs, such as ABCD1 and PMP70, is unclear. A *bona fide* translocon, such as the gated membrane channel complex found in mitochondria and the ER, may be required for the insertion of these multi-transmembrane PMPs. In fact, several key findings from my study point to PEX16 as a potential candidate that may act as a translocon for PMPs. As shown in Chapter 3, PEX16 is capable of recruiting various PMPs, including the multi-spanning PMP34 that has six TM domains (247), to the ER (Fig. 3.7) (77). Moreover, these ER-targeted PMPs are indeed integrated into the ER membranes (data not known), suggesting that PEX16 may be a critical component of the membrane insertion machinery for PMPs. Furthermore, over-expression of the N-terminal half of PEX16 (i.e.,

PEX16NT, refer to Fig. 3.1A) was found to induce a leakage of peroxisomal matrix content into the cytosol (data not shown), suggesting that the over-expression of this truncated PEX16 construct may lead to pore formation in peroxisomal membranes. To test the hypothesis that PEX16 may act as a translocon for PMPs, the ability of PEX16 to oligomerize with itself needs to be tested. It will also be of interest to examine the potential pore-forming ability of PEX16 using the planar bilayer technique which has been previously used to demonstrate the pore-forming activity for the peroxisomal matrix protein import receptor, PEX5 (248).

5.5 ER-peroxisome contact sites

5.5.1 Lipid transfer at ER-peroxisome contact sites

Our data presented in Chapter 4 demonstrates that the VAP-ACBD5 tether is important for peroxisome maintenance and cellular lipid homeostasis. We propose that this tether acts to bridge the ER and peroxisomal membranes, thereby bringing the two organelles in close opposition. The close proximity between them facilitates the transfer of membrane lipids from the ER to peroxisomes for peroxisomal membrane expansion. At the same time, it also allows for the lipid precursors, such as precursors of cholesterol and plasmalogens, to be transported to the ER from peroxisomes for their complete biosynthesis. However, how exactly these lipid molecules are being exchanged between the two organelles is not known. Although ACBD5 is shown to bind to acyl-CoAs via its N-terminal acyl-CoA binding domain (ACBD5) (225), it is not known whether this protein is also able to bind to other lipid molecules, thereby directly mediating the lipid transfer between peroxisomes and the ER. It is possible that ACBD5 acts only as a tether to bring the two opposing membranes in close apposition, but does not directly bind the lipids. In that case, other lipid binding proteins need to be present at the ER-peroxisome contact sites to shuttle the lipid molecules between the two organelles. To test this premise, the binding affinity of ACBD5 for various peroxisomal lipids needs to be measured. A BioID analysis of ACBD5 would also be helpful to identify other components that may directly mediate the lipid transfer at the ER-peroxisome contact sites, thereby enhancing our understanding about the lipid trafficking pathway between the two organelles.

5.5.2 Other tethers at ER-peroxisome contact sites

One common feature for MCSs is that MCSs between two organelles can be mediated by multiple tethers. For example, it has been shown that the ER-localized mitofusin 2 (Mfn2) complexes with mitochondrial Mfn2 to bridge the two organelles, and that this Mfn2-Mfn2 tether is required for efficient mitochondrial Ca^{2+} uptake (249). Another tethering complex that consists of ER resident VAPB and mitochondrial PTPIP51 has also been identified at the ER-mitochondria MCSs. Therefore, it is unlikely that the VAP-ACBD5 tether is the only tether between peroxisomes and the ER. Other tethering complexes may also exist at the ER-peroxisome MCSs.

One of the candidate tethering proteins is Extended-Synaptotagmin-1 (Esyt1) that was identified to be a PEX16 interactor in our BioID screen (Fig. 4.1 and Table 4.1). The Mammalian E-Syts (Esyt1, Esyt2, and Esyt3) are ER resident proteins that have been demonstrated to function in tethering the ER to PM. The tethering function is mediated by interaction between their C2 domains and the PM $PI(4,5)P_2$. Moreover, the recruitment of Esyt1 to the ER-PM contact sites seemed to be Ca^{2+} dependent. Based on the observation this E-syts-mediated tether is not required for store-operated Ca^{2+} entry and the fact that the E-Syts harbor a SMP (synaptotagmin-like mitochondrial-lipid binding protein) domain that is capable of binding lipids in a hydrophobic cavity (250), the authors proposed a potential role of the E-syts in lipid transfer between the ER and PM (251). On the other hand, PI(4,5)P2 in the peroxisomal membranes was shown to be bound by lysosomal protein Syt7 for the tethering between lysosomes and peroxisomes (146). Moreover, Scs2/22 (orthologs of VAPs), the tricalbins (Tcb1/2/3, orthologs of E-syts), and lst2 (related to mammalian TMEM16 ion channel family) were shown to mediate the tethering between the ER and PM independently of each other (156). Therefore, it is possible that E-syt1 serves as another tether at the ER-peroxisome MCSs by binding to peroxisomal PI(4,5)P2. To test this premise, the cellular localization of E-syt1 to peroxisomes, its binding affinity to peroxisomal PI(4,5)P2, and its effect on peroxisome maintenance and lipid homeostasis are important questions to be addressed in the future.

5.5.3 Other functions of ER-peroxisome contact sites

With the discovery of this novel ER-peroxisome tether in the mammalian cells, it is clear that peroxisomes, like mitochondria, form contact sites with the ER. Like the ER-mitochondria MCSs, the contact sites between the ER and peroxisomes are also important for the lipid exchange between them. Notably, a potential function of the ER-mitochondria MCSs in mitochondrial division has been proposed based on the observation from high-resolution EM tomography that the ER tubules wrap around mitochondria at specific sites where mitochondrial fission events occur (252). Further studies suggest that the ER associated inverted formin 2 (INF2) induces actin filament assembly at ER-mitochondria MCSs, thereby providing a driving force for the initial mitochondrial constriction (253). In addition, this initial constriction event occurring at ER-mitochondria MCSs appears to be independent of DLP1 and MFF, implying that it is an early event that facilitates the recruitment of DLP1 and assembly of fission machinery for mitochondrial division (252). As peroxisomes and mitochondria share partially their fission machinery and both organelles form contact sites with the ER, it is possible that the ER-peroxisome MCSs may serve a similar role in peroxisome division.

In the event of peroxisome division, the PEX11 family proteins initiate membrane remodeling and mediate the protrusion of peroxisomal membranes. FIS1 and MFF are recruited to the membrane extension, and concentrate at the site of constriction. FIS1/MFF then recruits cytosolic DLP1 to its site of action and cooperate with it to mediate the final scission of the peroxisomal membranes (25, 29, 30, 33, 71). Similar to mitochondria division, how the constriction sites on peroxisomal membrane extension are formed and how their positions are defined are not known. Interestingly, introducing recombinant Pex11p proteins into liposomes was shown to induce membrane constriction, and the reconstituted Pex11pβ was found at the constriction site, suggesting that Pex11pβ itself may have the ability to induce membrane constriction (254). However, it is also possible that other factors such as the ER may play a role in this process. Therefore, the potential involvement of the ER or actin assembly in peroxisome division is an interesting research question to be uncovered in the future. Specifically, the spatial relationship between the ER tubules (or ER-peroxisome contact sites) and the site of peroxisomal membrane constriction needs to be examined by

super-resolution microscopy. Whether the integrity of actin filaments affects peroxisome proliferation also needs to be tested.

5.6 Concluding Remarks

By taking together the recent novel findings and the data presented in this thesis, we propose a model for peroxisome maintenance in the mammalian system (Fig. 5.3). PMPs can be imported to peroxisomes via two distinct pathways: the indirect Group I pathway via the ER and the Group II pathway in which PMPs target directly to peroxisomes. Under basal conditions, PEX16 is first cotranslationally inserted into the ER, where it is able to recruit certain essential PMPs, including PEX3 (for insertion of other PMPs), PEX11 and MFF/FIS1/DLP1 (for subsequent growth and division), to the ER membranes. These PMPs together with PEX16 may accumulate in a specialized subdomain on the ER to generate the pre-peroxisomal vesicles or other pre-peroxisomal structures. These pre-peroxisomal structures can either fuse with pre-existing peroxisomes to provide lipids and essential PMPs for their steady-state maintenance, or they can mature to give rise to newly formed peroxisomes. In the latter scenario, matrix proteins are imported directly from the cytosol into these early peroxisomes to allow for the formation of mature functional peroxisomes. Under conditions where the amount of PMPs increases dramatically, such as exogenous over-expression of PMPs or induction of peroxisome proliferation via activation of PPARs, the ER pathway becomes saturated, resulting in PMPs targeting directly to peroxisomes to allow for their rapid growth and proliferation. Mitochondria are another potential contributor for membrane required for peroxisome growth, and the communication between these two organelles may be mediated by MDVs with unknown characteristics and functions. Similar to the ER-derived pre-peroxisomal structures, these MDVs may either fuse with pre-existing peroxisomes or form new ones *de novo*. At the same time, peroxisomes also form numerous contact sites with other organelles including the ER and mitochondria. At these contact sites, various lipid molecules, which are important for peroxisome maintenance and other metabolic functions, are exchanged between peroxisomes and the other organelles.

This model is likely a crude version of the mechanism by which the cells actually maintain peroxisomes. However, new technological advances in microscopy and gene editing will

likely bring about novel and creative experimental approaches to elucidate the mechanism of peroxisome maintenance. In summary, advancing the knowledge and details on the connection between peroxisomes and other organelles will bring about new functions that peroxisomes may play in both cellular homeostasis and diseases that have not been previously attributed to peroxisomes.

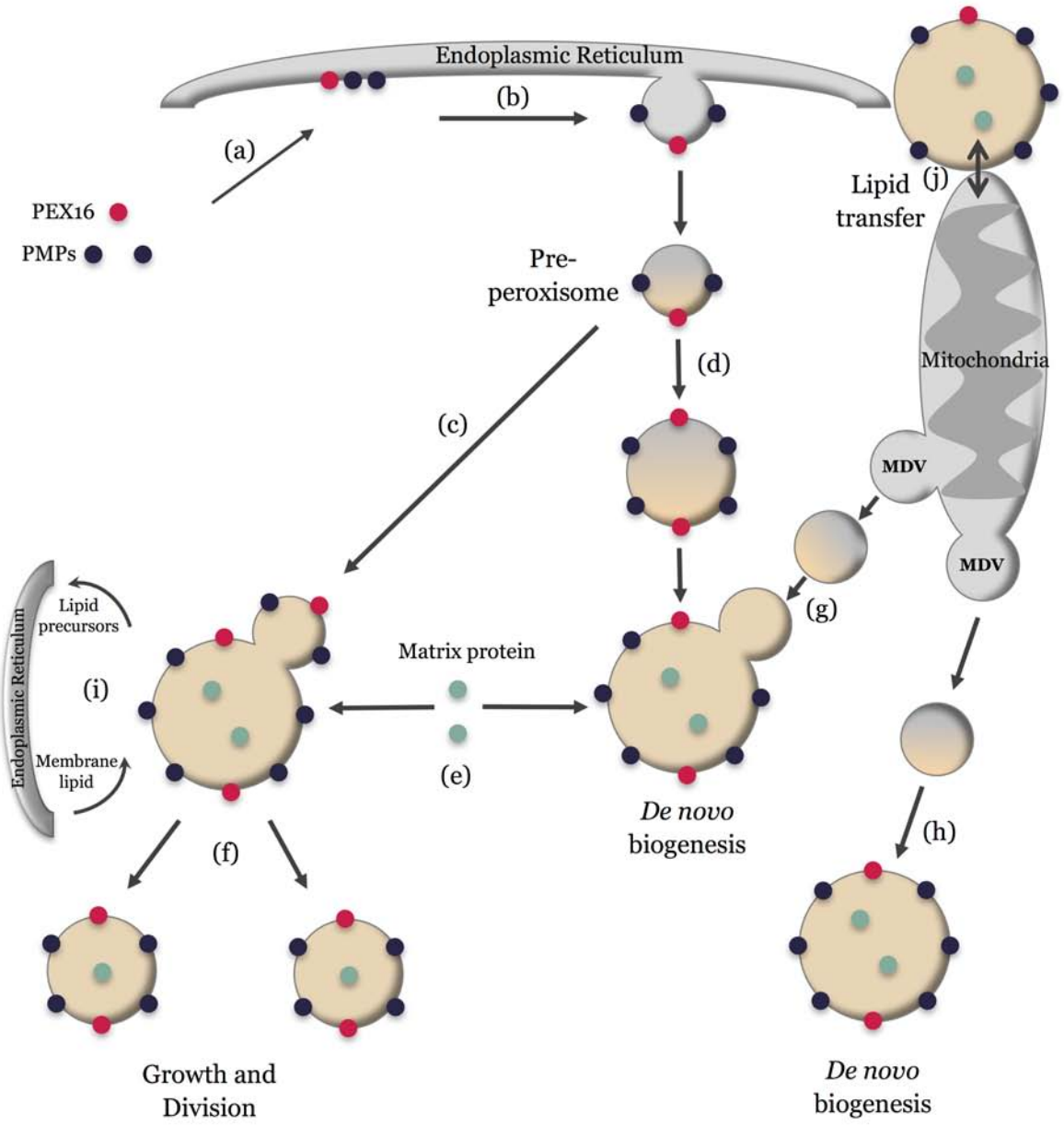

Figure 5.3 Model for peroxisome maintenance in mammalian cells
Mammalian peroxisomes can propagate via growth and division from pre-existing ones, as well as be derived *de novo* from other organelles, such as the ER and perhaps the mitochondria. (a) The *de novo* biogenesis of peroxisomes from the ER starts when PEX16 is first cotranslationally inserted into the ER, where it recruits other essential PMPs involved in membrane remodeling, such as the PEX11 family proteins, that induce membrane elongation and recruit the fission machinery proteins MFF and FIS1 to their sites of action (for subsequent growth and division) on the ER. The early-stage peroxin, PEX3, is also recruited to the ER by PEX16. (b) These PMPs together with PEX16 accumulate in a specialized subdomain on the ER, leading to the formation of the pre-peroxisomal vesicles or other pre-peroxisomal structures. (c) Once being released from the ER, these pre-peroxisomal structures can either fuse with pre-existing peroxisomes to provide lipid and essential proteins for their steady-state maintenance, or (d) they can mature into newly formed peroxisomes (Fig. 5.1). (e) Matrix proteins are

imported directly into peroxisomes from the cytosol by the protein import machinery comprised of the docking complex (PEX14/PEX13), the RING complex (PEX2/PEX10/PEX12), and the AAA-type ATPase complex (PEX1/PEX6/PEX16). (f) On the other hand, peroxisomes can also proliferate via growth and division from pre-existing ones. The fission machinery proteins, DLP1/Drp1, FIS1, and MFF, work cooperatively with the PEX11 family to mediate the fission of peroxisomes. (g) Another potential contributor for peroxisome biogenesis is mitochondria. The communication between these two organelles is partially mediated by the mitochondria-derived vesicles (MDVs) that could either (g) fuse with pre-existing peroxisomes to provide them with lipids and proteins, or (h) mature into functional peroxisomes. (i) Another function of the ER in peroxisome maintenance is to act as a donor for phospholipid (for the development of peroxisomal endomembrane system), lipid metabolites (for their metabolism), and lipid intermediates (for the biosynthesis of specialized lipids). The transfer of lipid between peroxisomes and the ER is mediated by a nonvesicular pathway in which membrane contact sites between the two organelles are required for this transfer. (j) Lipid exchange between peroxisomes and mitochondria may also occur via their membrane contact sites. These contact sites are most likely to be used for the exchange of lipid metabolites for lipid oxidation.

References

1. van den Bosch H, Schutgens RB, Wanders RJ, Tager JM. Biochemistry of peroxisomes. Annual review of biochemistry 1992;61:157-197.

2. Wanders RJ, Waterham HR. Peroxisomal disorders: the single peroxisomal enzyme deficiencies. Biochimica et biophysica acta 2006;1763(12):1707-1720.

3. Islinger M, Cardoso MJ, Schrader M. Be different--the diversity of peroxisomes in the animal kingdom. Biochimica et biophysica acta 2010;1803(8):881-897.

4. Steinberg SJ, Dodt G, Raymond GV, Braverman NE, Moser AB, Moser HW. Peroxisome biogenesis disorders. Biochimica et biophysica acta 2006;1763(12):1733-1748.

5. Issemann I, Green S. Activation of a member of the steroid hormone receptor superfamily by peroxisome proliferators. Nature 1990;347(6294):645-650.

6. Kliewer SA, Umesono K, Noonan DJ, Heyman RA, Evans RM. Convergence of 9-cis retinoic acid and peroxisome proliferator signalling pathways through heterodimer formation of their receptors. Nature 1992;358(6389):771-774.

7. Latruffe N, Vamecq J. Peroxisome proliferators and peroxisome proliferator activated receptors (PPARs) as regulators of lipid metabolism. Biochimie 1997;79(2-3):81-94.

8. Reddy JK. Peroxisome proliferators and peroxisome proliferator-activated receptor alpha: biotic and xenobiotic sensing. The American journal of pathology 2004;164(6):2305-2321.

9. Erdmann R, Veenhuis M, Mertens D, Kunau WH. Isolation of peroxisome-deficient mutants of Saccharomyces cerevisiae. Proceedings of the National Academy of Sciences of the United States of America 1989;86(14):5419-5423.

10. Tsukamoto T, Yokota S, Fujiki Y. Isolation and characterization of Chinese hamster ovary cell mutants defective in assembly of peroxisomes. The Journal of cell biology 1990;110(3):651-660.

11. Platta HW, Erdmann R. Peroxisomal dynamics. Trends in cell biology 2007;17(10):474-484.

12. Schrader M, Fahimi HD. The peroxisome: still a mysterious organelle. Histochemistry and cell biology 2008;129(4):421-440.

13. Fujiki Y, Okumoto K, Mukai S, Honsho M, Tamura S. Peroxisome biogenesis in mammalian cells. Frontiers in physiology 2014;5:307.

14. Santos MJ, Imanaka T, Shio H, Small GM, Lazarow PB. Peroxisomal membrane ghosts in Zellweger syndrome--aberrant organelle assembly. Science 1988;239(4847):1536-1538.

15. Honsho M, Tamura S, Shimozawa N, Suzuki Y, Kondo N, Fujiki Y. Mutation in PEX16 is causal in the peroxisome-deficient Zellweger syndrome of complementation group D. American journal of human genetics 1998;63(6):1622-1630.

16. South ST, Gould SJ. Peroxisome synthesis in the absence of preexisting peroxisomes. The Journal of cell biology 1999;144(2):255-266.

17. Matsuzono Y, Kinoshita N, Tamura S, Shimozawa N, Hamasaki M, Ghaedi K, Wanders RJ, Suzuki Y, Kondo N, Fujiki Y. Human PEX19: cDNA cloning by functional complementation, mutation analysis in a patient with Zellweger syndrome, and potential role in peroxisomal membrane assembly. Proceedings of the National Academy of Sciences of the United States of America 1999;96(5):2116-2121.

18. Sacksteder KA, Jones JM, South ST, Li X, Liu Y, Gould SJ. PEX19 binds multiple peroxisomal membrane proteins, is predominantly cytoplasmic, and is required for peroxisome membrane synthesis. The Journal of cell biology 2000;148(5):931-944.

19. Muntau AC, Mayerhofer PU, Paton BC, Kammerer S, Roscher AA. Defective peroxisome membrane synthesis due to mutations in human PEX3 causes Zellweger syndrome, complementation group G. American journal of human genetics 2000;67(4):967-975.

20. Ghaedi K, Honsho M, Shimozawa N, Suzuki Y, Kondo N, Fujiki Y. PEX3 is the causal gene responsible for peroxisome membrane assembly-defective Zellweger syndrome of complementation group G. American journal of human genetics 2000;67(4):976-981.

21. Ghaedi K, Tamura S, Okumoto K, Matsuzono Y, Fujiki Y. The peroxin pex3p initiates membrane assembly in peroxisome biogenesis. Molecular biology of the cell 2000;11(6):2085-2102.

22. Shimozawa N, Suzuki Y, Zhang Z, Imamura A, Ghaedi K, Fujiki Y, Kondo N. Identification of PEX3 as the gene mutated in a Zellweger syndrome patient lacking peroxisomal remnant structures. Hum Mol Genet 2000;9(13):1995-1999.

23. Hohfeld J, Veenhuis M, Kunau WH. PAS3, a Saccharomyces cerevisiae gene encoding a peroxisomal integral membrane protein essential for peroxisome biogenesis. The Journal of cell biology 1991;114(6):1167-1178.

24. Gotte K, Girzalsky W, Linkert M, Baumgart E, Kammerer S, Kunau WH, Erdmann R. Pex19p, a farnesylated protein essential for peroxisome biogenesis. Mol Cell Biol 1998;18(1):616-628.

25. Koch A, Thiemann M, Grabenbauer M, Yoon Y, McNiven MA, Schrader M. Dynamin-like protein 1 is involved in peroxisomal fission. The Journal of biological chemistry 2003;278(10):8597-8605.

26. Li X, Gould SJ. The dynamin-like GTPase DLP1 is essential for peroxisome division and is recruited to peroxisomes in part by PEX11. The Journal of biological chemistry 2003;278(19):17012-17020.

27. Tanaka A, Kobayashi S, Fujiki Y. Peroxisome division is impaired in a CHO cell mutant with an inactivating point-mutation in dynamin-like protein 1 gene. Experimental cell research 2006;312(9):1671-1684.

28. Waterham HR, Koster J, van Roermund CW, Mooyer PA, Wanders RJ, Leonard JV. A lethal defect of mitochondrial and peroxisomal fission. The New England journal of medicine 2007;356(17):1736-1741.

29. Koch A, Yoon Y, Bonekamp NA, McNiven MA, Schrader M. A role for Fis1 in both mitochondrial and peroxisomal fission in mammalian cells. Molecular biology of the cell 2005;16(11):5077-5086.

30. Kobayashi S, Tanaka A, Fujiki Y. Fis1, DLP1, and Pex11p coordinately regulate peroxisome morphogenesis. Experimental cell research 2007;313(8):1675-1686.

31. Gandre-Babbe S, van der Bliek AM. The novel tail-anchored membrane protein Mff controls mitochondrial and peroxisomal fission in mammalian cells. Molecular biology of the cell 2008;19(6):2402-2412.

32. Otera H, Wang C, Cleland MM, Setoguchi K, Yokota S, Youle RJ, Mihara K. Mff is an essential factor for mitochondrial recruitment of Drp1 during mitochondrial fission in mammalian cells. The Journal of cell biology 2010;191(6):1141-1158.

33. Koch J, Brocard C. PEX11 proteins attract Mff and human Fis1 to coordinate peroxisomal fission. Journal of cell science 2012;125(Pt 16):3813-3826.

34. Itoyama A, Michiyuki S, Honsho M, Yamamoto T, Moser A, Yoshida Y, Fujiki Y. Mff functions with Pex11pbeta and DLP1 in peroxisomal fission. Biology open 2013;2(10):998-1006.

35. Prinz WA. Bridging the gap: membrane contact sites in signaling, metabolism, and organelle dynamics. J Cell Biol 2014;205(6):759-769.

36. Helle SC, Kanfer G, Kolar K, Lang A, Michel AH, Kornmann B. Organization and function of membrane contact sites. Biochim Biophys Acta 2013;1833(11):2526-2541.

37. Schrader M, Grille S, Fahimi HD, Islinger M. Peroxisome interactions and cross-talk with other subcellular compartments in animal cells. Subcell Biochem 2013;69:1-22.

38. Shai N, Schuldiner M, Zalckvar E. No peroxisome is an island - Peroxisome contact sites. Biochim Biophys Acta 2016;1863(5):1061-1069.

39. Geuze HJ, Murk JL, Stroobants AK, Griffith JM, Kleijmeer MJ, Koster AJ, Verkleij AJ, Distel B, Tabak HF. Involvement of the endoplasmic reticulum in peroxisome formation. Mol Biol Cell 2003;14(7):2900-2907.

40. Hettema EH, Erdmann R, van der Klei I, Veenhuis M. Evolving models for peroxisome biogenesis. Curr Opin Cell Biol 2014;29:25-30.

41. Braverman NE, Moser AB. Functions of plasmalogen lipids in health and disease. Biochim Biophys Acta 2012;1822(9):1442-1452.

42. Kovacs WJ, Tape KN, Shackelford JE, Duan X, Kasumov T, Kelleher JK, Brunengraber H, Krisans SK. Localization of the pre-squalene segment of the isoprenoid biosynthetic pathway in mammalian peroxisomes. Histochemistry and cell biology 2007;127(3):273-290.

43. Yan M, Rachubinski DA, Joshi S, Rachubinski RA, Subramani S. Dysferlin domain-containing proteins, Pex30p and Pex31p, localized to two compartments, control the number and size of oleate-induced peroxisomes in Pichia pastoris. Mol Biol Cell 2008;19(3):885-898.

44. David C, Koch J, Oeljeklaus S, Laernsack A, Melchior S, Wiese S, Schummer A, Erdmann R, Warscheid B, Brocard C. A combined approach of quantitative interaction proteomics and live-cell imaging reveals a regulatory role for endoplasmic reticulum (ER) reticulon homology proteins in peroxisome biogenesis. Mol Cell Proteomics 2013;12(9):2408-2425.

45. Raychaudhuri S, Prinz WA. Nonvesicular phospholipid transfer between peroxisomes and the endoplasmic reticulum. Proc Natl Acad Sci U S A 2008;105(41):15785-15790.

46. Rhodin J. Correlation of ultrastructural organization and function in normal and experimentally changed proximal convoluted tubule cells of the mouse kidney. Aktiebolaget Godvil Stockholm: Karolinska Institute; 1954.

47. Bernhard W, Rouiller C. Microbodies and the problem of mitochondrial regeneration in liver cells. The Journal of biophysical and biochemical cytology 1956;2(4 Suppl):355-360.

48. De Duve C, Baudhuin P. Peroxisomes (microbodies and related particles). Physiological reviews 1966;46(2):323-357.

49. J R. In An Atlas of Ultrastructure. Philadelphia: Saunders; 1963.

50. AB Novikoff WS. The endoplasmic reticulum in the Golgi zone and its relations to microbodies, Golgi apparatus and autophagic vacuoles in rat liver cells. J Micros 1964;Oxford 3:187-206.

51. Higashi T, Peters T, Jr. Studies on Rat Liver Catalase. Ii. Incorporation of 14-C-Leucine into Catalase of Liver Cell Fractions in Vivo. The Journal of biological chemistry 1963;238:3952-3954.

52. Novikoff PM, Novikoff AB. Peroxisomes in absorptive cells of mammalian small intestine. The Journal of cell biology 1972;53(2):532-560.

53. Hora K, Ohno S, Oguchi H, Furukawa T, Furuta S. Three-dimensional study of glomerular slit diaphragm by the quick-freezing and deep-etching replica method. European journal of cell biology 1990;53(2):402-406.

54. Lazarow PB, Fujiki Y. Biogenesis of peroxisomes. Annual review of cell biology 1985;1:489-530.

55. Goldman BM, Blobel G. Biogenesis of peroxisomes: intracellular site of synthesis of catalase and uricase. Proceedings of the National Academy of Sciences of the United States of America 1978;75(10):5066-5070.

56. Lazarow PB, de Duve C. The synthesis and turnover of rat liver peroxisomes. V. Intracellular pathway of catalase synthesis. The Journal of cell biology 1973;59(2 Pt 1):507-524.

57. Fujiki Y, Rachubinski RA, Lazarow PB. Synthesis of a major integral membrane polypeptide of rat liver peroxisomes on free polysomes. Proceedings of the National Academy of Sciences of the United States of America 1984;81(22):7127-7131.

58. Miura S, Mori M, Takiguchi M, Tatibana M, Furuta S, Miyazawa S, Hashimoto T. Biosynthesis and intracellular transport of enzymes of peroxisomal beta-oxidation. The Journal of biological chemistry 1984;259(10):6397-6402.

59. Gould SG, Keller GA, Subramani S. Identification of a peroxisomal targeting signal at the carboxy terminus of firefly luciferase. J Cell Biol 1987;105(6 Pt 2):2923-2931.

60. Swinkels BW, Gould SJ, Bodnar AG, Rachubinski RA, Subramani S. A novel, cleavable peroxisomal targeting signal at the amino-terminus of the rat 3-ketoacyl-CoA thiolase. EMBO J 1991;10(11):3255-3262.

61. Hasan S, Platta HW, Erdmann R. Import of proteins into the peroxisomal matrix. Frontiers in physiology 2013;4:261.

62. Kim PK, Hettema EH. Multiple pathways for protein transport to peroxisomes. Journal of molecular biology 2015;427(6 Pt A):1176-1190.

63. Ma C, Agrawal G, Subramani S. Peroxisome assembly: matrix and membrane protein biogenesis. The Journal of cell biology 2011;193(1):7-16.

64. Tabak HF, Braakman I, van der Zand A. Peroxisome formation and maintenance are dependent on the endoplasmic reticulum. Annual review of biochemistry 2013;82:723-744.

65. Fakieh MH, Drake PJ, Lacey J, Munck JM, Motley AM, Hettema EH. Intra-ER sorting of the peroxisomal membrane protein Pex3 relies on its luminal domain. Biology open 2013;2(8):829-837.

66. Van Ael E, Fransen M. Targeting signals in peroxisomal membrane proteins. Biochimica et biophysica acta 2006;1763(12):1629-1638.

67. Theodoulou FL, Bernhardt K, Linka N, Baker A. Peroxisome membrane proteins: multiple trafficking routes and multiple functions? The Biochemical journal 2013;451(3):345-352.

68. Hettema EH, Girzalsky W, van Den Berg M, Erdmann R, Distel B. Saccharomyces cerevisiae pex3p and pex19p are required for proper localization and stability of peroxisomal membrane proteins. The EMBO journal 2000;19(2):223-233.

69. Snyder WB, Koller A, Choy AJ, Subramani S. The peroxin Pex19p interacts with multiple, integral membrane proteins at the peroxisomal membrane. The Journal of cell biology 2000;149(6):1171-1178.

70. Fang Y, Morrell JC, Jones JM, Gould SJ. PEX3 functions as a PEX19 docking factor in the import of class I peroxisomal membrane proteins. The Journal of cell biology 2004;164(6):863-875.

71. Huber A, Koch J, Kragler F, Brocard C, Hartig A. A subtle interplay between three Pex11 proteins shapes de novo formation and fission of peroxisomes. Traffic 2012;13(1):157-167.

72. Titorenko VI, Chan H, Rachubinski RA. Fusion of small peroxisomal vesicles in vitro reconstructs an early step in the in vivo multistep peroxisome assembly pathway of Yarrowia lipolytica. J Cell Biol 2000;148(1):29-44.

73. van der Zand A, Gent J, Braakman I, Tabak HF. Biochemically distinct vesicles from the endoplasmic reticulum fuse to form peroxisomes. Cell 2012;149(2):397-409.

74. Knoops K, Manivannan S, Cepinska MN, Krikken AM, Kram AM, Veenhuis M, van der Klei IJ. Preperoxisomal vesicles can form in the absence of Pex3. The Journal of cell biology 2014;204(5):659-668.

75. Hashiguchi N, Kojidani T, Imanaka T, Haraguchi T, Hiraoka Y, Baumgart E, Yokota S, Tsukamoto T, Osumi T. Peroxisomes are formed from complex membrane structures in PEX6-deficient CHO cells upon genetic complementation. Molecular biology of the cell 2002;13(2):711-722.

76. Baes M, Gressens P, Baumgart E, Carmeliet P, Casteels M, Fransen M, Evrard P, Fahimi D, Declercq PE, Collen D, van Veldhoven PP, Mannaerts GP. A mouse model for Zellweger syndrome. Nature genetics 1997;17(1):49-57.

77. Kim PK, Mullen RT, Schumann U, Lippincott-Schwartz J. The origin and maintenance of mammalian peroxisomes involves a de novo PEX16-dependent pathway from the ER. J Cell Biol 2006;173(4):521-532.

78. Aranovich A, Hua R, Rutenberg AD, Kim PK. PEX16 contributes to peroxisome maintenance by constantly trafficking PEX3 via the ER. Journal of cell science 2014;127(Pt 17):3675-3686.

79. Hua R, Gidda SK, Aranovich A, Mullen RT, Kim PK. Multiple Domains in PEX16 Mediate Its Trafficking and Recruitment of Peroxisomal Proteins to the ER. Traffic 2015;16(8):832-852.

80. Toro AA, Araya CA, Cordova GJ, Arredondo CA, Cardenas HG, Moreno RE, Venegas A, Koenig CS, Cancino J, Gonzalez A, Santos MJ. Pex3p-dependent peroxisomal biogenesis initiates in the endoplasmic reticulum of human fibroblasts. Journal of cellular biochemistry 2009;107(6):1083-1096.

81. South ST, Sacksteder KA, Li X, Liu Y, Gould SJ. Inhibitors of COPI and COPII do not block PEX3-mediated peroxisome synthesis. The Journal of cell biology 2000;149(7):1345-1360.

82. Voorn-Brouwer T, Kragt A, Tabak HF, Distel B. Peroxisomal membrane proteins are properly targeted to peroxisomes in the absence of COPI- and COPII-mediated vesicular transport. Journal of cell science 2001;114(Pt 11):2199-2204.

83. Lazarow PB. Peroxisome biogenesis: advances and conundrums. Current opinion in cell biology 2003;15(4):489-497.

84. Yonekawa S, Furuno A, Baba T, Fujiki Y, Ogasawara Y, Yamamoto A, Tagaya M, Tani K. Sec16B is involved in the endoplasmic reticulum export of the peroxisomal membrane biogenesis factor peroxin 16 (Pex16) in mammalian cells. Proceedings of the National Academy of Sciences of the United States of America 2011;108(31):12746-12751.

85. Titorenko VI, Rachubinski RA. Dynamics of peroxisome assembly and function. Trends in cell biology 2001;11(1):22-29.

86. Titorenko VI, Rachubinski RA. The life cycle of the peroxisome. Nature reviews Molecular cell biology 2001;2(5):357-368.

87. Suzuki Y, Orii T, Takiguchi M, Mori M, Hijikata M, Hashimoto T. Biosynthesis of membrane polypeptides of rat liver peroxisomes. Journal of biochemistry 1987;101(2):491-496.

88. Diestelkotter P, Just WW. In vitro insertion of the 22-kD peroxisomal membrane protein into isolated rat liver peroxisomes. The Journal of cell biology 1993;123(6 Pt 2):1717-1725.

89. Imanaka T, Takano T, Osumi T, Hashimoto T. Sorting of the 70-kDa peroxisomal membrane protein into rat liver peroxisomes in vitro. Annals of the New York Academy of Sciences 1996;804:663-665.

90. Matsuzono Y, Fujiki Y. In vitro transport of membrane proteins to peroxisomes by shuttling receptor Pex19p. The Journal of biological chemistry 2006;281(1):36-42.

91. Jones JM, Morrell JC, Gould SJ. PEX19 is a predominantly cytosolic chaperone and import receptor for class 1 peroxisomal membrane proteins. The Journal of cell biology 2004;164(1):57-67.

92. Yagita Y, Hiromasa T, Fujiki Y. Tail-anchored PEX26 targets peroxisomes via a PEX19-dependent and TRC40-independent class I pathway. The Journal of cell biology 2013;200(5):651-666.

93. Kashiwayama Y, Asahina K, Shibata H, Morita M, Muntau AC, Roscher AA, Wanders RJ, Shimozawa N, Sakaguchi M, Kato H, Imanaka T. Role of Pex19p in the targeting of PMP70 to peroxisome. Biochimica et biophysica acta 2005;1746(2):116-128.

94. Sato Y, Shibata H, Nakatsu T, Nakano H, Kashiwayama Y, Imanaka T, Kato H. Structural basis for docking of peroxisomal membrane protein carrier Pex19p onto its receptor Pex3p. The EMBO journal 2010;29(24):4083-4093.

95. Schmidt F, Dietrich D, Eylenstein R, Groemping Y, Stehle T, Dodt G. The role of conserved PEX3 regions in PEX19-binding and peroxisome biogenesis. Traffic 2012;13(9):1244-1260.

96. Matsuzaki T, Fujiki Y. The peroxisomal membrane protein import receptor Pex3p is directly transported to peroxisomes by a novel Pex19p- and Pex16p-dependent pathway. The Journal of cell biology 2008;183(7):1275-1286.

97. Titorenko VI, Rachubinski RA. Mutants of the yeast Yarrowia lipolytica defective in protein exit from the endoplasmic reticulum are also defective in peroxisome biogenesis. Mol Cell Biol 1998;18(5):2789-2803.

98. van der Zand A, Braakman I, Tabak HF. Peroxisomal membrane proteins insert into the endoplasmic reticulum. Molecular biology of the cell 2010;21(12):2057-2065.

99. Guo T, Kit YY, Nicaud JM, Le Dall MT, Sears SK, Vali H, Chan H, Rachubinski RA, Titorenko VI. Peroxisome division in the yeast Yarrowia lipolytica is regulated by a signal from inside the peroxisome. The Journal of cell biology 2003;162(7):1255-1266.

100. Guo T, Gregg C, Boukh-Viner T, Kyryakov P, Goldberg A, Bourque S, Banu F, Haile S, Milijevic S, San KH, Solomon J, Wong V, Titorenko VI. A signal from inside the peroxisome initiates its division by promoting the remodeling of the peroxisomal membrane. The Journal of cell biology 2007;177(2):289-303.

101. Fransen M, Wylin T, Brees C, Mannaerts GP, Van Veldhoven PP. Human pex19p binds peroxisomal integral membrane proteins at regions distinct from their sorting sequences. Mol Cell Biol 2001;21(13):4413-4424.

102. Honsho M, Hiroshige T, Fujiki Y. The membrane biogenesis peroxin Pex16p. Topogenesis and functional roles in peroxisomal membrane assembly. The Journal of biological chemistry 2002;277(46):44513-44524.

103. Schluter A, Real-Chicharro A, Gabaldon T, Sanchez-Jimenez F, Pujol A. PeroxisomeDB 2.0: an integrative view of the global peroxisomal metabolome. Nucleic acids research 2010;38(Database issue):D800-805.

104. Lev S. Non-vesicular lipid transport by lipid-transfer proteins and beyond. Nat Rev Mol Cell Biol 2010;11(10):739-750.

105. Jackson CL, Walch L, Verbavatz JM. Lipids and Their Trafficking: An Integral Part of Cellular Organization. Dev Cell 2016;39(2):139-153.

106. D'Angelo G, Vicinanza M, De Matteis MA. Lipid-transfer proteins in biosynthetic pathways. Curr Opin Cell Biol 2008;20(4):360-370.

107. Mesmin B, Bigay J, Moser von Filseck J, Lacas-Gervais S, Drin G, Antonny B. A four-step cycle driven by PI(4)P hydrolysis directs sterol/PI(4)P exchange by the ER-Golgi tether OSBP. Cell 2013;155(4):830-843.

108. Hanada K, Kumagai K, Yasuda S, Miura Y, Kawano M, Fukasawa M, Nishijima M. Molecular machinery for non-vesicular trafficking of ceramide. Nature 2003;426(6968):803-809.

109. Kumagai K, Kawano-Kawada M, Hanada K. Phosphoregulation of the ceramide transport protein CERT at serine 315 in the interaction with VAMP-associated protein (VAP) for inter-organelle trafficking of ceramide in mammalian cells. J Biol Chem 2014;289(15):10748-10760.

110. Toulmay A, Prinz WA. A conserved membrane-binding domain targets proteins to organelle contact sites. J Cell Sci 2012;125(Pt 1):49-58.

111. Binns D, Januszewski T, Chen Y, Hill J, Markin VS, Zhao Y, Gilpin C, Chapman KD, Anderson RG, Goodman JM. An intimate collaboration between peroxisomes and lipid bodies. J Cell Biol 2006;173(5):719-731.

112. Mehrshahi P, Stefano G, Andaloro JM, Brandizzi F, Froehlich JE, DellaPenna D. Transorganellar complementation redefines the biochemical continuity of endoplasmic reticulum and chloroplasts. Proc Natl Acad Sci U S A 2013;110(29):12126-12131.

113. Chapman KD, Trelease RN. Acquisition of membrane lipids by differentiating glyoxysomes: role of lipid bodies. The Journal of cell biology 1991;115(4):995-1007.

114. Lev S. Nonvesicular lipid transfer from the endoplasmic reticulum. Cold Spring Harbor perspectives in biology 2012;4(10).

115. Bascom RA, Chan H, Rachubinski RA. Peroxisome biogenesis occurs in an unsynchronized manner in close association with the endoplasmic reticulum in temperature-sensitive Yarrowia lipolytica Pex3p mutants. Mol Biol Cell 2003;14(3):939-957.

116. Blanchette-Mackie EJ, Dwyer NK, Barber T, Coxey RA, Takeda T, Rondinone CM, Theodorakis JL, Greenberg AS, Londos C. Perilipin is located on the surface layer of intracellular lipid droplets in adipocytes. Journal of lipid research 1995;36(6):1211-1226.

117. Knoblach B, Sun X, Coquelle N, Fagarasanu A, Poirier RL, Rachubinski RA. An ER-peroxisome tether exerts peroxisome population control in yeast. EMBO J 2013;32(18):2439-2453.

118. Scarpulla RC, Vega RB, Kelly DP. Transcriptional integration of mitochondrial biogenesis. Trends Endocrinol Metab 2012;23(9):459-466.

119. Mohanty A, McBride HM. Emerging roles of mitochondria in the evolution, biogenesis, and function of peroxisomes. Frontiers in physiology 2013;4:268.

120. Madrazo JA, Kelly DP. The PPAR trio: regulators of myocardial energy metabolism in health and disease. J Mol Cell Cardiol 2008;44(6):968-975.

121. Schreiber SN, Emter R, Hock MB, Knutti D, Cardenas J, Podvinec M, Oakeley EJ, Kralli A. The estrogen-related receptor alpha (ERRalpha) functions in PPARgamma coactivator 1alpha (PGC-1alpha)-induced mitochondrial biogenesis. Proceedings of the National Academy of Sciences of the United States of America 2004;101(17):6472-6477.

122. Schoonjans K, Martin G, Staels B, Auwerx J. Peroxisome proliferator-activated receptors, orphans with ligands and functions. Curr Opin Lipidol 1997;8(3):159-166.

123. Green S. PPAR: a mediator of peroxisome proliferator action. Mutat Res 1995;333(1-2):101-109.

124. Reddy JK, Hashimoto T. Peroxisomal beta-oxidation and peroxisome proliferator-activated receptor alpha: an adaptive metabolic system. Annual review of nutrition 2001;21:193-230.

125. Cohen Y, Klug YA, Dimitrov L, Erez Z, Chuartzman SG, Elinger D, Yofe I, Soliman K, Gartner J, Thoms S, Schekman R, Elbaz-Alon Y, Zalckvar E, Schuldiner M. Peroxisomes are juxtaposed to strategic sites on mitochondria. Mol Biosyst 2014;10(7):1742-1748.

126. Mattiazzi Usaj M, Brloznik M, Kaferle P, Zitnik M, Wolinski H, Leitner F, Kohlwein SD, Zupan B, Petrovic U. Genome-Wide Localization Study of Yeast Pex11 Identifies Peroxisome-Mitochondria Interactions through the ERMES Complex. J Mol Biol 2015;427(11):2072-2087.

127. McGuinness MC, Lu JF, Zhang HP, Dong GX, Heinzer AK, Watkins PA, Powers J, Smith KD. Role of ALDP (ABCD1) and mitochondria in X-linked adrenoleukodystrophy. Mol Cell Biol 2003;23(2):744-753.

128. Neuspiel M, Schauss AC, Braschi E, Zunino R, Rippstein P, Rachubinski RA, Andrade-Navarro MA, McBride HM. Cargo-selected transport from the mitochondria to peroxisomes is mediated by vesicular carriers. Current biology : CB 2008;18(2):102-108.

129. Braschi E, Goyon V, Zunino R, Mohanty A, Xu L, McBride HM. Vps35 mediates vesicle transport between the mitochondria and peroxisomes. Current biology : CB 2010;20(14):1310-1315.

130. Schrader M, Fahimi HD. Growth and Division of Peroxisomes. 2006;255:237-290.

131. Schrader M, Bonekamp NA, Islinger M. Fission and proliferation of peroxisomes. Biochimica et biophysica acta 2012;1822(9):1343-1357.

132. Rucktaschel R, Halbach A, Girzalsky W, Rottensteiner H, Erdmann R. De novo synthesis of peroxisomes upon mitochondrial targeting of Pex3p. European journal of cell biology 2010;89(12):947-954.

133. Sugiura A, Mattie S, Prudent J, McBride HM. Newly born peroxisomes are a hybrid of mitochondrial and ER-derived pre-peroxisomes. Nature 2017;542(7640):251-254.

134. Beller M, Thiel K, Thul PJ, Jackle H. Lipid droplets: a dynamic organelle moves into focus. FEBS Lett 2010;584(11):2176-2182.

135. Murphy DJ. The biogenesis and functions of lipid bodies in animals, plants and microorganisms. Prog Lipid Res 2001;40(5):325-438.

136. Barbosa AD, Savage DB, Siniossoglou S. Lipid droplet-organelle interactions: emerging roles in lipid metabolism. Curr Opin Cell Biol 2015;35:91-97.

137. Schrader M, Godinho LF, Costello JL, Islinger M. The different facets of organelle interplay-an overview of organelle interactions. Front Cell Dev Biol 2015;3:56.

138. Novikoff AB, Novikoff PM, Rosen OM, Rubin CS. Organelle relationships in cultured 3T3-L1 preadipocytes. J Cell Biol 1980;87(1):180-196.

139. Hayashi Y, Hayashi M, Hayashi H, Hara-Nishimura I, Nishimura M. Direct interaction between glyoxysomes and lipid bodies in cotyledons of the Arabidopsis thaliana ped1 mutant. Protoplasma 2001;218(1-2):83-94.

140. Schrader M. Tubulo-reticular clusters of peroxisomes in living COS-7 cells: dynamic behavior and association with lipid droplets. J Histochem Cytochem 2001;49(11):1421-1429.

141. Dirkx R, Vanhorebeek I, Martens K, Schad A, Grabenbauer M, Fahimi D, Declercq P, Van Veldhoven PP, Baes M. Absence of peroxisomes in mouse hepatocytes causes mitochondrial and ER abnormalities. Hepatology 2005;41(4):868-878.

142. Zhang SO, Trimble R, Guo F, Mak HY. Lipid droplets as ubiquitous fat storage organelles in C. elegans. BMC Cell Biol 2010;11:96.

143. Pu J, Ha CW, Zhang S, Jung JP, Huh WK, Liu P. Interactomic study on interaction between lipid droplets and mitochondria. Protein Cell 2011;2(6):487-496.

144. Thazar-Poulot N, Miquel M, Fobis-Loisy I, Gaude T. Peroxisome extensions deliver the Arabidopsis SDP1 lipase to oil bodies. Proc Natl Acad Sci U S A 2015;112(13):4158-4163.

145. Schrul B, Kopito RR. Peroxin-dependent targeting of a lipid-droplet-destined membrane protein to ER subdomains. Nat Cell Biol 2016;18(7):740-751.

146. Chu BB, Liao YC, Qi W, Xie C, Du X, Wang J, Yang H, Miao HH, Li BL, Song BL. Cholesterol transport through lysosome-peroxisome membrane contacts. Cell 2015;161(2):291-306.

147. Liscum L, Munn NJ. Intracellular cholesterol transport. Biochim Biophys Acta 1999;1438(1):19-37.

148. Brown MS, Goldstein JL. A receptor-mediated pathway for cholesterol homeostasis. Science 1986;232(4746):34-47.

149. Chang TY, Chang CC, Ohgami N, Yamauchi Y. Cholesterol sensing, trafficking, and esterification. Annu Rev Cell Dev Biol 2006;22:129-157.

150. English AR, Voeltz GK. Endoplasmic reticulum structure and interconnections with other organelles. Cold Spring Harb Perspect Biol 2013;5(4):a013227.

151. Soussan L, Burakov D, Daniels MP, Toister-Achituv M, Porat A, Yarden Y, Elazar Z. ERG30, a VAP-33-related protein, functions in protein transport mediated by COPI vesicles. J Cell Biol 1999;146(2):301-311.

152. Weir ML, Xie H, Klip A, Trimble WS. VAP-A binds promiscuously to both v- and tSNAREs. Biochem Biophys Res Commun 2001;286(3):616-621.

153. Alpy F, Rousseau A, Schwab Y, Legueux F, Stoll I, Wendling C, Spiegelhalter C, Kessler P, Mathelin C, Rio MC, Levine TP, Tomasetto C. STARD3 or STARD3NL and VAP form a novel molecular tether between late endosomes and the ER. J Cell Sci 2013;126(Pt 23):5500-5512.

154. Rocha N, Kuijl C, van der Kant R, Janssen L, Houben D, Janssen H, Zwart W, Neefjes J. Cholesterol sensor ORP1L contacts the ER protein VAP to control Rab7-RILP-p150 Glued and late endosome positioning. J Cell Biol 2009;185(7):1209-1225.

155. De Vos KJ, Morotz GM, Stoica R, Tudor EL, Lau KF, Ackerley S, Warley A, Shaw CE, Miller CC. VAPB interacts with the mitochondrial protein PTPIP51 to regulate calcium homeostasis. Hum Mol Genet 2012;21(6):1299-1311.

156. Manford AG, Stefan CJ, Yuan HL, Macgurn JA, Emr SD. ER-to-plasma membrane tethering proteins regulate cell signaling and ER morphology. Dev Cell 2012;23(6):1129-1140.

157. Murphy SE, Levine TP. VAP, a Versatile Access Point for the Endoplasmic Reticulum: Review and analysis of FFAT-like motifs in the VAPome. Biochim Biophys Acta 2016;1861(8 Pt B):952-961.

158. Wyles JP, Ridgway ND. VAMP-associated protein-A regulates partitioning of oxysterol-binding protein-related protein-9 between the endoplasmic reticulum and Golgi apparatus. Experimental cell research 2004;297(2):533-547.

159. Loewen CJ, Roy A, Levine TP. A conserved ER targeting motif in three families of lipid binding proteins and in Opi1p binds VAP. EMBO J 2003;22(9):2025-2035.

160. Lev S, Ben Halevy D, Peretti D, Dahan N. The VAP protein family: from cellular functions to motor neuron disease. Trends Cell Biol 2008;18(6):282-290.

161. Jansen M, Ohsaki Y, Rega LR, Bittman R, Olkkonen VM, Ikonen E. Role of ORPs in sterol transport from plasma membrane to ER and lipid droplets in mammalian cells. Traffic 2011;12(2):218-231.

162. Kanekura K, Nishimoto I, Aiso S, Matsuoka M. Characterization of amyotrophic lateral sclerosis-linked P56S mutation of vesicle-associated membrane protein-associated protein B (VAPB/ALS8). J Biol Chem 2006;281(40):30223-30233.

163. Suzuki H, Kanekura K, Levine TP, Kohno K, Olkkonen VM, Aiso S, Matsuoka M. ALS-linked P56S-VAPB, an aggregated loss-of-function mutant of VAPB, predisposes motor neurons to ER stress-related death by inducing aggregation of co-expressed wild-type VAPB. J Neurochem 2009;108(4):973-985.

164. Tsuda H, Han SM, Yang Y, Tong C, Lin YQ, Mohan K, Haueter C, Zoghbi A, Harati Y, Kwan J, Miller MA, Bellen HJ. The amyotrophic lateral sclerosis 8 protein VAPB is cleaved, secreted, and acts as a ligand for Eph receptors. Cell 2008;133(6):963-977.

165. Nishimura AL, Mitne-Neto M, Silva HC, Richieri-Costa A, Middleton S, Cascio D, Kok F, Oliveira JR, Gillingwater T, Webb J, Skehel P, Zatz M. A mutation in the vesicle-trafficking protein VAPB causes late-onset spinal muscular atrophy and amyotrophic lateral sclerosis. Am J Hum Genet 2004;75(5):822-831.

166. Qiu L, Qiao T, Beers M, Tan W, Wang H, Yang B, Xu Z. Widespread aggregation of mutant VAPB associated with ALS does not cause motor neuron degeneration or modulate mutant SOD1 aggregation and toxicity in mice. Mol Neurodegener 2013;8:1.

167. Teuling E, Ahmed S, Haasdijk E, Demmers J, Steinmetz MO, Akhmanova A, Jaarsma D, Hoogenraad CC. Motor neuron disease-associated mutant vesicle-associated membrane protein-associated protein (VAP) B recruits wild-type VAPs into endoplasmic reticulum-derived tubular aggregates. J Neurosci 2007;27(36):9801-9815.

168. Langou K, Moumen A, Pellegrino C, Aebischer J, Medina I, Aebischer P, Raoul C. AAV-mediated expression of wild-type and ALS-linked mutant VAPB selectively triggers death of motoneurons through a Ca2+-dependent ER-associated pathway. J Neurochem 2010;114(3):795-809.

169. Gkogkas C, Middleton S, Kremer AM, Wardrope C, Hannah M, Gillingwater TH, Skehel P. VAPB interacts with and modulates the activity of ATF6. Hum Mol Genet 2008;17(11):1517-1526.

170. Boillee S, Vande Velde C, Cleveland DW. ALS: a disease of motor neurons and their nonneuronal neighbors. Neuron 2006;52(1):39-59.

171. Hailey DW, Rambold AS, Satpute-Krishnan P, Mitra K, Sougrat R, Kim PK, Lippincott-Schwartz J. Mitochondria supply membranes for autophagosome biogenesis during starvation. Cell 2010;141(4):656-667.

172. Clark SM, Di Leo R, Van Cauwenberghe OR, Mullen RT, Shelp BJ. Subcellular localization and expression of multiple tomato gamma-aminobutyrate transaminases that utilize both pyruvate and glyoxylate. Journal of experimental botany 2009;60(11):3255-3267.

173. Shockey JM, Gidda SK, Chapital DC, Kuan JC, Dhanoa PK, Bland JM, Rothstein SJ, Mullen RT, Dyer JM. Tung tree DGAT1 and DGAT2 have nonredundant functions in triacylglycerol biosynthesis and are localized to different subdomains of the endoplasmic reticulum. The Plant cell 2006;18(9):2294-2313.

174. Karnik SK, Trelease RN. Arabidopsis peroxin 16 trafficks through the ER and an intermediate compartment to pre-existing peroxisomes via overlapping molecular targeting signals. Journal of experimental botany 2007;58(7):1677-1693.

175. Lingard MJ, Gidda SK, Bingham S, Rothstein SJ, Mullen RT, Trelease RN. Arabidopsis PEROXIN11c-e, FISSION1b, and DYNAMIN-RELATED PROTEIN3A cooperate in cell cycle-associated replication of peroxisomes. The Plant cell 2008;20(6):1567-1585.

176. Roux KJ, Kim DI, Raida M, Burke B. A promiscuous biotin ligase fusion protein identifies proximal and interacting proteins in mammalian cells. J Cell Biol 2012;196(6):801-810.

177. Coyaud E, Mis M, Laurent EM, Dunham WH, Couzens AL, Robitaille M, Gingras AC, Angers S, Raught B. BioID-based Identification of Skp Cullin F-box (SCF)beta-TrCP1/2 E3 Ligase Substrates. Mol Cell Proteomics 2015;14(7):1781-1795.

178. Deutsch EW, Mendoza L, Shteynberg D, Farrah T, Lam H, Tasman N, Sun Z, Nilsson E, Pratt B, Prazen B, Eng JK, Martin DB, Nesvizhskii AI, Aebersold R. A guided tour of the Trans-Proteomic Pipeline. Proteomics 2010;10(6):1150-1159.

179. Pedrioli PG. Trans-proteomic pipeline: a pipeline for proteomic analysis. Methods Mol Biol 2010;604:213-238.

180. Liu G, Zhang J, Larsen B, Stark C, Breitkreutz A, Lin ZY, Breitkreutz BJ, Ding Y, Colwill K, Pasculescu A, Pawson T, Wrana JL, Nesvizhskii AI, Raught B, Tyers M*, et al.* ProHits: integrated software for mass spectrometry-based interaction proteomics. Nat Biotechnol 2010;28(10):1015-1017.

181. Kessner D, Chambers M, Burke R, Agus D, Mallick P. ProteoWizard: open source software for rapid proteomics tools development. Bioinformatics 2008;24(21):2534-2536.

182. Craig R, Beavis RC. TANDEM: matching proteins with tandem mass spectra. Bioinformatics 2004;20(9):1466-1467.

183. Eng JK, Jahan TA, Hoopmann MR. Comet: an open-source MS/MS sequence database search tool. Proteomics 2013;13(1):22-24.

184. Schermelleh L, Heintzmann R, Leonhardt H. A guide to super-resolution fluorescence microscopy. J Cell Biol 2010;190(2):165-175.

185. Jaqaman K, Loerke D, Mettlen M, Kuwata H, Grinstein S, Schmid SL, Danuser G. Robust single-particle tracking in live-cell time-lapse sequences. Nat Methods 2008;5(8):695-702.

186. Kunce CM, Trelease RN, Turley RB. Purification and biosynthesis of cottonseed (Gossypium hirsutum L.) catalase. The Biochemical journal 1988;251(1):147-155.

187. Matsuzono Y, Matsuzaki T, Fujiki Y. Functional domain mapping of peroxin Pex19p: interaction with Pex3p is essential for function and translocation. Journal of cell science 2006;119(Pt 17):3539-3550.

188. Kim PK, Mullen RT. PEX16: a multifaceted regulator of peroxisome biogenesis. Front Physiol 2013;4:241.

189. Hegde RS, Kang SW. The concept of translocational regulation. The Journal of cell biology 2008;182(2):225-232.

190. Wessels HP, Spiess M. Insertion of a multispanning membrane protein occurs sequentially and requires only one signal sequence. Cell 1988;55(1):61-70.

191. Brocard CB, Boucher KK, Jedeszko C, Kim PK, Walton PA. Requirement for microtubules and dynein motors in the earliest stages of peroxisome biogenesis. Traffic 2005;6(5):386-395.

192. Trimble WS, Cowan DM, Scheller RH. VAMP-1: a synaptic vesicle-associated integral membrane protein. Proceedings of the National Academy of Sciences of the United States of America 1988;85(12):4538-4542.

193. Kim PK, Hollerbach C, Trimble WS, Leber B, Andrews DW. Identification of the endoplasmic reticulum targeting signal in vesicle-associated membrane proteins. The Journal of biological chemistry 1999;274(52):36876-36882.

194. Lu G, Chen J, Espinoza LA, Garfield S, Toshiyuki S, Akiko H, Huppler A, Wang QJ. Protein kinase D 3 is localized in vesicular structures and interacts with vesicle-associated membrane protein 2. Cellular signalling 2007;19(4):867-879.

195. Halbach A, Landgraf C, Lorenzen S, Rosenkranz K, Volkmer-Engert R, Erdmann R, Rottensteiner H. Targeting of the tail-anchored peroxisomal membrane proteins PEX26 and PEX15 occurs through C-terminal PEX19-binding sites. Journal of cell science 2006;119(Pt 12):2508-2517.

196. Warren DS, Morrell JC, Moser HW, Valle D, Gould SJ. Identification of PEX10, the gene defective in complementation group 7 of the peroxisome-biogenesis disorders. American journal of human genetics 1998;63(2):347-359.

197. Abe I, Fujiki Y. cDNA cloning and characterization of a constitutively expressed isoform of the human peroxin Pex11p. Biochem Biophys Res Commun 1998;252(2):529-533.

198. Nemoto Y, De Camilli P. Recruitment of an alternatively spliced form of synaptojanin 2 to mitochondria by the interaction with the PDZ domain of a mitochondrial outer membrane protein. The EMBO journal 1999;18(11):2991-3006.

199. Horie C, Suzuki H, Sakaguchi M, Mihara K. Characterization of signal that directs C-tail-anchored proteins to mammalian mitochondrial outer membrane. Molecular biology of the cell 2002;13(5):1615-1625.

200. Lin Y, Cluette-Brown JE, Goodman HM. The peroxisome deficient Arabidopsis mutant sse1 exhibits impaired fatty acid synthesis. Plant physiology 2004;135(2):814-827.

201. Fukao Y, Hayashi Y, Mano S, Hayashi M, Nishimura M. Developmental analysis of a putative ATP/ADP carrier protein localized on glyoxysomal membranes during the peroxisome transition in pumpkin cotyledons. Plant & cell physiology 2001;42(8):835-841.

202. Hunt JE, Trelease RN. Sorting pathway and molecular targeting signals for the Arabidopsis peroxin 3. Biochemical and Biophysical Research Communications 2004;314(2):586-596.

203. Motley AM, Hettema EH. Yeast peroxisomes multiply by growth and division. The Journal of cell biology 2007;178(3):399-410.

204. Higy M, Junne T, Spiess M. Topogenesis of membrane proteins at the endoplasmic reticulum. Biochemistry 2004;43(40):12716-12722.

205. Walton PA, Wendland M, Subramani S, Rachubinski RA, Welch WJ. Involvement of 70-kD heat-shock proteins in peroxisomal import. The Journal of cell biology 1994;125(5):1037-1046.

206. Hua R, Kim PK. Multiple paths to peroxisomes: Mechanism of peroxisome maintenance in mammals. Biochimica et biophysica acta 2016;1863(5):881-891.

207. Agrawal G, Subramani S. De novo peroxisome biogenesis: Evolving concepts and conundrums. Biochimica et biophysica acta 2016;1863(5):892-901.

208. Schrader M, Costello JL, Godinho LF, Azadi AS, Islinger M. Proliferation and fission of peroxisomes - An update. Biochimica et biophysica acta 2016;1863(5):971-983.

209. Antonenkov VD, Hiltunen JK. Transfer of metabolites across the peroxisomal membrane. Biochimica et biophysica acta 2012;1822(9):1374-1386.

210. Hunt MC, Tillander V, Alexson SE. Regulation of peroxisomal lipid metabolism: the role of acyl-CoA and coenzyme A metabolizing enzymes. Biochimie 2014;98:45-55.

211. Lam SK, Yoda N, Schekman R. A vesicle carrier that mediates peroxisome protein traffic from the endoplasmic reticulum. Proc Natl Acad Sci U S A 2010;107(50):21523-21528.

212. Agrawal G, Joshi S, Subramani S. Cell-free sorting of peroxisomal membrane proteins from the endoplasmic reticulum. Proc Natl Acad Sci U S A 2011;108(22):9113-9118.

213. Ng SK, Liu F, Lai J, Low W, Jedd G. A tether for Woronin body inheritance is associated with evolutionary variation in organelle positioning. PLoS Genet 2009;5(6):e1000521.

214. Gupta GD, Coyaud E, Goncalves J, Mojarad BA, Liu Y, Wu Q, Gheiratmand L, Comartin D, Tkach JM, Cheung SW, Bashkurov M, Hasegan M, Knight JD, Lin ZY, Schueler M*, et al.* A Dynamic Protein Interaction Landscape of the Human Centrosome-Cilium Interface. Cell 2015;163(6):1484-1499.

215. Cole A, Wang Z, Coyaud E, Voisin V, Gronda M, Jitkova Y, Mattson R, Hurren R, Babovic S, Maclean N, Restall I, Wang X, Jeyaraju DV, Sukhai MA, Prabha S*, et al.* Inhibition of the Mitochondrial Protease ClpP as a Therapeutic Strategy for Human Acute Myeloid Leukemia. Cancer Cell 2015;27(6):864-876.

216. Huttlin EL, Ting L, Bruckner RJ, Gebreab F, Gygi MP, Szpyt J, Tam S, Zarraga G, Colby G, Baltier K, Dong R, Guarani V, Vaites LP, Ordureau A, Rad R*, et al.* The BioPlex Network: A Systematic Exploration of the Human Interactome. Cell 2015;162(2):425-440.

217. Nishimura AL, Al-Chalabi A, Zatz M. A common founder for amyotrophic lateral sclerosis type 8 (ALS8) in the Brazilian population. Hum Genet 2005;118(3-4):499-500.

218. Navone F, Genevini P, Borgese N. Autophagy and Neurodegeneration: Insights from a Cultured Cell Model of ALS. Cells 2015;4(3):354-386.

219. Farr RL, Lismont C, Terlecky SR, Fransen M. Peroxisome biogenesis in mammalian cells: The impact of genes and environment. Biochimica et biophysica acta 2016;1863(5):1049-1060.

220. Krisans SK. The role of peroxisomes in cholesterol metabolism. Am J Respir Cell Mol Biol 1992;7(4):358-364.

221. Faust PL, Kovacs WJ. Cholesterol biosynthesis and ER stress in peroxisome deficiency. Biochimie 2014;98:75-85.

222. Itzkovitz B, Jiralerspong S, Nimmo G, Loscalzo M, Horovitz DD, Snowden A, Moser A, Steinberg S, Braverman N. Functional characterization of novel mutations in GNPAT and AGPS, causing rhizomelic chondrodysplasia punctata (RCDP) types 2 and 3. Hum Mutat 2012;33(1):189-197.

223. Eisenberg-Bord M, Shai N, Schuldiner M, Bohnert M. A Tether Is a Tether Is a Tether: Tethering at Membrane Contact Sites. Dev Cell 2016;39(4):395-409.

224. Ferdinandusse S, Falkenberg KD, Koster J, Mooyer PA, Jones R, van Roermund CW, Pizzino A, Schrader M, Wanders RJ, Vanderver A, Waterham HR. ACBD5 deficiency causes a defect in peroxisomal very long-chain fatty acid metabolism. J Med Genet 2016.

225. Yagita Y, Shinohara K, Abe Y, Nakagawa K, Al-Owain M, Alkuraya FS, Fujiki Y. Deficiency of a retinal dystrophy protein ACBD5 impairs peroxisomal beta-oxidation of very-long-chain fatty acids. J Biol Chem 2016.

226. Marques VD, Barreira AA, Davis MB, Abou-Sleiman PM, Silva WA, Jr., Zago MA, Sobreira C, Fazan V, Marques W, Jr. Expanding the phenotypes of the Pro56Ser VAPB mutation: proximal SMA with dysautonomia. Muscle Nerve 2006;34(6):731-739.

227. Schliebs W, Kunau WH. Peroxisome membrane biogenesis: the stage is set. Current biology : CB 2004;14(10):R397-399.

228. Lin Y, Sun L, Nguyen LV, Rachubinski RA, Goodman HM. The Pex16p homolog SSE1 and storage organelle formation in Arabidopsis seeds. Science 1999;284(5412):328-330.

229. Nakayama M, Sato H, Okuda T, Fujisawa N, Kono N, Arai H, Suzuki E, Umeda M, Ishikawa HO, Matsuno K. Drosophila carrying pex3 or pex16 mutations are models of Zellweger syndrome that reflect its symptoms associated with the absence of peroxisomes. PloS one 2011;6(8):e22984.

230. Sugiura A, McLelland GL, Fon EA, McBride HM. A new pathway for mitochondrial quality control: mitochondrial-derived vesicles. The EMBO journal 2014;33(19):2142-2156.

231. Schmidt F, Treiber N, Zocher G, Bjelic S, Steinmetz MO, Kalbacher H, Stehle T, Dodt G. Insights into peroxisome function from the structure of PEX3 in complex with a soluble fragment of PEX19. The Journal of biological chemistry 2010;285(33):25410-25417.

232. Chen Y, Pieuchot L, Loh RA, Yang J, Kari TM, Wong JY, Jedd G. Hydrophobic handoff for direct delivery of peroxisome tail-anchored proteins. Nature communications 2014;5:5790.

233. Smith BK, Mukai K, Lally JS, Maher AC, Gurd BJ, Heigenhauser GJ, Spriet LL, Holloway GP. AMP-activated protein kinase is required for exercise-induced peroxisome proliferator-activated receptor co-activator 1 translocation to subsarcolemmal mitochondria in skeletal muscle. The Journal of physiology 2013;591(Pt 6):1551-1561.

234. Anthonio EA, Brees C, Baumgart-Vogt E, Hongu T, Huybrechts SJ, Van Dijck P, Mannaerts GP, Kanaho Y, Van Veldhoven PP, Fransen M. Small G proteins in peroxisome biogenesis: the potential involvement of ADP-ribosylation factor 6. BMC cell biology 2009;10:58.

235. Ebberink MS, Koster J, Visser G, Spronsen F, Stolte-Dijkstra I, Smit GP, Fock JM, Kemp S, Wanders RJ, Waterham HR. A novel defect of peroxisome division due to a homozygous non-sense mutation in the PEX11beta gene. J Med Genet 2012;49(5):307-313.

236. Joshi AS, Huang X, Choudhary V, Levine TP, Hu J, Prinz WA. A family of membrane-shaping proteins at ER subdomains regulates pre-peroxisomal vesicle biogenesis. J Cell Biol 2016;215(4):515-529.

237. Huybrechts SJ, Van Veldhoven PP, Brees C, Mannaerts GP, Los GV, Fransen M. Peroxisome dynamics in cultured mammalian cells. Traffic 2009;10(11):1722-1733.

238. Nagotu S, Saraya R, Otzen M, Veenhuis M, van der Klei IJ. Peroxisome proliferation in Hansenula polymorpha requires Dnm1p which mediates fission but not de novo formation. Biochimica et biophysica acta 2008;1783(5):760-769.

239. Delille HK, Agricola B, Guimaraes SC, Borta H, Luers GH, Fransen M, Schrader M. Pex11pbeta-mediated growth and division of mammalian peroxisomes follows a maturation pathway. Journal of cell science 2010;123(Pt 16):2750-2762.

240. Koch J, Pranjic K, Huber A, Ellinger A, Hartig A, Kragler F, Brocard C. PEX11 family members are membrane elongation factors that coordinate peroxisome proliferation and maintenance. Journal of cell science 2010;123(Pt 19):3389-3400.

241. Lingard MJ, Trelease RN. Five Arabidopsis peroxin 11 homologs individually promote peroxisome elongation, duplication or aggregation. Journal of cell science 2006;119(Pt 9):1961-1972.

242. Hu J, Baker A, Bartel B, Linka N, Mullen RT, Reumann S, Zolman BK. Plant peroxisomes: biogenesis and function. The Plant cell 2012;24(6):2279-2303.

243. Gronemeyer T, Wiese S, Grinhagens S, Schollenberger L, Satyagraha A, Huber LA, Meyer HE, Warscheid B, Just WW. Localization of Rab proteins to peroxisomes: a proteomics and immunofluorescence study. FEBS Lett 2013;587(4):328-338.

244. English AR, Voeltz GK. Rab10 GTPase regulates ER dynamics and morphology. Nat Cell Biol 2013;15(2):169-178.

245. McNew JA, Sogaard M, Lampen NM, Machida S, Ye RR, Lacomis L, Tempst P, Rothman JE, Sollner TH. Ykt6p, a prenylated SNARE essential for endoplasmic reticulum-Golgi transport. J Biol Chem 1997;272(28):17776-17783.

246. Kweon Y, Rothe A, Conibear E, Stevens TH. Ykt6p is a multifunctional yeast R-SNARE that is required for multiple membrane transport pathways to the vacuole. Mol Biol Cell 2003;14(5):1868-1881.

247. Honsho M, Fujiki Y. Topogenesis of peroxisomal membrane protein requires a short, positively charged intervening-loop sequence and flanking hydrophobic segments. study using human membrane protein PMP34. J Biol Chem 2001;276(12):9375-9382.

248. Meinecke M, Cizmowski C, Schliebs W, Kruger V, Beck S, Wagner R, Erdmann R. The peroxisomal importomer constitutes a large and highly dynamic pore. Nat Cell Biol 2010;12(3):273-277.

249. de Brito OM, Scorrano L. Mitofusin 2 tethers endoplasmic reticulum to mitochondria. Nature 2008;456(7222):605-610.

250. Reinisch KM, De Camilli P. SMP-domain proteins at membrane contact sites: Structure and function. Biochim Biophys Acta 2016;1861(8 Pt B):924-927.

251. Giordano F, Saheki Y, Idevall-Hagren O, Colombo SF, Pirruccello M, Milosevic I, Gracheva EO, Bagriantsev SN, Borgese N, De Camilli P. PI(4,5)P(2)-dependent and Ca(2+)-regulated ER-PM interactions mediated by the extended synaptotagmins. Cell 2013;153(7):1494-1509.

252. Friedman JR, Lackner LL, West M, DiBenedetto JR, Nunnari J, Voeltz GK. ER tubules mark sites of mitochondrial division. Science 2011;334(6054):358-362.

253. Korobova F, Ramabhadran V, Higgs HN. An actin-dependent step in mitochondrial fission mediated by the ER-associated formin INF2. Science 2013;339(6118):464-467.

254. Yoshida Y, Niwa H, Honsho M, Itoyama A, Fujiki Y. Pex11mediates peroxisomal proliferation by promoting deformation of the lipid membrane. Biol Open 2015;4(6):710-721.